

**Re-Analysis of the MWX Fracture Stimulation Data
From the Paludal Zone of the Mesaverde Formation**

Annual Report, FY 1988

**M.B. Smith
W.K. Miller II**

Work Performed Under Contract No.: DE-AC21-87MC24264

**For
U.S. Department of Energy
Office of Fossil Energy
Morgantown Energy Technology Center
P.O. Box 880
Morgantown, West Virginia 26507-0880**

**By
Nolte-Smith, Inc.
7030 S. Yale, Suite 502
Tulsa, Oklahoma 74136**

November 1988

TABLE OF CONTENTS

	<u>PAGE</u>
LIST OF FIGURES AND TABLES	iii
INTRODUCTION	1
SUMMARY	3
DISCUSSION	7
Stress Data Summary	7
Paludal Zone Stress Data Analysis	7
Micro-Frac Tests	7
Large Volume Stress Tests	8
Summary of Paludal Stress Analyses	10
Stress Correlation Analysis	12
Gamma-Ray Lithology Correlation	12
Sonic Log Correlation	14
Stress Profiles	15
Large Zone Stress Test Results	15
Minifrac #1 - Paludal Zone, MWX-1	16
Pressure Decline Analysis	16
Pressure History Match	19
Minifrac #2 - Paludal Zone, MWX-1	21
Pressure Decline Analysis	22
Pressure History Match	22
Pressure History Match of Propped Fracture Treatment .	24
CONCLUSIONS	27
REFERENCES	29
FIGURES AND TABLES	31
APPENDIX - Minifrac and Fracture Treatment Computer Simulations	85

LIST OF FIGURES AND TABLES

FIGURE	PAGE
1. Geologic Cross-Section of MWX-1	32
2. Pressure Decline Plot (Vs. Square Root Time), Test 1, MWX-1	33
3. Comparison of Square Root Time Plot Vs. Linear Plot for Determining Closure Stress, Test 4, Zone 2P2	34
4. Comparison of Square Root Time Plot Vs. Linear Plot for Determining Closure Stress, Test 3, Zone 2P3	35
5. Pressure Vs. Time for Step-Rate/Flowback Test, MWX-1, Paludal ..	36
6. Analysis of Paludal Step-Rate Test	37
7. Pressure and Pressure Derivative Vs. Time for First Flowback Test, MWX-1, Paludal	38
8. Pressure Vs. Time for Pump-In/Flowback Test, MWX-1, Paludal	39
9. Pressure and Pressure Derivative Vs. Time for Second Flowback Test, MWX-1, Paludal	40
10. Comparison of NSI and Sandia Frac Gradients for MWX Paludal Test Zones	41
11. K Factor Vs. Mean Gamma-Ray for All Test Zones	42
12. K Factor Vs. Gamma-Ray Showing Bilinear Correlation	43
13. Measured Frac Gradient Vs. Frac Gradient Calculated from Linear K/GR Correlation	44
14. Measured Frac Gradient Vs. Frac Gradient Calculated from Bilinear K/GR Correlation	45
15. Measured K Factor Vs. K Factor Calculated from MWX-2 Sonic Log for Fluvial and Marine Zones	46
16. Measured Frac Gradient Vs. Calculated Frac Gradient from the Sonic Log K/ Measured K Correlation	47
17. Measured Vs. Log Derived Stress Comparison for Both MWX Data and Published Data	48
18. Stress Profile Through the Paludal Zone in MWX-1 Using the Linear K Factor/ GR Correlation	49
19. Stress Profile Through the Paludal Zone in MWX-1 Using the Bilinear K Factor/ GR Correlation	50
20. BHP Vs. Time and Square Root Time for MWX-1 Paludal Minifrac #1.	51
21. Smoothed Stress Profile Through Paludal Zone in MWX-1	52
22. Minifrac #1 Pressure Decline Type Curve Match, $P(c) = 6411$ psi, $t(o) = 43.1$ minutes	53
23. Fluid Efficiency Vs. Dimensionless Closure Time	54
24. Minifrac #1 Pressure Decline Type Curve Match, $P(c) = 5890$ psi, $t(o) = 43.1$ minutes	55
25. Minifrac #1 Pressure Decline Type Curve Match, $P(c) = 5890$ psi, $t(o) = 63.4$ minutes	56
26. Revised Smoothed Stress Profile Through MWX-1 Paludal Zone	57
27. Pressure History Match of MWX-1, Minifrac #1 Injection	58
28. Post-Minifrac #1 Temperature Log	59
29. Computed Fracture Width-Height Profile for Minifrac #1 Pressure History Match	60
30. Comparison of Created Fracture Height From Temperature Log and Predicted Height from Pressure History Match, Minifrac #1.....	61
31. Pressure Decline History Match for MWX-1, Minifrac #1	62

FIGURES (Cont.)	PAGE
32. BHP Vs. Time and Square Root Time for MWX-1 Paludal Minifrac #2.	63
33. Minifrac #2 Pressure Decline Type Curve Match	64
34. Pressure History Match of MWX-1, Minifrac #2 Injection	65
35. Computed Fracture Width-Height Profile for Minifrac #2 Pressure History Match	66
36. Comparison of Created Fracture Height From Temperature Log and Predicted Height from Pressure History Match, Minifrac #2	67
37. Pressure Decline History Match for MWX-1, Minifrac #2	68
38. Nolte-Smith Log-Log Plot of Net BHTP During MWX-1 Paludal Fracturing Treatment	69
39. Pressure History Match of Paludal Frac Treatment Using a Leak-Off Coefficient of 0.0001 ft/min**0.5	70
40. Comparison of Minifrac and Main Frac Treatment Net Treating Pressures Vs. Injected Volume	71
41. Estimated Sand Geometry for Paludal Sands 3 and 4	72
42. Simulated Pressure History for Paludal Fracturing Treatment Assuming a Tip Screen-out at 50 Minutes	73
43. Post-Frac Temperature Log, MWX-1 Paludal Frac Treatment	74
44. Computed Fracture Width-Height Profile for Main Fracture Treatment Pressure History Match	75

TABLES	PAGE
1. Sandia Stress Test Results	76
2. Paludal Stress Data Re-Analysis Results	77
3. Stress, Sonic Log, and Mean Gamma-Ray Data Considered for Correlation Analysis	78
4. Leak-Off Coefficient Calculations for MWX-1 Minifrac #1, P(c) = 6411 psi, t(o) = 43.1 minutes	79
5. Leak-Off Coefficient Calculations for MWX-1 Minifrac #1, P(c) = 5890 psi, t(o) = 43.1 minutes	80
6. Leak-Off Coefficient Calculations for MWX-1 Minifrac #1, P(c) = 5890 psi, t(o) = 63.4 minutes	81
7. Summary of Results from Pressure Decline Analysis, MWX-1 Minifrac #1	82
8. Leak-Off Coefficient Calculations for MWX-1 Minifrac #2	83
9. MWX-1 Paludal Zone Fracture Treatment Schedule	84

INTRODUCTION

Historically, producing natural gas from low permeability formations has been uneconomical and inefficient due to the low natural flow rates. While massive hydraulic fracturing has resulted in significant improvements in production from blanket sands, the results have been disappointing for lenticular tight gas reservoirs. In 1980, the National Petroleum Council estimated that these lenticular reservoirs contained in excess of 370 Tcf of gas, or over 40 percent of the estimated reserves in the U.S. tight gas basins. More recently (1987), the U.S. Geological Survey estimated that gas-in-place in the Piceance Basin lenticular sands alone exceeded 400 Tcf with estimated recoverable gas at 68 Tcf.

For a number of years the U.S. Department of Energy has been engaged in research to enhance gas recovery from "tight gas sands", particularly the lenticular sandstone formations common to the Western United States. The purpose of this research is to establish the production potential from lenticular reservoirs, improve existing production technology; and ultimately, to demonstrate the economic feasibility of drilling and completing wells in this unconventional gas source.

To investigate these Western U.S. tight gas sands, DOE established the Multi-Well Experiment (MWX), a field research facility near Rifle, Colorado, where three closely spaced wells were drilled through the lenticular Mesaverde formation in the Piceance basin. Testing included extensive coring and core analysis, production testing, and instrumented fracture stimulation experiments. Because one of the more important aspects of the MWX project was to establish the predictability of well stimulation procedures, extensive pre-frac testing was conducted in the Paludal, Coastal, and Fluvial zones.

This report concentrates on a review and re-analysis of the MWX stimulation data for the Paludal zone. The Paludal was deposited in environments of lenticular distributary channels and adjacent coal swamps, with sandstones occurring both as channel fillings and splay deposits. The objectives of the DOE Paludal experiments were 1) to characterize the lenticular sandstones for reservoir quality and size, 2) to determine fracture geometry and behavior in a lenticular environment, and 3) to successfully stimulate lenticular sandstones in the complex, coal-bearing interval. While the Paludal experiments were successful and informative in many ways, there still remained some questionable aspects of the testing at its conclusion; the most noted being the unexpected, abnormally high injection pressures during the fracture tests and main fracture treatment.

The primary goal of the Paludal stimulation data review was to establish the conditions affecting fracture geometry and behavior in this lenticular environment; and determine the degree of predictability of fracture behavior from pre-frac testing. Since variations of in situ stress are the primary control mechanism over fracture geometry, a major effort was made by DOE to collect in situ stress data in the Paludal and its bounding layers. As the first step in evaluating the final utility of the stress testing program in terms of: 1) testing theories of fracture geometry in a field scale environment, and 2) examining the usefulness of pre-frac testing for improving the predictability of well stimulations; much of this in situ stress test data was reviewed, and, in some instances, re-analyzed. The objectives of this initial portion of the review were to confirm the stress results showing that significant stress differences can exist in lenticular formations, to evaluate the micro-frac testing procedure utilized for the MWX wells, and to examine correlations between measured stresses and other formation properties. As reported herein, formation properties correlations with in situ stress were obtainable for deriving a stress profile.

The derived in situ stress profile was then used in a fracture simulator to history match the net treating pressures obtained on the two Paludal minifrac and the main fracture treatment. This analysis was preceded by re-analyzing the two minifrac pressure declines to determine the fluid leak-off properties for use in the simulator. As reported, this review and re-analysis of the MWX Paludal data resulted in some very significant differences from previous analyses. The derived stress profile possessed some unique differences, the leak-off coefficients calculated were much lower than previous analysis, and the history match of the net treating pressures revealed that, in fact, the measured pressures were not abnormally high and quite predictable. The results of post-frac temperature logs from the minifrac and main treatment are confirmed with the generated height from the simulator.

This work will be followed up with a similar review of the MWX stimulation data obtained for the Coastal and Fluvial zones in the Mesaverde formation. A collective analysis of the results from the three zones will then be conducted to formulate general guidelines for future testing and analysis of fracturing data from lenticular sandstone reservoirs.

SUMMARY

Review of Paludal Stress Data

The micro-frac stress tests for the seven Paludal zones in MWX-2 and MWX-3 were re-analyzed using a plot of pressure versus the square-root of shut-in time to determine closure pressure. This method relies on linear flow behavior and is referred to in the report as the "reservoir type" method. The results from this method were compared to those obtained in previous analyses which estimated closure pressure from the instantaneous shut-in pressure (ISIP). While both methods showed good agreement for most tests, it was concluded that the "reservoir type" analysis was generally superior; yielding clearer, more definitive results than a subjective pick of an ISIP.

Large volume stress tests were performed in Paludal sands 3 and 4 on wells MWX-1 and MWX-3. These included a step-rate test/flowback and pump-in/flowback test. The re-analysis of these tests showed good agreement with the previous analysis, using similar methods.

A point clearly indicated by this analysis was that significant stress differences (on the order of 0.2 psi/ft or 1500 psi) can exist in this layered, heterogeneous formation. This somewhat unexpected phenomenon has been extensively commented on in previous MWX publications and was verified with this re-analysis.

Also, considering the good agreement between the two analysis procedures and the complexity of the Paludal zone, it seemed certain that similar agreement would prevail for stress tests in the lower Marine, and uphole Coastal and Fluvial zones. Therefore, the previous analyses for these zones was used in addition to the Paludal results in looking for correlations between in situ stress and other formation properties.

Stress Correlation Analysis

This section examined correlations between measured in situ stress and other rock properties such as lithology and acoustic velocity. Stress results considered included those from 38 tests from the four Mesaverde zones including the Fluvial, Coastal, Paludal, and Marine. K factor, derived from the measured closure stress, was used in this analysis instead of closure stress to normalize out the effects of depth and pore pressure.

Using the gamma-ray measurements to define lithology, a

correlation existed between stress (K factor) and lithology (gamma-ray). When data from test zones with a high standard deviation in gamma-ray (indicating complex, layered lithology) and also from those that are in or near coal seams were eliminated from consideration, the correlation was very strong.

K factor values derived from the Poisson's Ratio from the acoustic log showed a non 1:1 correlation with measured K factor. The stresses derived with this correlation were not as accurate as those from the gamma-ray correlation. Comparing the non-adjusted sonic log K values from the MWX tests to published data, the MWX data did not follow the strong linear correlation observed in other areas.

Stress Profile

A stress profile was derived for the Paludal zone in MWX-1, using the gamma-ray lithology correlation. The results from large volume stress tests performed in MWX-1 showed good agreement with the profile results. A smoothed version of the profile was used as the basis for pressure/height analysis and for modeling the two minifrac and main fracture treatment performed in the Paludal zone in MWX-1.

Minifrac No. 1

From the square-root of shut-in time plot of the minifrac pressure decline, a closure pressure was evident at about 6400 psi, or the same as predicted from the derived stress profile for the lower Paludal sand perforated (Zone 3). This being 600 psi higher than the measured stress in the Paludal Zone 4, led to questioning the validity and applicability of the pressure decline type curve analysis for complex conditions where different layers are closing at different time intervals during the pressure decline. Several scenarios were used in performing the analysis including (1) a gross height of 135 ft (from temperature log) with a leak-off height of 55 ft (Zones 3 and 4), (2) a gross height of 55 ft (assuming that the higher stress boundary layers close relatively quick after shut-down, and (3) a gross height of 25 ft, assuming continued injection into Zone 4 until the time at which Zone 3 is closed, from fluid being squeezed from the higher stress zone to the lower stress zone through either the fracture or through crossflow in the wellbore. The results from these cases yielded leak-off coefficients ranging from 0.00009 to 0.003 ft/min**0.5, an impossible range for designing a fracture treatment. Some of these values were eliminated, though, as reported herein, to arrive at a much smaller range of from 0.0001 to 0.0002 ft/min**0.5 or an order-of-magnitude smaller than calculated in the previous analysis.

In analyzing the pressure decline data, it was evident

that the analysis techniques are not without weakness for complex stress conditions such as the Paludal. Coupled with history matching of the actual injection and decline pressures, though, it is still a powerful tool.

Using the stress profile from the gamma-ray lithology correlation (with only minor adjustments), a leak-off coefficient of $0.0001 \text{ ft/min}^{*0.5}$, and published rheology data for 30 lb. non-crosslinked gel; modeling obtained a very close history match with the measured net bottomhole injection pressures. The predicted height from the model also very closely approximated the results of the post-frac temperature log, including the top and bottom of the fracture.

To ascertain the validity of using the lower leak-off coefficient, one requirement in history matching the injection pressures was that the model predicted fluid efficiency match that calculated in the pressure decline analysis. Additionally, model predicted pressure declines were generated for 0.0001 , 0.0002 , 0.0003 , and $0.001 \text{ ft/min}^{*0.5}$ leak-off coefficients for comparison to the actual decline. This analysis showed the early time decline to follow higher leak-off, but that from 20 minutes to the end of the recorded pressures, the decline closely approximated $0.0001 \text{ ft/min}^{*0.5}$. Since the lower perforated sand closed at 20 minutes, the early higher leak-off was either "real" to this zone or anomalous as caused by fluid crossflow. The later is thought to be the case, the lower leak-off value being more consistent with core analysis which saw very few natural fractures in this zone and calculated permeabilities in the 1-3 microdarcy range.

Minifrac No. 2

The pressure decline analysis for the second minifrac was complicated by the fact that the pressure was not recorded down to a closure pressure. As on the analysis of the first minifrac, several different ratios of leak-off to gross height were evaluated; resulting in calculated leak-off coefficients ranging from 0.00004 to $0.0006 \text{ ft/min}^{*0.5}$. Using a leak-off coefficient of 0.0001 and the previously revised stress profile, a good pressure history match was obtained with the measured pressures. The modeled height was once again very close to the post-minifrac temperature log interpretation and the modeling of the pressure decline was consistent with the lower leak-off value used.

To summarize the analysis of the two minifracs, a detailed stress profile was generated; which, when coupled with the best approximation of leak-off from pressure decline analysis, gave good history matches with the injection pressures. This was supported by matching the modeled height with temperature evaluation logs and the consistency of the low leak-off coefficient with the observed pressure decline and fluid

efficiency. The major conclusions were (1) leak-off coefficient was an order-of-magnitude smaller than previous analyses predicted and (2) injection pressures during the Paludal fracturing tests were not abnormally high as previously charged.

Main Fracture Treatment

Using the same stress profile and leak-off coefficient used to model the minifrac, a good pressure history match was obtained for the propped fracture treatment up to about 50 minutes. At this time the pressure started increasing very rapidly, suggesting a possible screen-out. This was ruled out, though, as the primary cause since the crosslinked gel should have resulted in even lower leak-off than calculated on the minifrac. Comparing the minifrac and main treatment pressures on a volume basis revealed similar behavior, the volume of the minifrac not large enough to reach the point of abnormally increasing pressures.

Looking at how far the proppant had traveled after 50 minutes, the simulator predicted a propped length of 300 feet. When compared to the estimated sand geometry for Paludal Zones 3 and 4, it was postulated that proppant reached the outer boundary(s) of the sand splay and/or channel and that the stress of the shalier rock beyond this point was high enough to restrict fracture width and cause proppant bridging. Attempts to simulate the pressure increase were relatively unsuccessful due to the complex nature of the situation.

The modeled height from the original history match very closely approximated the interpreted post-frac temperature log. These were also consistent with the limited borehole seismic data obtained.

DISCUSSION

STRESS DATA SUMMARY

This section presents a summary of much of the closure stress data obtained during the MWX fracture testing program. Most of the stress testing was concentrated in the Coastal, Paludal, and Marine zones, with four tests being conducted in the Fluvial zone. Figure 1 is a geologic cross-section of MWX-1 showing the four zones.¹ Most of the tests conducted in wells MWX-2 and MWX-3 were performed using the small volume (micro-frac) procedure, which typically consists of pumping low volumes of low viscosity fluid into a 1-2 foot interval at 5-20 GPM and measuring the shut-in pressure (Instantaneous Shut-In Pressure).^{2,3,4} Because of the low volume injected and the apparent small fracture volume created, theoretically the fracture should close quickly after shut-in and the closure stress can be approximated by the ISIP. Stress tests in MWX-1 were performed on larger perforated intervals and larger volume injections used to measure closure stress, e.g. pump-in/flow-backs, step-rate tests, etc.

Table 1 shows Sandia's published results for the stress tests performed in MWX-2 and MWX-3.⁵ The designation for the test zone is "well no.-zone-test zone", e.g. 2F1 designates stress test zone no. 1 in the Fluvial zone of MWX-2. Also shown in Table 1 for each test depth are the gamma-ray reading, pore pressure, overburden pressure and K-factor. The K-factor is discussed later. It should be noted that the closure stress results in Table 1 were obtained by subjective picking of an ISIP from a plot of pressure versus time.

Included in NSI's analysis of the stress data are seven of the micro-frac tests in the Paludal zone. It was hoped that detailed analysis of the tests would lead to correlations between closure stress and formation parameters quantifiable by log analysis. Also, if the Sandia results in the Paludal zone could be accurately verified, then stress results from outside the zone could be assumed valid and possibly used for similar correlation analysis.

PALUDAL ZONE STRESS DATA ANALYSIS

MICRO-FRAC TESTS

The micro-frac tests for the seven Paludal zones in MWX-2 and MWX-3 were analyzed in detail and the results reported in an earlier Topical Report - "In Situ Stress Analysis", July, 1988.⁶ Detailed plots of the data were included in that report

and will not be repeated here. The main tool used to determine closure pressure was the plot of pressure versus square root of shut-in time - Figure 2 showing an example from Test 1, Zone 2P2.⁷ This analysis procedure consists of looking for linear flow behavior in the pressure data, with a deviation from this behavior indicating closure pressure. This is in contrast to the micro-frac analysis which estimates closure from the ISIP. For many tests the ISIP analysis may be too subjective, and "reservoir type" analysis may yield a more definitive fracture closure.

There were many instances in the data where there was a definitive deviation from linear behavior on a square root of time plot, and little or no indication of an ISIP on the corresponding linear plot. One example of this is shown in Figure 3, the square root plot indicating a closure stress of 6000 psi and the linear plot providing little character for picking an ISIP. While Sandia showed a closure stress of 5745 psi for this zone from an earlier test, the linear plot would indicate a much higher value than this - probably between 5970 and 6100 psi. This is probably due to an increasing closure stress in the water saturated, porous sand section.

There are also instances in the data where there is good agreement between the square root of time analysis and the ISIP in a zone. For example the square root plot in Figure 4 shows a deviation from linearity at 6290 psi and Sandia's pick of the ISIP on the linear plot was 6325 psi. If closure stress remains constant in a zone (as it should for any case other than a liquid saturated porous zone), and there is good agreement initially between the square root analysis and the ISIP, this agreement should hold for other tests in the same zone.

Common to the data sets analyzed from the Paludal zone was the fact that the square root analysis gave a clearer definition of closure stress than trying to pick the ISIP. In performing the re-analysis of this data, we concluded that "reservoir type" methods for determining closure stress were generally superior to the ISIP technique, even for small volume tests. This does not imply the infallibility of the square root time analysis, it only points out that this method tends to yield clearer, often more definitive results than using a subjective pick of an ISIP. The results from the re-analysis of the Paludal micro-frac tests are reported later in combination with the results from the large volume stress tests performed in the Paludal zone.

LARGE VOLUME STRESS TESTS

The large volume tests were performed using two distinctly different methods. One was breakdown/shut-in with fluid being

injected into the zone and the well shut-in downhole to monitor the pressure decline. The ISIP technique was then used to determine closure stress. This type test was performed on MWX-1 interval 7256-7284 feet and on MWX-3 interval 7080-7102 feet inclusive of two perforated intervals corresponding to Paludal Sands 3 and 4. The other type test performed was the pump-in/flowback test, which was performed in the Paludal Sands 3 and 4 in MWX-1 (perforated intervals: 7076-7100 ft. and 7120-7144 ft.). The focus of this discussion is on the flowback tests, as no detailed pressure data was available for the breakdown tests.

A pump-in/flowback test is the preferred method for determining closure stress in low permeability formations.⁸ If a correct flowback rate is chosen, closure pressure can be seen as a change in curvature of the pressure decline. Any series of flowback tests should start with a step-rate injection, which helps characterize fracture extension pressure which serves as an upper limit on closure pressure. The detailed data plots for this group of tests on MWX-1 was included in the Topical Report: "In Situ Stress Analysis" and are not repeated here. Only those plots required for this discussion are included in the text.

Figure 5 shows the pressure record for the step-rate injection/flowback test performed in Paludal Sands 3 and 4 in MWX-1. Sandia's analysis of the step-rate test is shown in Figure 6 along with NSI's re-analysis of the same data. The results indicate a fracture extension pressure of 5940 psi from Sandia and 6010 psi from NSI. The difference lies in Sandia plotting the pressure mid-point of each time step and NSI plotting the stabilized pressure at the end of each time step. The later is the more widely accepted method for analysis.

Figure 7 shows the decline pressure for the flowback following the step-rate test. Also included on this plot, is the pressure derivative (or slope) curve for better defining where the change in curvature on the pressure versus time curve occurs, this point of acceleration in the rate of pressure decline being closure pressure. In Figure 7, closure pressure appears to be at around 5800 psi. The pressure derivative curve shows little change in slope from about 6000 psi to 5800 psi, suggesting that closure may be as high as 5900 psi, which is what Sandia determined. 5800 psi was chosen because this is where the rate of pressure decline starts to accelerate. This is in excellent agreement with the closure stress of 5805 psi found in the breakdown stress test conducted on the MWX-3 interval 7080-7100 feet.

Following the step-rate test/decline, a pump-in/flowback test was conducted at a rate of 8 BPM. The pressure record for this test is shown in Figure 8. When the decline pressure and pressure derivative were plotted versus time (Figure 9), there

was little character in the data and no obvious inflection point indicative of closure pressure. During testing, data was recorded down to a pressure of about 5600 psi, however the later portion of the data is no longer available for analysis. The results of any analysis on this test would be suspect at best.

Following the flowback tests, two minifracs were performed in the same Paludal interval in MWX-1. Unfortunately, the pressure declines were hampered by surface line freezing problems and insufficient data recorded to get back to the closure pressure measured on the step-rate test. This data will be further analyzed and interpreted in the later fracture modeling section.

SUMMARY OF PALUDAL STRESS ANALYSES

Table 2 shows the results of the seven Paludal micro-frac stress test zones for which pressure data was available. The first column designates the test, e.g. 2PlTST3 indicates Test 3 in zone 2Pl. Both Sandia's and NSI's closure stresses are listed for comparison. There was fairly good agreement between test results. The pore pressure column in Table 2 gives the values reported in the literature and the values in the overburden pressure column assumes a gradient of 1.05 psi/foot.⁹ Fracture gradients for both Sandia and NSI are calculated simply by dividing the closure stress by depth.

For shale intervals, pore pressure is assumed equal to that in nearby porous sandstones. For the geologic environment of the Mesaverde Group, this seems to be a reasonable assumption since the formations are being "unloaded" (e.g. overburden is being reduced) during recent geologic time. Overpressured shales are common in younger sediments such as the Gulf Coast where rapid sedimentation (and the resultant increase in overburden pressure) along with salt dome intrusions for the particular case of the Gulf Coast, are loading and compressing the shale formations faster than the resulting excess pore pressures can escape from such low permeability rocks.

Finally, a "K factor" was calculated to attempt to normalize out effects of depth and pore pressure in comparing the stress results from different zones. Other studies¹⁰ have noted a general linear relation between fracture closure pressure, depth, and pore pressure which might be written as

$$\sigma_c = K (OB - P_{res}) + P_{res} \quad (1)$$

where σ_c is closure pressure, "OB" is the overburden pressure,

and P_{res} is reservoir or pore pressure. This can be rewritten as

$$K = (\sigma_c - P_{res}) / (OB - P_{res}) \quad (2)$$

and it is often further assumed that "K" is related to the elastic properties of the rock by

$$K = \nu / (1 - \nu) .$$

No assumption is implied here by the use of "K", it is simply a convenient means of comparing stress test results from zones at different depths with different pore pressures.

Overall, there was good agreement between the Sandia stress results and those from the NSI re-analysis. Figure 10 shows a plot of NSI frac gradient versus Sandia frac gradient. Even though one may be concerned with the subjective nature of the ISIP analysis, the results matched well with the more objective "reservoir" type approach. Linear regression of the points plotted, with the y intercept of the plot forced to zero, yield a line with a slope of 0.999, and a coefficient of linearity $R = 0.961$. This indicates a very strong linear correlation for the relation $Y = 0.999 X$. Since the Paludal appears to be the most complex of the various zones of the Mesaverde Group, this good agreement implies that an ISIP analysis of micro-frac stress tests does yield a consistent, repeatable result for in situ stress if proper care is taken with the testing and analysis. However, linear flow analysis (e.g. square root of time plots) can, in many instances, provide a more definitive and objective analysis method.

Another point clearly indicated by Figure 10 is that significant stress differences (on the order of 0.2 psi/ft or 1500 psi) can exist in this layered, heterogeneous formation. This somewhat unexpected phenomenon has been extensively commented on in previous MWX publications and was verified with this re-analysis.

Also, considering the agreement between the two analysis procedures and the complexity of the Paludal zone, it seems certain that similar agreement would prevail for stress tests in the lower Marine, and uphole Coastal and Fluvial zones. Therefore, the previous Sandia stress analyses for these zones was used in the subsequent analysis in looking for correlations between in situ stress and other formation properties.

STRESS CORRELATION ANALYSIS

This section of the report examines correlations between measured closure stress and other rock properties such as lithology and acoustic velocity. An average gamma ray value for each particular test zone (an eleven foot interval centered around the zone) was used to "define" lithology. An attempt is made to build a correlation with the value of K factor derived from a sonic log, but it is not found to be as accurate as the gamma ray correlation; the gamma ray correlation having other advantages.

GAMMA RAY LITHOLOGY CORRELATION

Table 3 presents the stress test results which were considered for this analysis, including four tests from the Fluvial, eleven from the Coastal, twelve from the Paludal, and eleven from the Marine zone. The "Gamma Ray" column in Table 3 gives the average GR over the 2 foot perforated test interval and the "Mean Gamma" is the mean GR value over the eleven foot interval surrounding the test zone. The "Std Dev" column gives the standard deviation in gamma ray associated with the mean gamma ray results. "K (Stress)" and "Frac Gradient" are based on published data, the re-analysis of the Paludal data verifying the accuracy of the earlier results. "K (Sonic)" is K factor results based on sonic log data from MWX-2 where reliable data was available. The Poisson's Ratio from the sonic log, averaged over ten feet, was used to calculate "K" using the relationship $K = \nu / (1 - \nu)$. The Poisson's Ratio values used in this analysis were those determined from the original MWX log analysis. No attempt has been made to review the basic log data for reanalysis of the shear and compressional wave velocities. The basic logs were reviewed to insure there were no adverse wellbore effects in the zones of interest.

When K factor was plotted versus the mean gamma ray values, Figure 11, there appeared to be a general relation between stress and lithology, as noted throughout the MWX testing. However, there was significant scatter to the data. In the Paludal analysis, data from a stress test was deemed unsuitable for correlation analysis if it was in or near a coal section, or if the mean gamma ray value had a large standard deviation, e.g. complex layered lithology. These zones from the Paludal section were eliminated from the overall correlation analysis and tests from other zones, such as the Coastal and Fluvial, were evaluated for suitability based on these criteria. As seen in Figure 11, when data obtained near a coal section or with a high gamma ray deviation were separated out, the remaining data showed a strong trend of increasing stress (as characterized by "K") with increasing gamma ray.

Figure 12 shows the "filtered" K factor data plotted. It is hypothesized that the correlation between K factor and gamma ray may be bilinear. While the data with a mean gamma ray value greater than approximately 90 API Units shows some scatter, it appears to flatten out. This flat spot occurs at or near $K = 1$, which implies that closure pressure is equal to the overburden pressure. If closure stress equals or exceeds overburden stress, injection may tend to create or open a horizontal fracture(s) instead of the expected vertical fracture. This would tend to complicate the analysis of injection/decline tests since the true closure stress may not be measured - the true stress possibly being higher than the overburden. Regardless, if the behavior implied in Figure 12 is assumed to be true, then one relationship exists between "K" and gamma ray for gamma ray values less than about 90 API Units and above this value, the relationship can be defined simply by $K = 1$. This correlation enables one to determine the stress value for any zone based on its mean gamma ray value, overburden stress, and local pore pressure using Equation 1.

It is unclear whether K factor derived from the lithology correlation actually measures resistance to vertical fracturing, or, for shalier/siltier formations, measures overburden pressure. The linear trend below $GR = 90$ API Units, when extrapolated, may yield the closure stress for a vertical fracture. If one assumes this to be true, Figure 12 shows that for a given GR value over 90, the K factor (and closure stress) derived from this correlation would significantly exceed that derived from the bilinear correlation. Given this uncertainty, stress profiles were constructed for both the linear and bilinear correlations.

The best fit line through the GR data less than 90 API Units in Figure 12 describes the linear correlation for all GR values. The equation for this line, determined by linear regression, is given as:

$$K = MGR * 0.01532 - 0.458$$

where "MGR" is the "mean gamma ray" value for a zone and this line has a coefficient of linearity $R = 0.88$, indicating a highly linear grouping. For the bilinear correlation the equation above would be used for GR less than 90. For GR equal to or greater than 90, K would equal 1.0.

Using the linear correlation above, and Equation 1, the expected frac gradients for the stress test zones can be calculated. Figure 13 shows the strong agreement between the measured versus "calculated" frac gradients determined with this method. A flattening is evident for frac gradients

greater than 1.05 (the approximate overburden gradient). Use of the bilinear correlation takes calculated frac gradients greater than 1.05 and assigns them a value of 1.05, giving a slightly better relation as seen in Figure 14. Given a base uncertainty in the average closure stress measurement of 50 to 100 psi, this simple lithology correlation appears to be quite accurate.

SONIC LOG CORRELATION

Sonic log data from MWX-2 was investigated in an attempt to determine if a relationship existed between stress properties derived from the sonic log and actual stresses measured in the micro-frac tests. K factor was calculated using the Poisson's Ratio determined from the sonic log data. Figure 15 shows the K factors determined from the sonic log for the Fluvial and Marine zones in MWX-2 versus the measured K factors from closure stresses, the data having a coefficient of linearity of $R = 0.88$. While the Paludal zone data was also investigated, it showed poor linearity when sonic log K was plotted versus measured K (only four points available for analysis). While it is evident from Figure 15 that a relation exists between sonic derived and measured K, it is NOT 1:1, and Equation 2 cannot be used to calculate closure stress.

Based on a linear regression fit, the correlation in Figure 15 can be defined as

$$K(\text{cor}) = 5.2 * K(\text{log}) - 0.82 ,$$

where $K(\text{cor})$ is the sonic log derived K corrected to the best fit line. Using the corrected K, a comparison of calculated frac gradients was made to the measured gradients as shown in Figure 16. Again, no Paludal data was included. While a reasonable relation appears to exist, the average error between calculated and measured stress is not quite as good as that found for the bilinear lithology correlation. When compared to other published sonic derived versus measured stress data, Figure 17, the MWX data clearly shows a poorer correlation.¹¹ The following table shows the comparison between the correlations derived from the sonic log and GR log, with the GR correlations showing the most accuracy.

<u>Correlation</u>	<u>Paludal Zone Data</u>	<u>Coefficient of Linearity (R)</u>	<u>Average Error (psi)</u>
Sonic Log	Included	0.69	360
Sonic Log	Not Included	0.88	257
GR Log	Included	0.93	200
GR Log	Not Included	0.94	206

STRESS PROFILES

The two lithology correlations (linear and bilinear) were used to generate stress profiles for the Paludal frac zone in MWX-1 and its surrounding layers as seen in Figures 18 and 19. These profiles provide the basis for history matching the treating pressures from the Paludal minifrac and propped fracture treatment. Of particular interest is the indication of a high stress "shale" between the two perforated intervals in the frac zone. This, along with the possibly higher stress in the lower perforated frac interval than in the upper interval, would contribute to the apparently high treating pressures recorded for the MWX-1 Paludal fracture treatments.⁹

LARGE ZONE STRESS TEST RESULTS

In addition to the micro-frac tests used to generate the Paludal zone stress profiles, several larger volume stress tests were conducted in MWX-1 and MWX-3. Since this data was not included in deriving the lithology correlation or the stress profiles, it is useful to compare the results of these tests to the generated stress profile.

In the MWX-1 frac zone, the first flowback test yielded a closure stress of 5900 psi (original Sandia analysis) to 5800 psi (re-analysis discussed previously). The average stress across the upper perforated interval of the frac zone is 5890 psi - clearly excellent agreement. The breakdown test in MWX-3, in an equivalent lithology to the MWX-1 frac interval, yielded a closure stress of 5800 psi, again in good agreement with the profile results. For the second flowback test in the Paludal zone in MWX-1, the original Sandia analysis result was 6100 psi. However, as previously discussed, there are several questions about this test and the results. From the stress profile, the average closure stress through this lower perforated interval is about 6400 psi. As shown later this is the same as the earliest time closure measured on the first minifrac in this zone.

The good agreement between the large volume stress test measurements and the stress profiles provides confidence both in the overall stress profiles and in their use for history matching the fracturing pressures. The following discusses the analysis of the minifrac data and the pressure history matches of the two minifrac and main fracture treatment conducted in the Paludal zone in MWX-1.

MWX-1, MINIFRAC #1 - PALUDAL ZONE

The first minifrac performed in the Paludal zone in MWX-1 consisted of pumping 15,000 gals. of non-crosslinked 30 lbs./1000 gals. gel, at an average injection rate of 10 BPM. A prepad of 2,100 gals. of low pH methanol was used to reduce formation damage and aid fluid recovery. During the minifrac injection/decline, a quartz crystal pressure gauge was installed at 6700 feet. Following the minifrac decline a temperature survey was run to evaluate fracture height growth.¹²

MINIFRAC #1 PRESSURE DECLINE ANALYSIS

Figure 20 shows plots of bottomhole pressure versus time for the injection/decline and pressure decline versus the square root of shut-in time. From the square root of time plot there is a distinct change in the slope of the pressure decline at 6411 psi, indicating fracture closure at a shut-in time of 20.3 minutes. Looking at the stress profile in Figure 21 (from the linear lithology correlation), this corresponds to the average closure pressure in the lower Paludal sand. If only the lower sand was closed at this point, which appears to be the case, then several questions must be answered before the pressure decline analysis can be used to determine the leak-off coefficient. One must know what happens to the fluid in the higher stress intervals if the leak-off rate is less than or equal to leak-off in the interval in which the fracture remains open. While some of the fluid will obviously leak-off to the formation, the large stress difference may cause the remainder of the fluid to be squeezed back into the "lower" stress zone(s), giving the same effect as continued injection. With injection time in the equation for leak-off coefficient, this is very important.

Of even greater importance than the use of the correct injection time, is what gross height and leak-off height to use in the calculation of leak-off coefficient. At the end of pumping, gross height was about 135 feet (post-minifrac temperature log) and the leak-off height was 55 feet (combined sand intervals). But, after the high stress intervals close, is the gross height only the 55 feet? And taking it one step further, after the lower sand closes, is the gross and leak-off heights only 25 feet in the upper sand? This degree of variance in height will dramatically change the resultant leak-off coefficient calculated.

To analyze the Minifrac #1 pressure decline, the closure pressure of 6411 psi was assumed to be the fracture closing only in the lower sand and the rate of pressure decline following this closure was extrapolated to 5890 psi (the average closure of the upper sand indicated by Figure 21) to

determine when fracture closure in the upper sand would be reached. This extrapolation gave a final closure time of 148.5 minutes, or 7.3 times longer than the closure indicated in Figure 20.

With two possible closure pressures and times, three possible gross heights, and two possible leak-off heights; combinations of these variables were used in the pressure decline analysis to calculate fluid efficiency and leak-off coefficient for each. The intent was then to try to match the fluid efficiency in the history match of the net treating pressures to try to determine which fluid leak-off coefficient appeared to be the most correct. Granted, none of the values calculated would be absolutely correct because of the changing conditions during the pressure decline, one might be revealed as more correct than the others.

Figure 22 is the first pressure decline type curve match for the closure pressure of 6411 psi at a closure time of 20.3 minutes.⁷ Table 4 shows the corresponding worksheet on which the fluid efficiency and leak-off calculations are presented. From Figure 22, the match pressure P^* (not related to reservoir pressure) is 400 psi. Using this value, along with other data presented in the table, a fluid efficiency of 0.28 was calculated. This compares very close to the efficiency determined from the time-to-close and the plot shown in Figure 23, and suggests little or no leak-off to a secondary source such as natural fissures.⁷ For a gross height of 135 ft. and a leak-off height of 55 ft. (values used in Sandia's analysis) a leak-off coefficient of $0.0028 \text{ ft/min}^{0.5}$ was calculated. This is twice as high as their results, since they apparently used the later closure pressure and time for their analysis. The later closure analysis is presented shortly. The second scenario looked at for the early time closure was a gross height of 55 ft., assuming all of the fracture closed very early with the exception of the two main sand intervals, and a leak-off height of 55 feet. This resulted in a much lower estimate of leak-off coefficient, i.e. $0.00047 \text{ ft/min}^{0.5}$.

Figure 24 shows the pressure decline match for an assumed closure pressure of 5890 psi at a closure time of 148.5 minutes (assumed because the pressure decline never reached the lower closure of the upper sand), resulting in a match pressure, P^* , of 192 psi. Using this value in the calculation worksheet, Table 5, a fluid efficiency of 0.69 was calculated from pressures and from the time-to close, the efficiency was 0.63. These are once again reasonably close, which would suggest that no secondary leak-off source was interfering with the analysis. For the later time closure, four scenarios were used for calculating leak-off coefficient. The first assumed a gross height of 135 ft. and a leak-off height of 25 ft., this lower leak-off height being reflective of only the upper sand open during most of the pressure decline. This resulted in a leak-

off coefficient of $0.003 \text{ ft/min}^{0.5}$. Changing leak-off height to 55 ft. resulted in a coefficient of $0.0014 \text{ ft/min}^{0.5}$, or very close to that determined by Sandia. The third scenario looked at the case where most of the fracture closed relatively quick in comparison to the upper sand, leaving only the 25 foot sand open. In this case the leak-off height was equal to the gross height of 25 ft. and a leak-off coefficient of $0.0001 \text{ ft/min}^{0.5}$ was calculated. The final case was for a gross and leak-off height of 55 ft., assuming that leak-off prior to closure of the lower sand contributed significantly to the character of the pressure decline. This resulted in a calculated leak-off coefficient of $0.00022 \text{ ft/min}^{0.5}$. At this point in the analysis, it became evident that using only the pressure decline analysis to determine leak-off coefficient in a complex zone such as the Paludal could be misleading in the conclusions drawn.

The third type curve analysis, Figure 25 and Table 6, assumed that even after shut-down, fluid was being squeezed from the higher stress intervals into the lowest stress interval (upper sand). In effect this would be the same as continued injection up to the point of closure in the lower sand at a shut-in time of 20.3 minutes. Thus, for this analysis, the pump time was the surface injection time of 43.1 minutes plus the early closure time of 20.3 minutes or a total injection time of 63.4 minutes. Also, this would reduce the later closure time from 148.5 to 128.2 minutes. To take this approach, would require that only the upper sand be contributing to leak-off; the leak-off height being fixed at 25 feet. Looking at two cases, a leak-off coefficient of $0.0025 \text{ ft/min}^{0.5}$ was calculated using a gross height of 135 ft. and a coefficient of $0.00009 \text{ ft/min}^{0.5}$ was determined for a gross height of 25 feet.

Table 7 is a summary of the eight possible cases looked at in performing the pressure decline analysis on the Paludal Minifrac #1 in MWX-1. From this it implies that the leak-off coefficient could be anywhere between 0.00009 and $0.003 \text{ ft/min}^{0.5}$, an impossible range for use in designing a fracture treatment. Some might be eliminated, though, with a certain degree of confidence. For instance, both of those values calculated for the early time closure (Cases 1 and 2) can be eliminated because it is of the belief that at least part of the fracture was still open for a much longer time. It is also unlikely that the gross "effective" fracture height during the pressure decline was 135 feet, most of the fracture having closed after a shut-in time of 20 minutes. Thus, Cases 3, 4, and 7 could be ruled out with some lesser degree of confidence. This would leave only Cases 5, 6, and 8, which are all around 0.0001 - $0.0002 \text{ ft/min}^{0.5}$ or an order-of-magnitude lower than calculated in previous analyses.

In analyzing this data, it was evident that the pressure

decline analysis is not without weakness in determining leak-off coefficient for complex stress conditions such as the Paludal and its surrounding layers. Coupled with history matching of the actual injection and decline pressures, though, it is still a powerful tool. In the history match, a wide range of leak-off values can be used to get an injection pressure history match simply with minor alterations in fluid viscosity and modulus (keeping these parameters realistic). But, the fluid efficiency and pressure decline must be consistent with the leak-off coefficient used. In the previous analysis, fluid efficiency was not considered. The following discusses the pressure history match of Minifrac #1.

MINIFRAC #1 PRESSURE HISTORY MATCH

Using the linear lithology correlation from the gamma-ray log (Figure 21) and the results from the pressure decline analysis, an attempt was made to history match the injection pressures recorded on the first Paludal minifrac in MWX-1. As discussed previously, the best estimate of leak-off coefficient from the pressure decline was 0.0001 to 0.0002 ft/min** 0.5 , with fluid efficiency somewhere in the range of 0.57 to 0.66 . Fluid properties for a non-crosslinked gel were obtained from Dowell's rheology manual¹³, these expected to be about the same for the linear gel system used for the minifrac. Prior to pumping the actual minifrac, 40 bbls of water, 60 bbls of methanol, and 140 bbls of gel were pumped; leaving the gel in the wellbore during a shut-down for a hammer test. The shut-in period was 1.5 hours or sufficient time for the gel to heat up and break. Following this assumption, very low viscosity fluid properties were used in the model to simulate early time minifrac injection pressures.

The initial attempt to match the minifrac injection pressures used a leak-off coefficient of 0.0001 ft/min** 0.5 . Only very minor modifications to the stress profile (Figure 26) were required in the fracture model to obtain the history match shown in Figure 27 and to match the results of the post-minifrac temperature log shown in Figure 28. This would indicate that, in fact, the treating pressures for Minifrac #1 were not abnormally high as indicated by the original analysis of this data; but, instead could be very closely explained using a more detailed analysis. The I/O for the computer model runs used to generate this and other matches in this report are included in the Appendix. Comparing the stress profile in Figure 26 to that in the previous Figure 21, the changes required were:

<u>Zone (ft)</u>	<u>Initial Stress (psi)</u>	<u>Revised Stress (psi)</u>
7015-7049	7560	7275
7049-7057	8600	7300
7057-7072	6840	6800
7147-7165	6860	7000
7165-7175	7820	8000

Of these changes, only the zone from 7049-7057 ft was significant, and this zone was relatively thin and directly below a thick coal bed. Minor modifications were also required to the modulus values. In the pay, modulus was increased from 3.8 to $4 \times 10^{**6}$ psi; and above and below the pay, modulus was decreased from 5 to $4.5 \times 10^{**6}$ psi - these changes being within log and laboratory measurement error of the values reported by Sandia.

Figure 29 shows the width profile generated for the pressure history match of Minifrac #1, the top and bottom of the fracture indicated at about 7045 and 7155 ft, respectively; or a modeled height of 110 ft as compared to Sandia's interpreted height of 135 ft from the post-frac temperature log. Figure 30 shows the comparison of the width profile and temperature log on the same scale. While not an exact match, the temperature log was run 22 hours after injection and only has a 10 degree variance over the fractured interval, leaving some room for interpretation.

To obtain the minifrac pressure history match required that the fluid efficiency calculated by the computer model match that determined in the pressure decline analysis, both from pressures and the time-to-close. For the $0.0001 \text{ ft/min}^{**0.5}$ case, the computer model predicted an efficiency of about 0.63. This is very close to the efficiency of 0.66 calculated for the pressure decline Case No. 5 shown in Table 7. This implies that most of the pressure decline was dominated by only leak-off to the lower stress, upper Paludal sand. To evaluate this further, an attempt was made to match the pressure decline. Leak-off coefficients of 0.0001, 0.0002, 0.0003, and $0.001 \text{ ft/min}^{**0.5}$ were evaluated as seen in Figure 31. While there is no good match with any one of these, several important observations can be made from the comparison. One, the leak-off coefficient is NOT $0.0014 \text{ ft/min}^{**0.5}$ as suggested by the previous analysis, the projected decline for this coefficient being much steeper. Also, using this high of a leak-off coefficient in the computer model results in a fluid efficiency of less than 0.2, NOT consistent with the pressure decline analysis efficiency of 0.66.

A second observation from Figure 31 was that the early time actual data, i.e. less than about 20 minutes or the early closure time observed in Figure 20, seemed to decline faster than predicted for the 0.0001-0.0003 coefficients. Beyond 20

minutes, the actual decline, while 150-200 psi lower, seemed to parallel the $0.0001 \text{ ft/min}^{0.5}$ curve. One might hypothesize from this that early in the decline, before the lower Paludal sand closed at 20 minutes, that the "effective" leak-off coefficient was higher than $0.0001 \text{ ft/min}^{0.5}$. This would cause the faster decline seen early in the data. How much higher this early leak-off value is, though, can not be determined. One might only speculate at what would cause such behavior. Two reasons are most apparent, these being 1) higher leak-off in the lower Paludal sand and/or 2) crossflow from the higher stress sand to the lower stress sand. From the pressure decline analysis, there did not appear to be any significant leak-off to a secondary source such as natural fissures, the efficiencies calculated from pressures and time-to-close being very close. Thus, while not impossible, one would not expect the lower Paludal sand to have natural fissures while the upper sand did not. Assuming that both sands were relatively free of fissures and that leak-off in the lower sand was also $0.0001 \text{ ft/min}^{0.5}$, then crossflow could explain the behavior seen. With the stress in the lower sand 600 psi higher than the upper sand, flow from the lower sand into the upper sand, via the wellbore (or possibly the open fracture), would create the same effect as continued injection into the upper sand. Looking at this case in Table 7, Case 8, a leak-off coefficient of $0.00009 \text{ ft/min}^{0.5}$ was calculated. While the efficiency of 0.57 is slightly lower than the model projected value, it is still within the range of an acceptable match.

From this analysis and discussion, there is still some question as to the actual leak-off rate during injection. Most likely it was on the order of 0.0001 to $0.0002 \text{ ft/min}^{0.5}$ for both Paludal sands. This would be consistent with the core analysis which did not see any natural fissures and calculated permeabilities in the 1-3 microdarcy range. It becomes quite apparent, though, that the pressure decline analysis has limitations when used alone to analyze pressure data obtained in a non-uniform, complex stress distribution. To avoid misinterpretation, both leak-off coefficient and fluid efficiency must be consistent in the pressure decline analysis and the history matching of injection/decline pressures. The following history matching of Minifrac #2 and the main fracture treatment on the Paludal zone in MWX-1 will lend support to this analysis.

MWX-1, MINIFRAC #2 - PALUDAL ZONE

The second minifrac conducted in the Paludal zone in MWX-1 consisted of pumping 30,000 gals (twice the volume pumped on the first minifrac) of 60 lbs/1000 gals un-crosslinked gel, a more viscous fluid. The average injection rate was 10 BPM, the same as the first minifrac.

MINIFRAC #2 PRESSURE DECLINE ANALYSIS

Figure 32 shows plots of bottomhole pressure versus time for the injection/decline and pressure decline versus the square root of shut-in time. From the square root plot there does not appear to be any indication of closure, as would be expected since the decline only reached a bottomhole pressure of 6529 psi or over 100 psi above the lower Paludal sand closure of 6400 psi.

To analyze the pressure decline from the second minifrac, the available data was type curve matched as shown in Figure 33 resulting in a P^* match pressure of 103 psi. This is relatively close to Sandia's match pressure of 120 psi. As with the analysis of the first minifrac, multiple combinations of gross to leak-off height were investigated. Figure 34 is the post-minifrac temperature log which shows a gross created height of 150 feet. Using 55 ft for the total Paludal leak-off height and 25 ft for leak-off height in the upper sand only, three different cases were looked at as presented in Table 8. The first assumes that the entire fracture (135 ft) remains open throughout the entire pressure decline and that both Paludal sands (55 ft) are also open during the entire decline. This results in a calculated leak-off coefficient of 0.0006 ft/min**0.5, or very close to that calculated by Sandia. The second case looked at having only the Paludal sands open during the decline, i.e. the higher stress boundary layers closing very quick after shut-down of injection. Using 55 ft for both gross and leak-off height, a leak-off coefficient of 0.00008 ft/min**0.5 was calculated. Suspecting that the lower sand closed early in the decline, the third case looked at a gross and leak-off height of 25 ft (the upper sand only). This resulted in a calculated leak-off coefficient of 0.00004 ft/min**0.5.

Case 1 in Table 8 is not thought to be a realistic assumption, the higher stress shales and siltier boundary layers expected to close very quick after shut-down squeezing their fluid back into the Paludal sands. Thus, the higher leak-off coefficient of 0.0006 is not thought to be correct. Instead, one of the lower values is thought to be more representative of what actually happened based on the results of the first minifrac pressure decline analysis and history match.

MINIFRAC #2 PRESSURE HISTORY MATCH

To history match the second Paludal minifrac, the revised stress profile in Figure 26 (also used to obtain the history match of Minifrac #1) and a leak-off coefficient of 0.0001 ft/min**0.5 was used. Rheology data for the 60 lb non-crosslinked gel was obtained from the service company manuals.

As on the first minifrac, the actual minifrac was preceded by pumping a methanol prepad and flushing part way with the gel before shutting down for a water hammer test. On this particular test, 3800 gals of gel was pumped into the wellbore prior to the shut-down and remained static for 71 minutes. With the total flush volume being about 8400 gals, this put gel about midway down the hole. The temperature at this point would be great enough to break the un-crosslinked gel in this time period, this being evident in the low initial treating pressures on both minifracs. Thus, a stage of lower viscosity gel was included in the model to simulate this initial condition.

The pressure history match of Minifrac #2, shown in Figure 34, was obtained with only minor adjustments to the viscosity data. No adjustments were required in the stress profile or any of the other input parameters. Once again, the computed net treating pressure very closely matched the actual measurements; indicating that, in fact, the treating pressures were NOT abnormally high as suggested by previous analysis.

Figure 35 shows the width profile computed by NSI's model at the end of injection of the minifrac. This shows the top of the fracture at 7025 ft and the bottom at about 7165 ft, for a total created height of 140 feet. This is very close to the temperature log interpretation shown in Figure 36. While the estimated height from the temperature log is slightly greater, i.e. 150 ft, the top and bottom of the modeled fracture are within a few feet of the chosen fracture top and bottom. This lends confidence to the stress profile and model used to perform this simulation, and supports the re-analysis of the data from the first minifrac.

The pressure decline following the minifrac was also compared to the computer model predicted declines for various leak-off coefficients. This is shown in Figure 37. As this same type analysis showed on the first minifrac, the leak-off coefficient could not have been nearly as high as calculated in the previous analysis, i.e. $0.0007 \text{ ft/min}^{0.5}$. In fact, it is only early in the actual decline data that the leak-off coefficient seems to track the $0.0002 \text{ ft/min}^{0.5}$ curve. Beyond about 50 minutes, the actual decline is much slower and more characteristic of a coefficient between 0.00005 and $0.0001 \text{ ft/min}^{0.5}$. As mentioned for the first minifrac, these lower values would be more consistent with the core analysis which showed no natural fissures and permeabilities in the 2-3 microdarcy range.

To summarize, a detailed stress profile has been generated that has been used to history match the net treating pressures for both minifracs performed in the Paludal zone in MWX-1. While the pressure decline type curve analysis provided a wide range of possible leak-off coefficients, the fluid efficiency determined from pressures and the time-to-close was consistent

with the lower values, i.e. $0.0001 \text{ ft/min}^{0.5}$ on Minifrac #1 and $0.00005-0.0001 \text{ ft/min}^{0.5}$ on Minifrac #2. Also, the actual decline pressures were characteristic of these lower values. Based on the decline analysis and history matching of injection and decline pressures, there is no indication that the leak-off coefficients are nearly as high as those calculated in the previous analysis. In addition, the model generated injection pressures are very close to the actual measured pressures; this contradicting the charge of abnormally high treating pressures on all Paludal fracturing tests. In fact, modeling of the actual pressures was relatively straight forward, given a few minor adjustments to the original stress profile. This profile and the other parameters generated in this study are tested further in the following history match of the main propped fracture treatment pumped in the same Paludal zone.

PRESSURE HISTORY MATCH OF PROPPED FRACTURE TREATMENT

The propped fracture treatment performed in the Paludal zone of MWX-1 consisted of pumping the schedule shown in Table 9 at an average injection rate of 20 BPM. The treatment was pumped down the annulus of 7 inch, 29 lb casing and 2-7/8 inch tubing, with an HP pressure transducer hung in the tubing at 6700 ft to monitor bottomhole treating pressure. Three planned shut-downs were performed during the pad stage to measure the instantaneous shut-in pressure for use in performing Nierode's leak-off analysis. These occurred after pumping 8,000, 12,000, and 17,000 gals of pad into the formation. One other "unexpected" shut-down occurred after having pumped 104 bbls of pad into the wellbore, this due to trouble with the bottomhole pressure processor. This left gel in the hot wellbore for 40 minutes, probably time enough for the gel to break. Thus, in the following simulations, the early pad fluid was modeled with lower viscosity.

Figure 38 shows the Nolte-Smith log-log plot of the net bottomhole treating pressure (BHTP-5890) versus time for the fracture treatment, time zero being the time when gel was on the perforations after the unexpected 40 minute shut-down. All fluid injected into the formation prior to this (water and methanol) was thought to have leaked-off during the shut-in period. As shown by the figure, at about 50 minutes the net BHTP started increasing at an abnormal rate indicating that fracture extension had stopped. Attempts to history match this abnormal behavior were unsuccessful. Figure 39 shows the best pressure history match obtained, using a leak-off coefficient of $0.0001 \text{ ft/min}^{0.5}$ and the same stress profile used to history match the minifrac. The crosslinked gel used should have resulted in an even lower leak-off rate than the uncrosslinked gels used on the minifrac. This made improbable the possibility of an early screen-out due to excessive leak-off and attention was turned to looking at other possible

causes.

To evaluate why the abnormally increasing pressure was not observed on the minifrac, the pressures for the two minifrac and the main fracture treatment were compared on a volume basis. As shown in Figure 40, all three injections tracked each other very close, with the BHTP increasing with each subsequent injection as would be expected due to increasing fluid viscosity. This figure shows that the amount of fluid pumped on the minifrac was insufficient to reach the point at which the pressure started increasing on the main treatment.

Looking at how far proppant had traveled after 50 minutes of injection, the simulator predicted a propped length of about 300 feet. Comparing this to the estimated sand geometry in Figure 41 for Paludal Zones 3 and 4, it could be postulated that the proppant reached the outer boundaries of the sand splay and/or the channel and the stress of the shalier rock beyond this point was high enough to restrict fracture width and cause proppant bridging. This would not necessarily stop the fluid, though, from continuing to extend the fracture far beyond this point as suggested by the modeled lengths of the minifrac. If, in fact, the azimuths shown are reasonably accurate, then the proppant would have reached the boundary of the channel first in the upper Zone 3 sand and effectively "screened-out", causing most of the treatment to then go into the lower sand. With the lower sand having a 600 psi higher stress than the upper zone, the injection pressure would then start to increase at a higher rate. It would again be expected, though, to level off at a more reasonable slope for a confined height, unrestricted extension fracture, i.e. 1/8 to 1/4 slope. This behavior was not observed and could be because proppant reached the outer boundaries of the splay shortly after reaching the channel boundaries.

In an attempt to simulate the increasing pressures using the limited sand lens theory, the modeled fracture was forced to screen-out at about 50 minutes to observed what the predicted pressure increase would look like. As seen in Figure 42, with the entire fracture screened-out, the pressure increases even faster than observed. This lends support to the theory that the fracture stopped growing in only one zone, and possibly in only one fracture wing in one zone, followed by additional periodic wing screen-outs in the other zone.

The post-frac pressure decline could not be meaningfully analyzed as such because of the abnormally high pressures in the later portion of the treatment and the likelihood of insufficient breaker added to the gel. At 200 degrees F, the 40 lb. crosslinked gel will not break very readily and the rate of pressure decline will be very low, i.e. much lower than observed on the minifrac. The attempted post-frac pressure decline type curve analysis performed in the previous analysis¹² may have seen a part of the fracture close, but not the major

portion. Their calculated leak-off coefficients of 0.0012-0.0015 ft/min**0.5 are inconsistent with their reported fluid efficiency of 0.74. In the history match of the injection pressures using a leak-off coefficient of 0.0001 ft/min**0.5 (Figure 39), the model predicted fluid efficiency was about 0.85. Using a coefficient of 0.001 would have resulted in an efficiency of about 0.2 as shown earlier in the modeling of the minifrac. The very slow post-frac pressure decline was not consistent with their high leak-off coefficients.

Figure 43 shows the post-frac temperature log run 28 hours after frac. As interpreted by Sandia, the fracture top was at about 7000 feet. Due to sand fill in the wellbore, the tool could not be lowered below 7087 ft to see the bottom of the fracture. In comparison, NSI's model predicted height (Figure 44) for the history match case in Figure 39 showed the fracture top and bottom to be at about 6985 ft and 7175 ft, respectively; or a total created height of about 190 feet. This is consistent with the limited borehole seismic signals obtained, which all fell within a 200 ft height window.¹²

To summarize, the stress profile used to model both minifrac seemed to also explain very closely the results of the main fracture treatment. The high rate of pressure increase at the end of the treatment is not thought to have been caused by a screen-out in the conventional sense, i.e. higher than expected leak-off and dehydration of fluid from the slurry. Instead, the high pressure is thought to have been caused when proppant reached the outer boundaries of the sand lens structures; the fracture continuing to grow outside these boundaries, but the width pinching down at this point. The pressure decline data was of little use in trying to determine a leak-off coefficient because of the complicated nature of the fracture at the end of injection and the apparent gel breakage problems. Any analysis of this data would be highly suspect. The fluid efficiency of 0.74, determined in the previous analysis, was inconsistent with their high calculated leak-off values. And finally, in re-analyzing the data, the simulation of the net BHTP, prior to the abnormal pressure increase, was very close to actual measurements; indicating once again that the pressures during the Paludal fracturing tests and the fracture treatment were about what should have been expected. This is further supported by the compared results of the post-frac temperature log and the model predicted height, as well as the results of the limited borehole seismic data.

CONCLUSIONS

The re-analysis of the Paludal stress data, plotting pressure versus the square-root of shut-in time, showed reasonably good agreement with the previous stress results estimated from the ISIP's. The square-root of time method, though, was generally superior; yielding clearer, more definitive results. Using stress data from the Paludal, Coastal, Fluvial, and Marine zones; good correlations were found to exist between in situ stress and lithology (gamma-ray log) and acoustic velocity (sonic log). The superior lithology correlation provided a detailed stress profile for fracture modeling of the Paludal minifrac and main propped fracture treatment.

In analyzing the two minifrac, it was evident that the pressure decline type curve analysis has certain limitations. In a complex stress environment, such as the Paludal and surrounding beds, multiple closures (occurring at different times during the decline) must be considered and what effect this has on the fractures' gross and leak-off heights used in the leak-off calculations. The leak-off values determined in the re-analysis, using both the type curve analysis and history matching of the injection and decline pressures, were an order of magnitude lower than the previous analysis reported.

The model history matching of the two minifrac and main treatment revealed that the injection pressures were not abnormally high as previously charged. In fact, the analysis was reasonably straight forward, given minor adjustments to the derived stress profile and service company rheology data. The main difference in this and the previous analysis was the use of a more detailed stress profile, the lower leak-off values not having a significant effect on the model predicted injection pressures.

The results of the modeling of the Paludal fracture treatment suggested that the propped portion of the fracture did not extend beyond the boundaries of the sand lens, this being consistent with the estimated Paludal sand geometry at the MWX site. This type behavior is not unique; a similar undocumented case being experienced in a limited sand lens in the Uinta Basin. In this particular case, the abnormally increasing pressure was observed at the end of a minifrac (i.e. no proppant to bridge). The modeled length of the fracture at the point of the start of abnormally increasing pressure closely agreed with the radius of investigation calculated from pressure transient analysis; and was also verified with the behavior of the main treatment, which screened-out shortly after sand reached the outer extremity of the lens. These two cases would seem to indicate a high degree of difficulty associated with extending a propped fracture beyond the

boundaries of a sand lens. Even if a propped fracture could be extended through the higher stress rock between the sand lenses, the proppant in this region would likely be squeezed back into the lenses during closure, leaving little or no conductivity to interconnect the lenses with the wellbore. Thus, the limited size and reserves of each lens becomes a very important economic consideration for completing and stimulating this unconventional gas source.

The results of this re-analysis study are in no way intended to discourage the exploitation of tight gas resources from lenticular sandstones. If anything, it points out the need for further study of this unconventional energy source.

REFERENCES

1. Sandia National Laboratories: Multiwell Experiment Final Report: II. The Paludal Interval of the Mesaverde Formation, Sandia Report SAND88-1008, UC-92, May, 1988.
2. Kehle, R.O.: "The Determination of Tectonic Stresses Through Analysis of Hydraulic Well Fracturing," J. of Geophysical Research, Vol. 69, No. 2, Jan. 15, 1964.
3. McLennan, J.D. and Rogiers, J.C.: "How Instantaneous Are Instantaneous Shut-In Pressures," SPE 11064 presented at 57th Ann. Conf. of SPE, New Orleans, LA., Sept. 26-29, 1982.
4. Warpinski, N.R.: "Investigation of the Accuracy and Reliability of In Situ Stress Measurements Using Hydraulic Fracturing in Perforated Cased Holes," Proceedings 24th U.S. Symposium on Rock Mechanics, June, 1983.
5. Warpinski, N.R., Branagan, P., and Wilmer, R.: "In Situ Stress Measurements at DOE's Multi-Well Experiment Site, Mesaverde Group, Rifle, Colorado," SPE 12142 presented at 58th Ann. Conf. of SPE, San Francisco, CA., Oct. 5-8, 1983.
6. Smith, M.B.: MWX Stimulation Data Review, Topical Report: In Situ Stress Analysis, NSI Report No. 80709S, DOE Contract No. DE-AC21-87MC24264, July, 1988.
7. Nolte, K.G.: "Determination of Fracture Parameters From Fracturing Pressure Decline," SPE 8341 presented at 54th Ann. Conf. of SPE, Las Vegas, Nevada, Sept. 1979.
8. Nolte, K.G.: "Fracture Design Considerations Based on Pressure Analysis," SPE 10911 presented at 1982 Cotton Valley Symposium, Tyler, TX., May 20.
9. Warpinski, N.R. and Teufel, L.W.: "In Situ Stresses in Low-Permeability, Nonmarine Rocks," SPE/DOE 16402.
10. Breckels, I.M. and Van Eekelen, H.A.M.: "Relationship Between Horizontal Stress and Depth in Sedimentary Basins," SPE 10336 presented at 56th Ann. Conf. of SPE, San Antonio, TX., Oct. 5-7, 1981.
11. Veatch, R.W., Jr., and Moschovidis, Z.A.: "An Overview of Recent Advances in Hydraulic Fracturing Technology," SPE 14085 presented at 1986 SPE International Mtg., Beijing, China, March 17-20, 1986.

12. Warpinski, N.R., Branagan, P.T., Sattler, A.R., Lorenz, J.C., Northrop, D.A., Mann, R.L., and Frohne, K.H.: "Fracturing and Testing Case Study of Paludal, Tight, Lenticular Gas Sands," SPE/DOE 13876 presented at Low-Permeability Gas Reservoirs Symposium, Denver, CO., May 19-22, 1985.
13. Fracturing Fluids Design Data, Dowell Schlumberger, August, 1986.

FIGURES AND TABLES

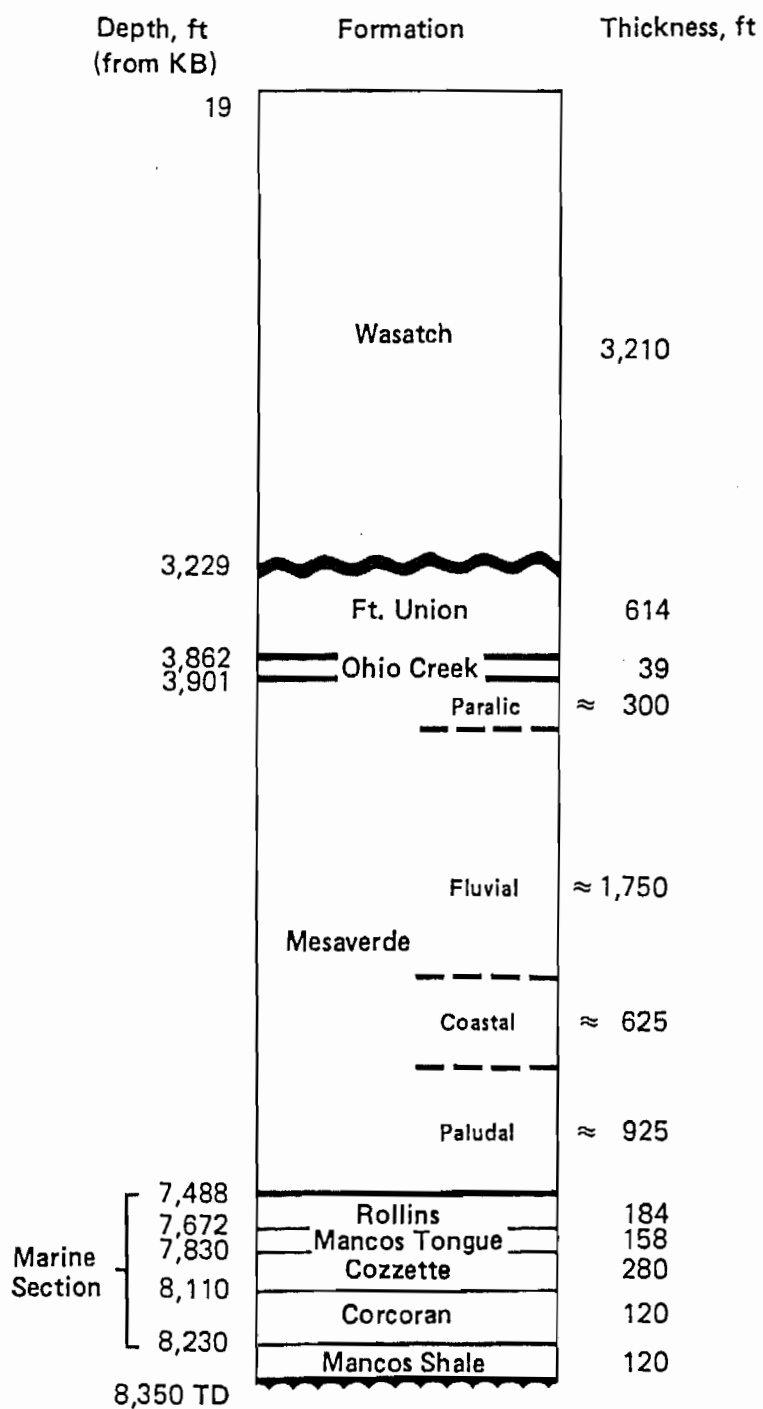


FIGURE 1: Geologic Cross-Section of MWX-1.

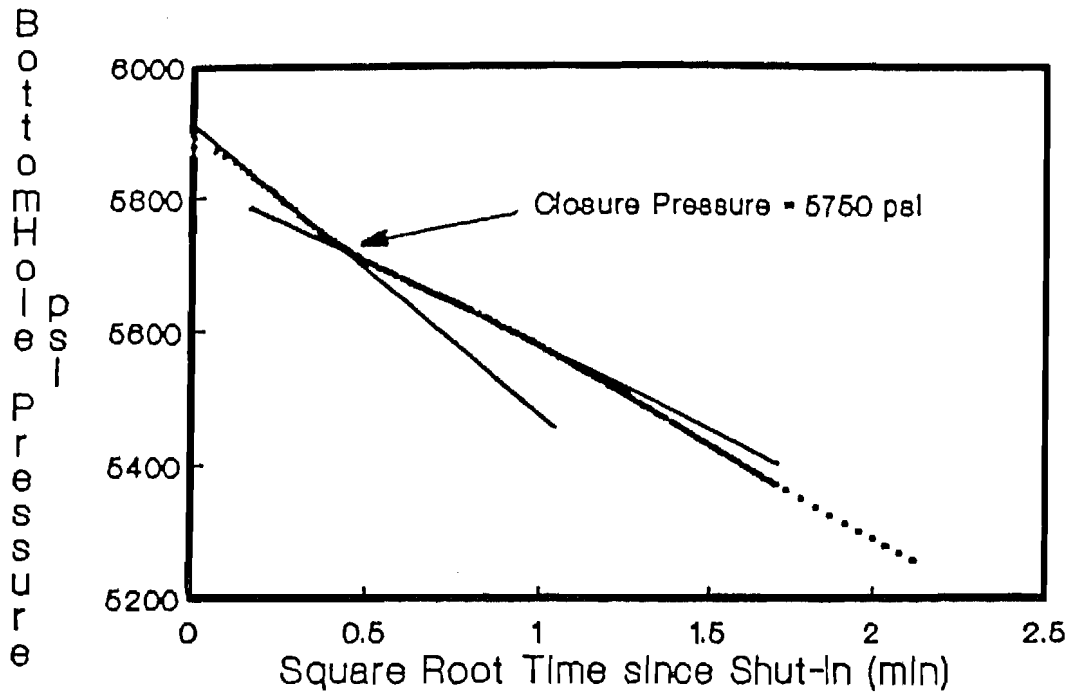


FIGURE 2: Pressure Decline Plot (vs. Square Root Time), Test 1, Zone 2P2.

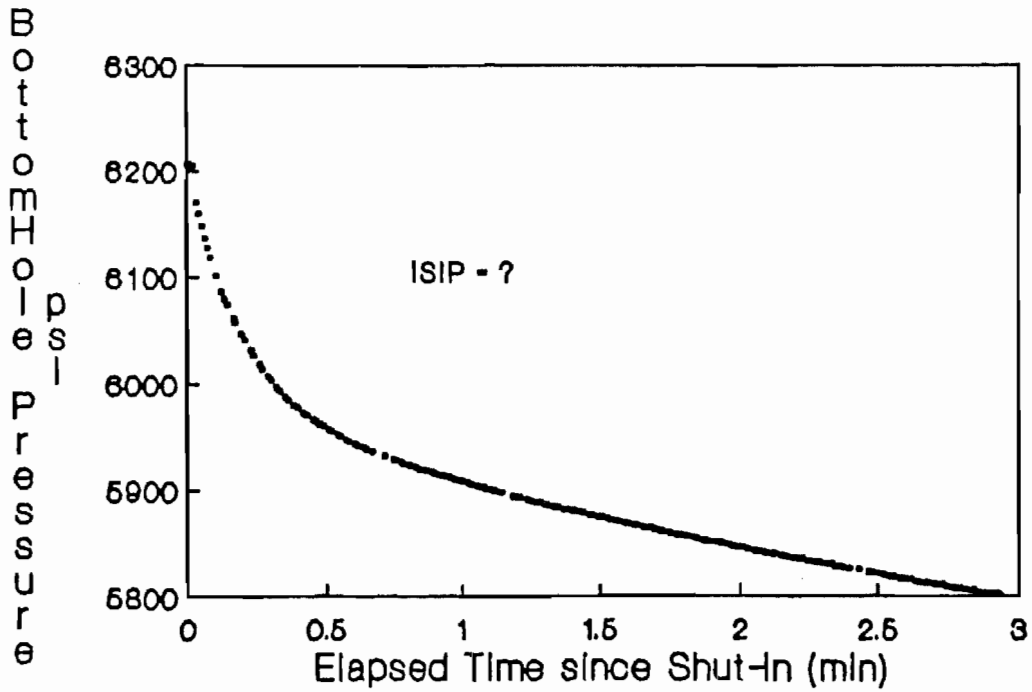
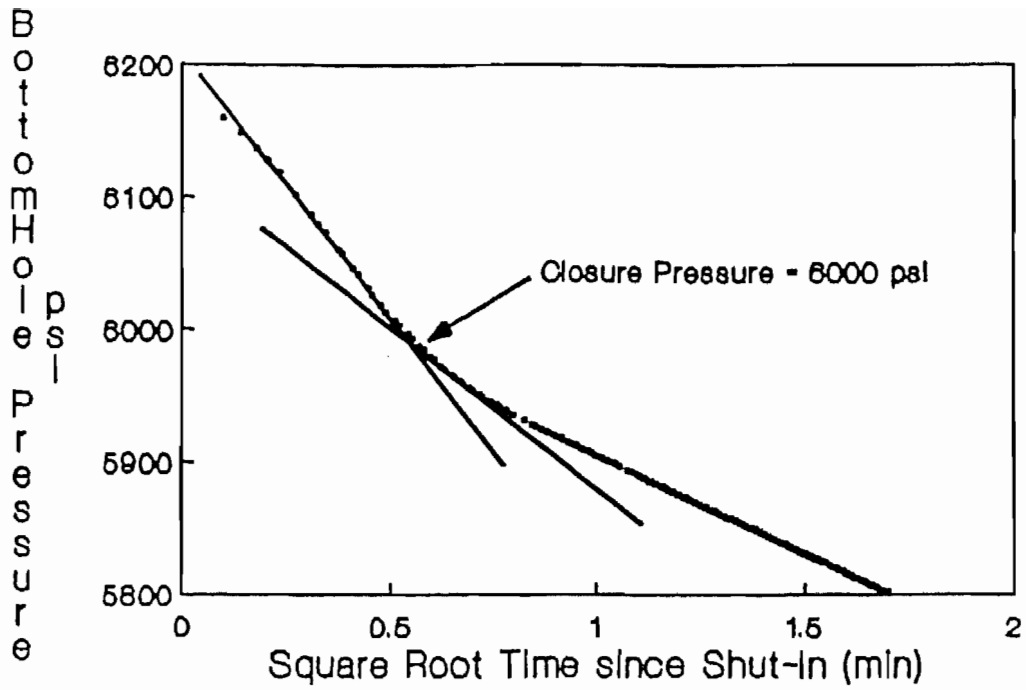


FIGURE 3: Comparison of Square Root Time Plot Vs. Linear Plot for Determining Closure Stress, Test 4, Zone 2P2.

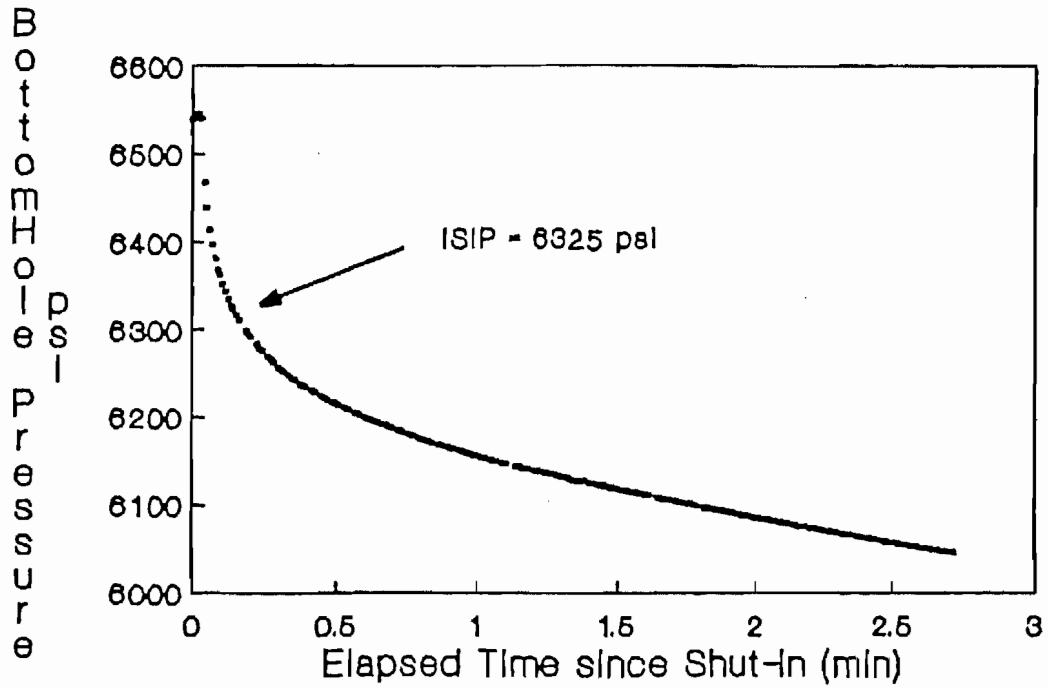
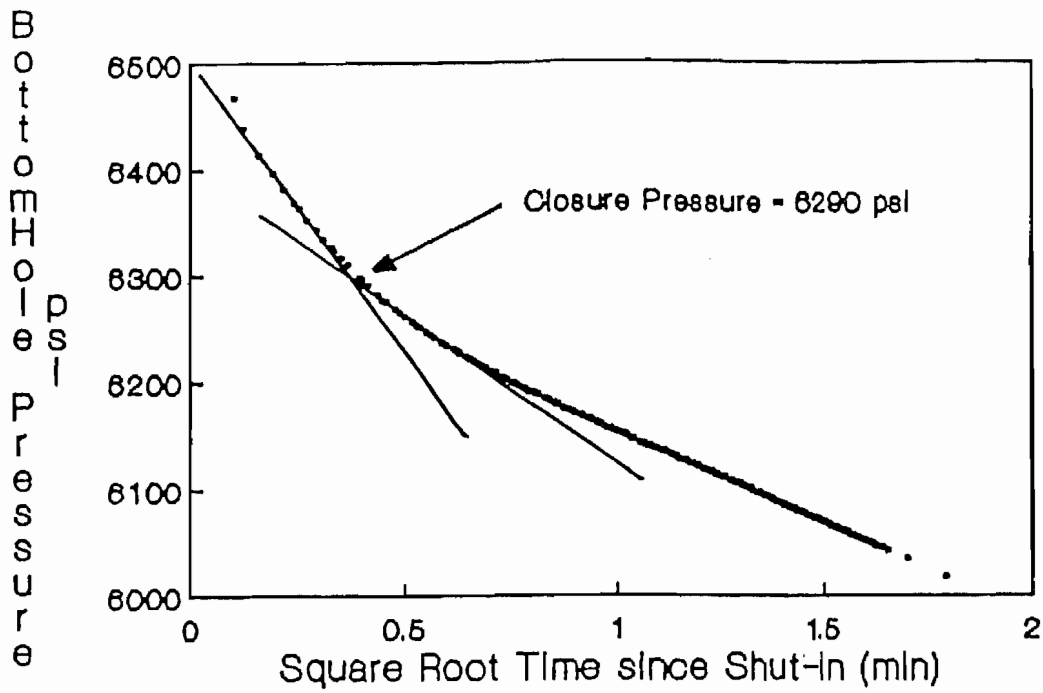


FIGURE 4: Comparison of Square Root Time Plot Vs. Linear Plot for Determining Closure Stress, Test 3, Zone 2P3.

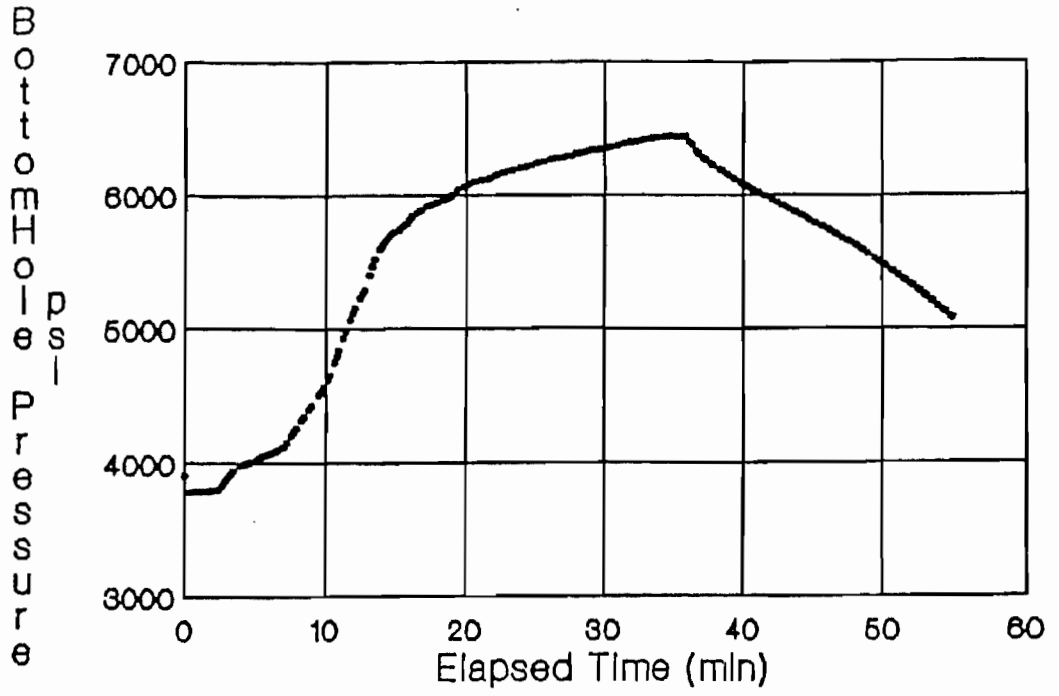


FIGURE 5: Pressure Vs. Time for the Step-Rate/Flowback Test in the MWX-1 Paludal Frac Zone.

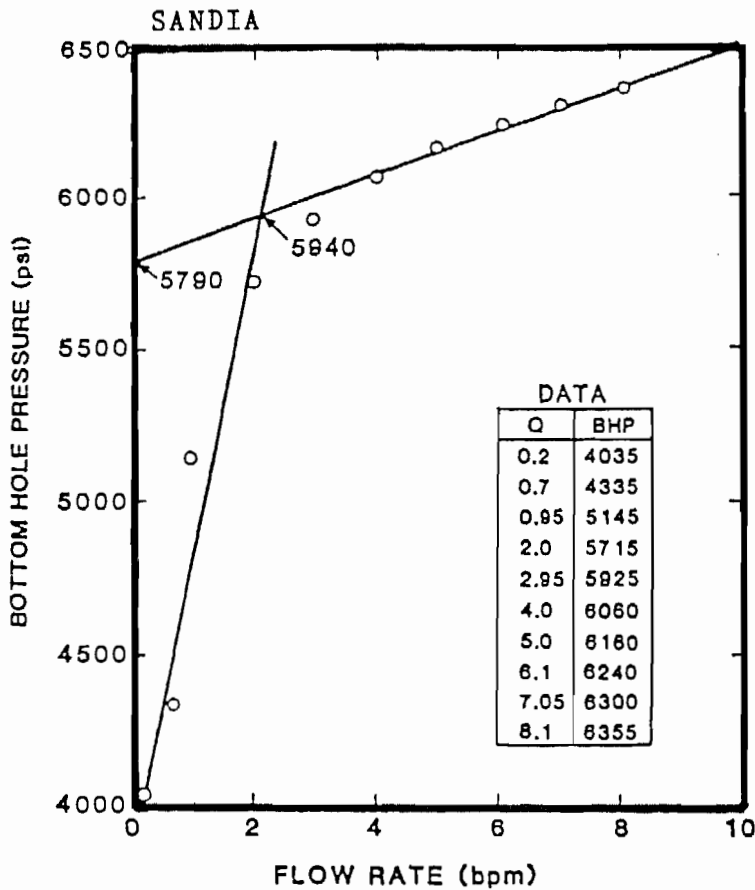
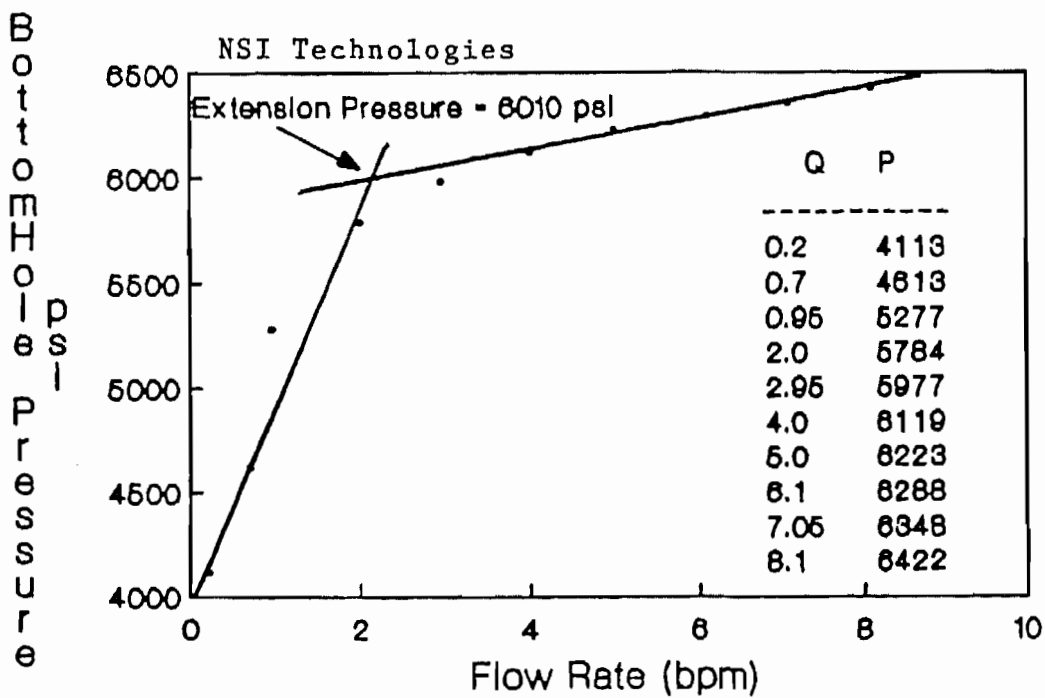


FIGURE 6: Analysis of Step-Rate Injection on Paludal Frac Zone in MWX-1.



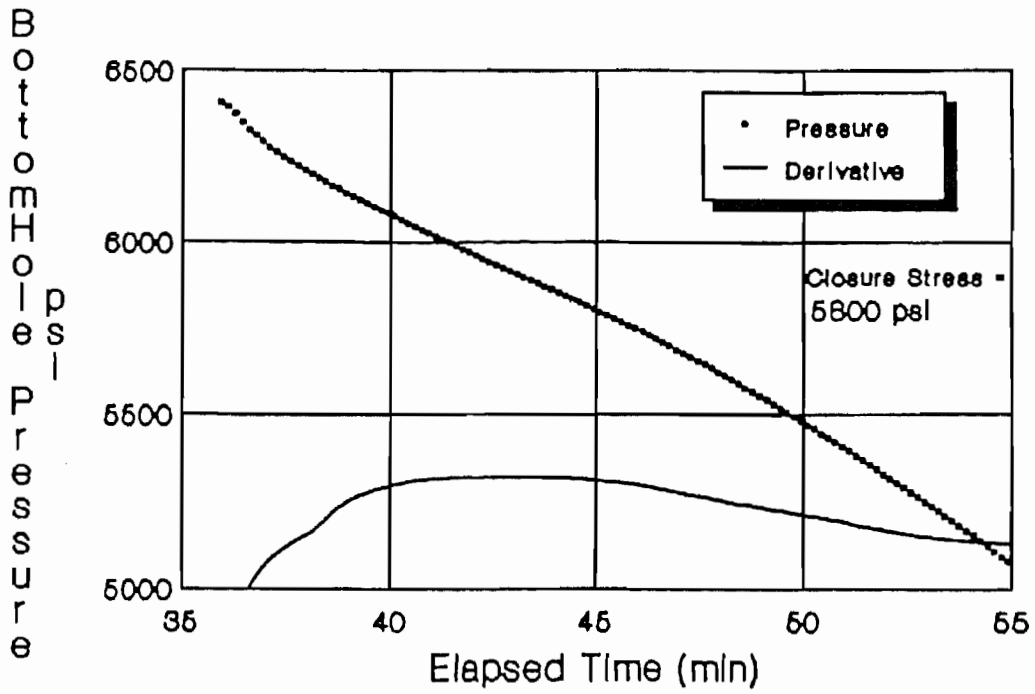


FIGURE 7: Plot of Pressure and Pressure Derivative Versus Time for the First Flowback Test, MWX-1 Paludal Frac Zone.

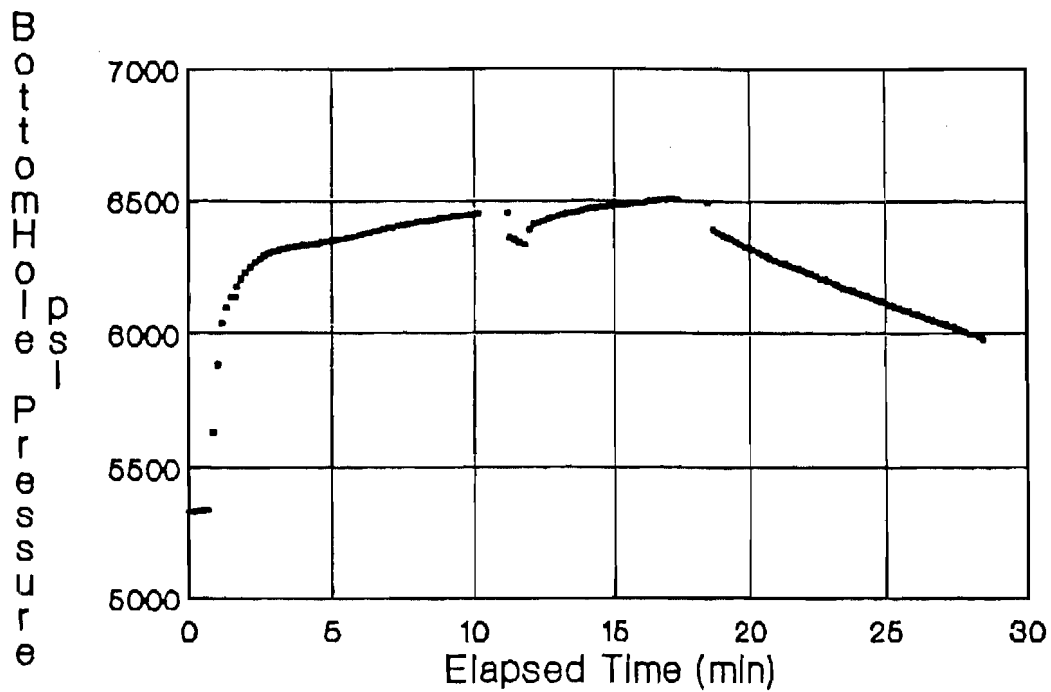


FIGURE 8: Pressure Versus Time for the Pump-In/Flowback Test in the MWX-1 Paludal Frac Zone.

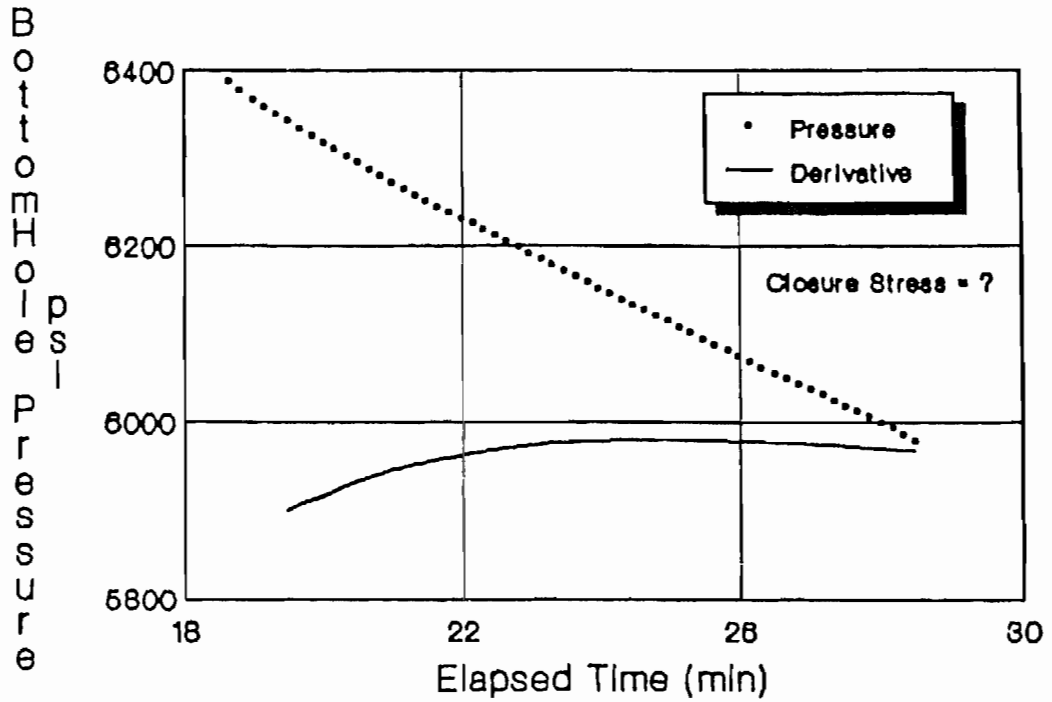


FIGURE 9: Plot of Pressure and Pressure Derivative Versus Time for the Second Flowback Test in the MWX-1 Paludal Frac Zone.

NSI VERSUS SANDIA FRAC GRADIENTS PALUDAL PRESSURE DATA

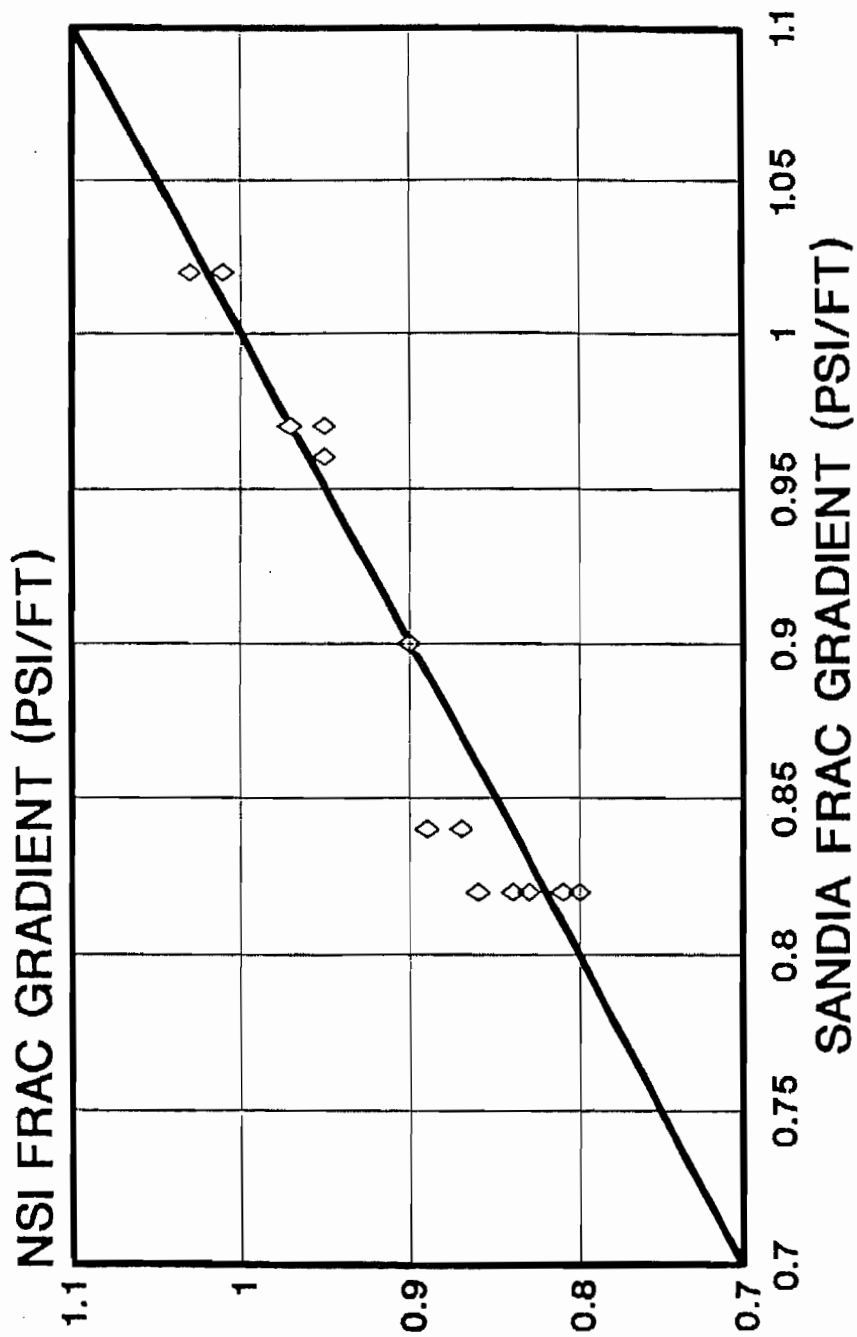


FIGURE 10: Comparison of NSI and Sandia Frac Gradients for MWX Paludal Test Zones.

K FACTOR vs. GAMMA RAY

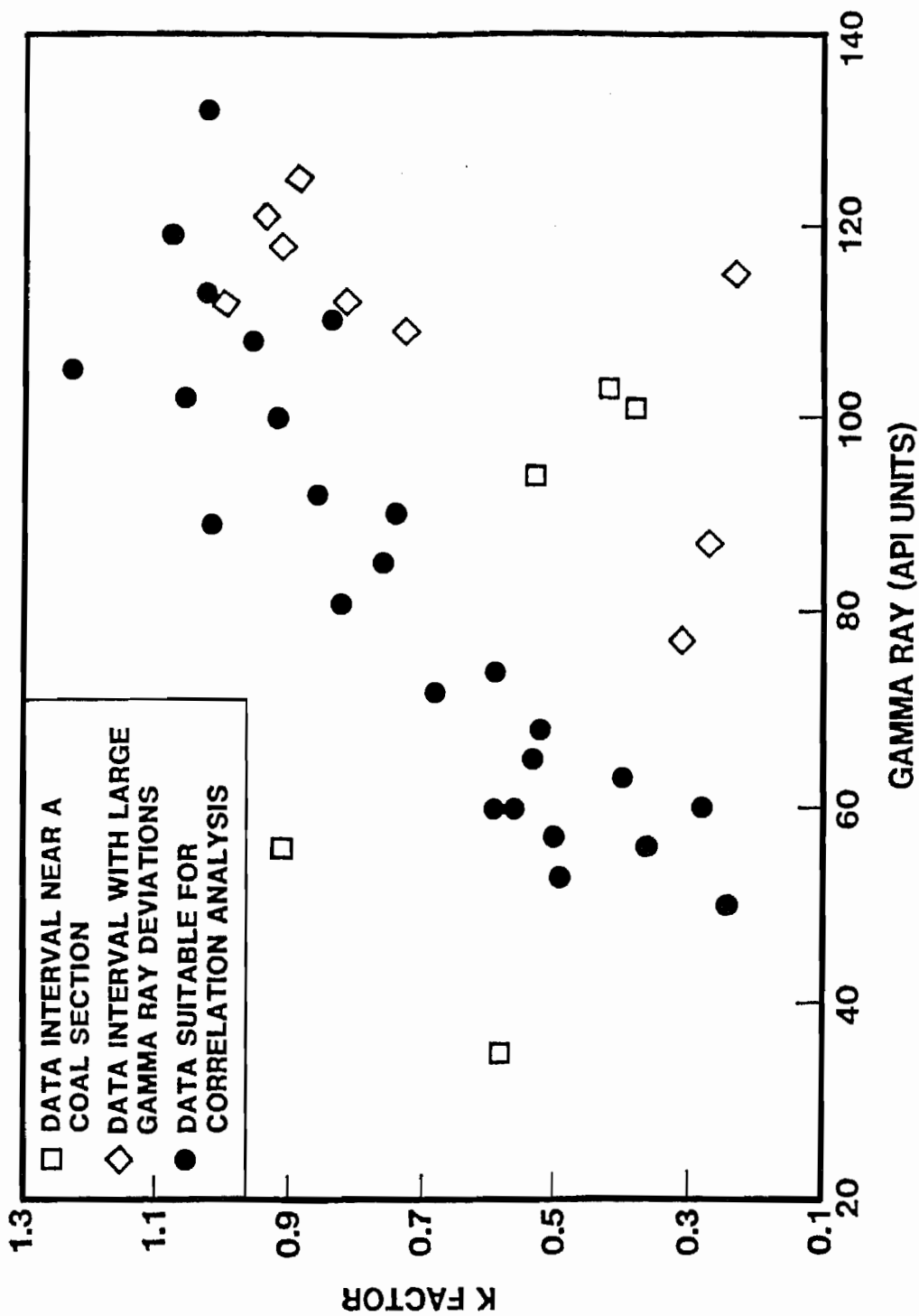


FIGURE 11: K Factor (Based on Measured Stress Results) Versus Mean Gamma Ray for all Test Zones.

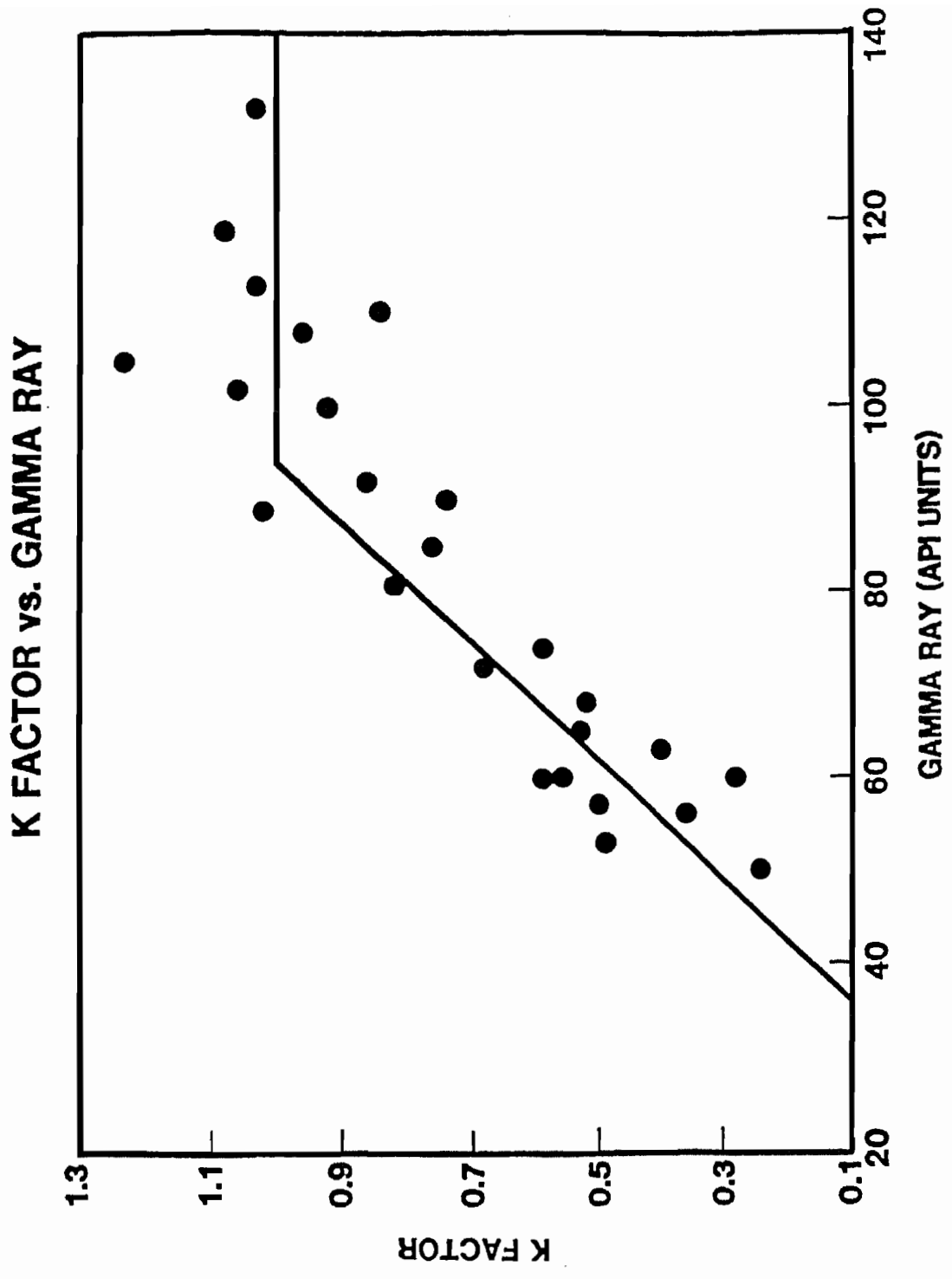


FIGURE 12: K Factor Versus Gamma Ray Showing Bilinear Correlation.

FRAC GRADIENT COMPARISON (LINEAR CORRELATION)

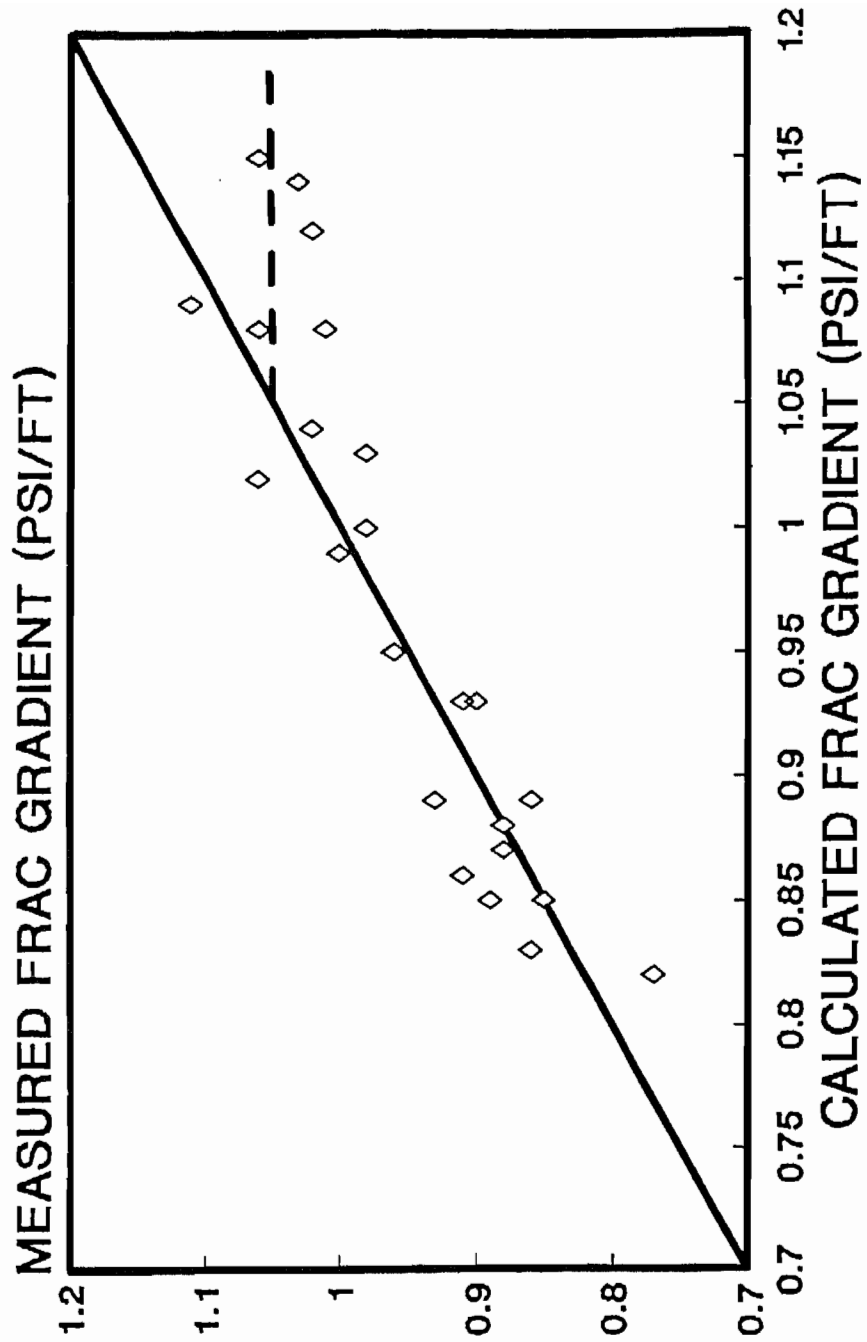


FIGURE 13: Measured Frac Gradient vs. Frac Gradient Calculated from the Linear K/GR Correlation.

FRAC GRADIENT COMPARISON (LINEAR CORRELATION)

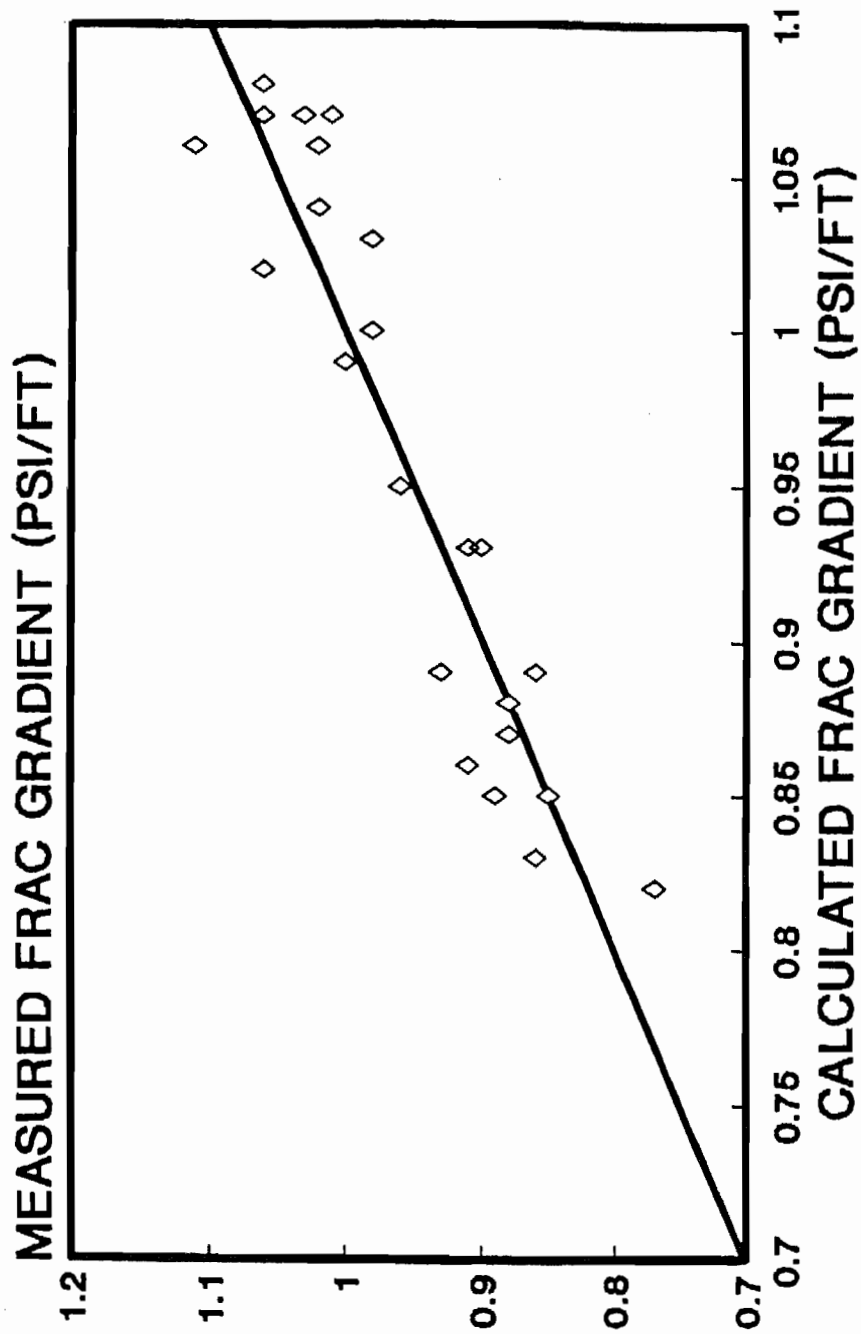


FIGURE 14: Measured Frac Gradient vs. Frac Gradient Calculated from the Bilinear K Factor/GR Correlation.

MEASURED K vs. SONIC LOG K

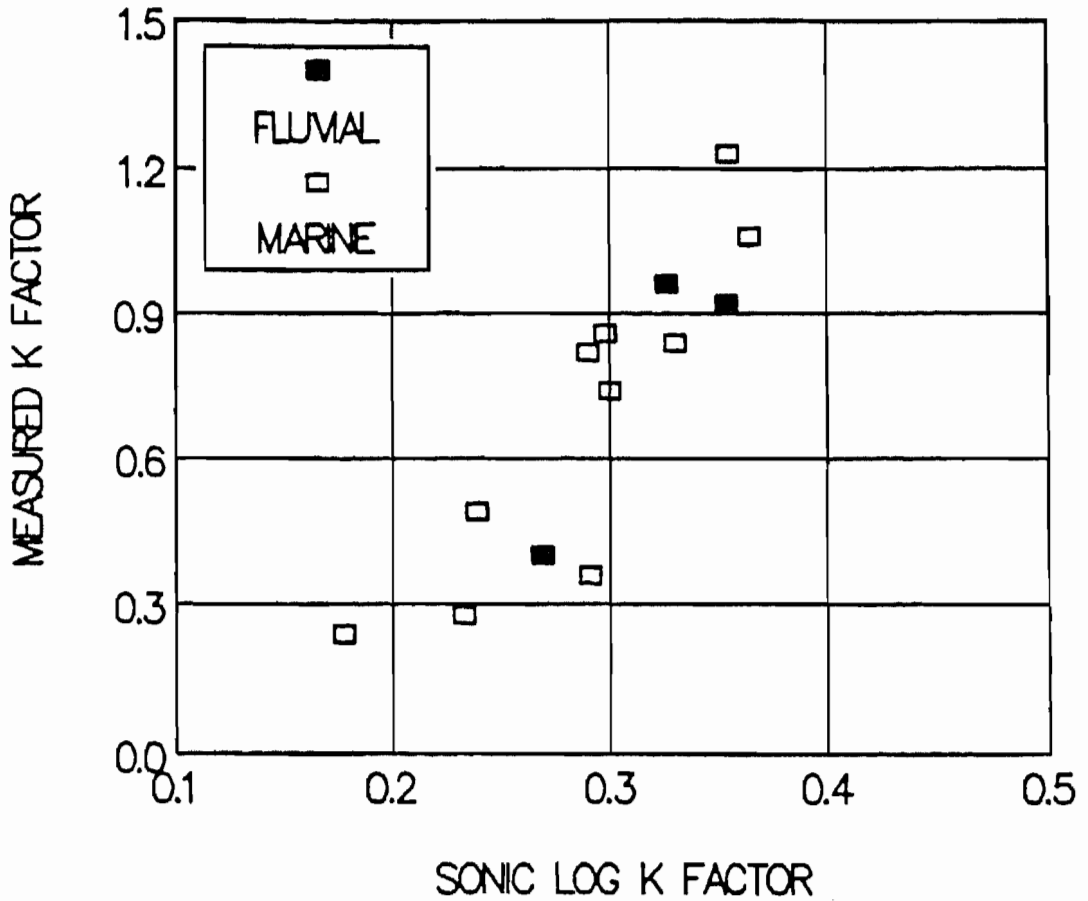


FIGURE 15: Measured K Factor vs. K Factor Calculated from the MWX-2 Sonic Log for the Combined Fluvial and Marine Zones.

FRAC GRADIENT COMPARISON
(MEASURED vs. CALCULATED)

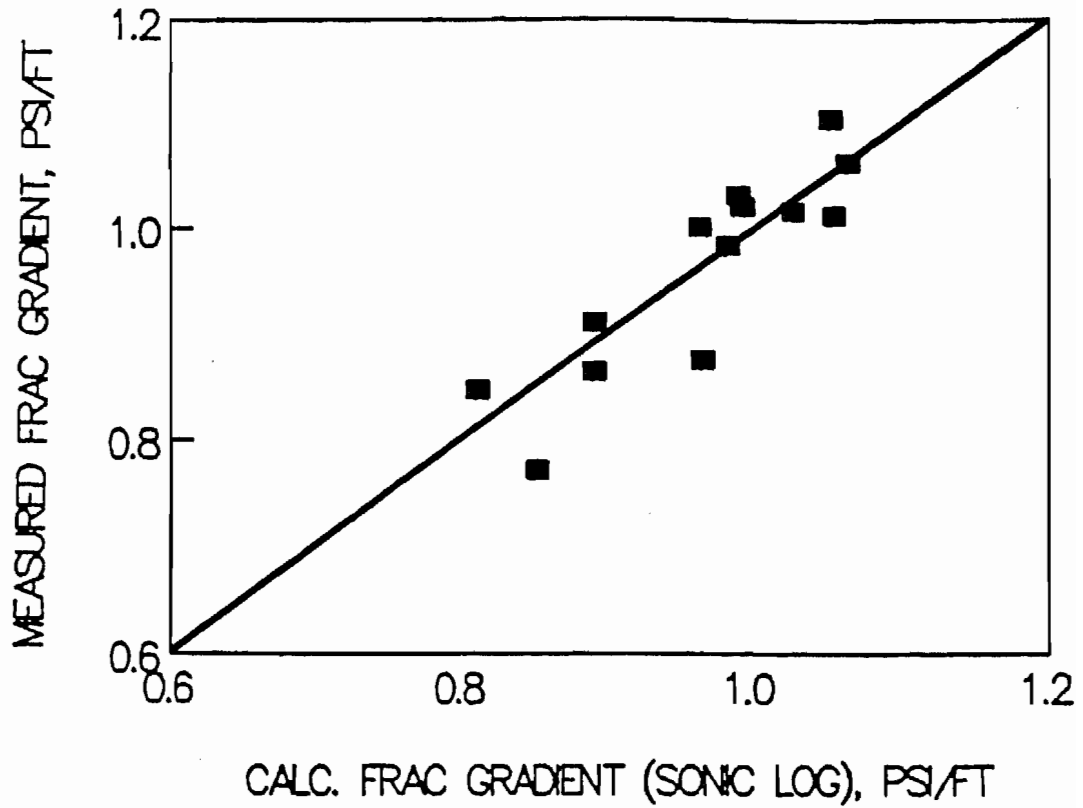


FIGURE 16: Measured Frac Gradient vs. Calculated Frac Gradient from the Sonic Log K/Measured K Correlation.

STRESS COMPARISON

(MEASURED vs. SONIC LOG DERIVED)

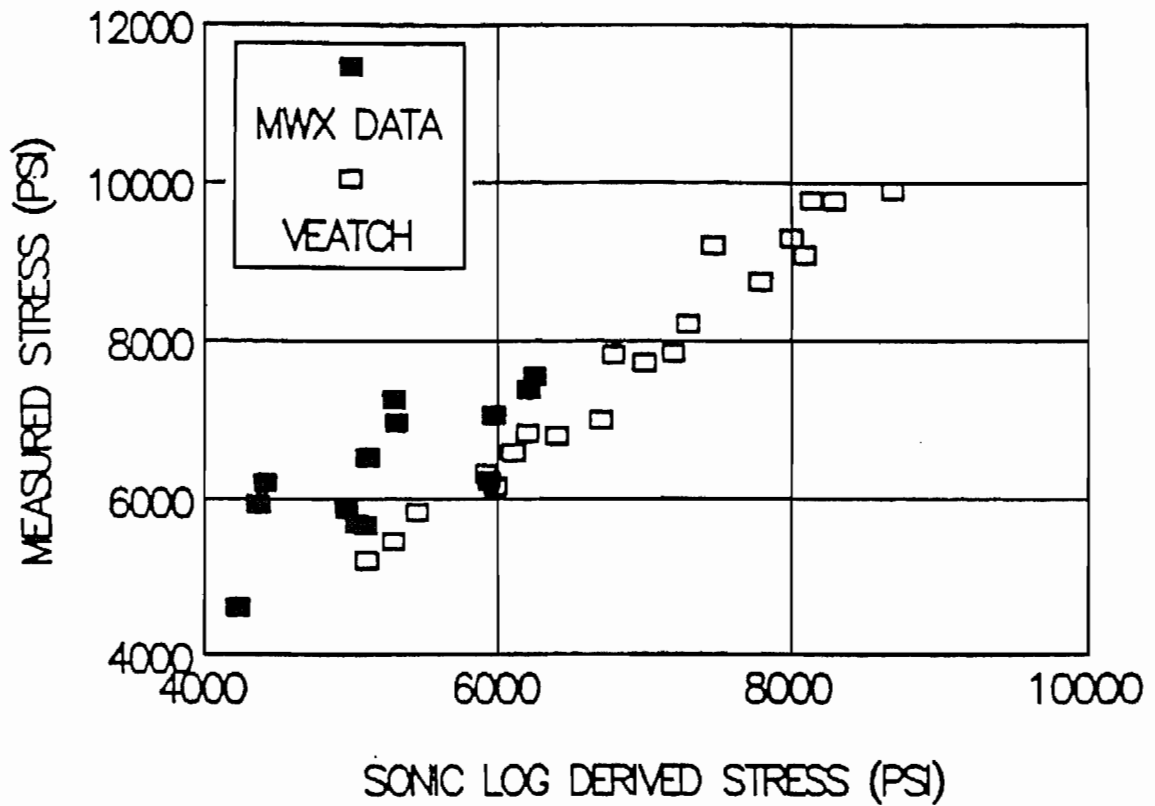


FIGURE 17: Measured vs. Log Derived Stress Comparison for Both MWX Data and Published Data.

STRESS PROFILE USING THE LINEAR CORRELATION

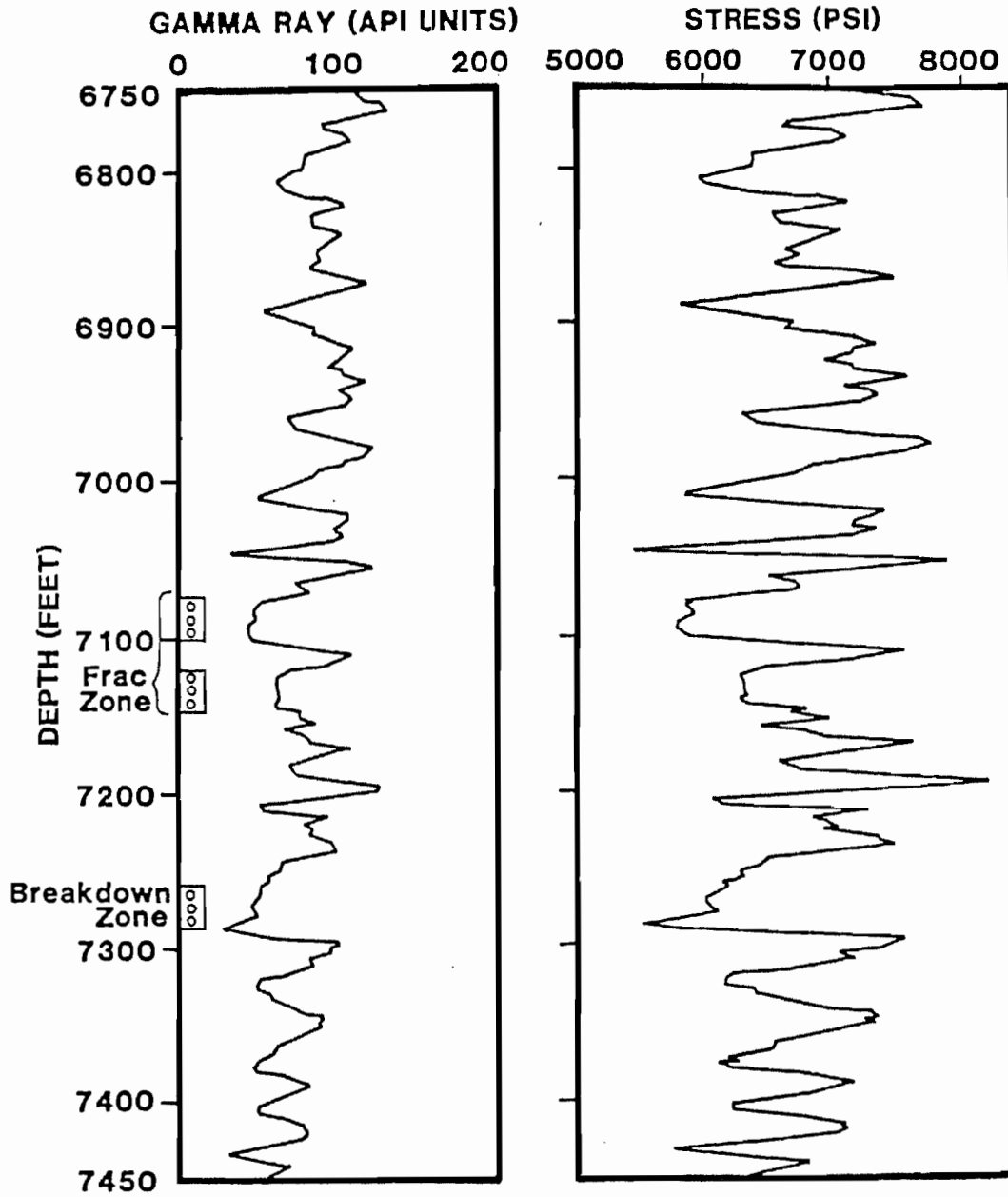


FIGURE 18: Stress Profile Through the Paludal Zone in MWX-1 Using the Linear K Factor/GR Correlation.

STRESS PROFILE USING THE BILINEAR CORRELATION

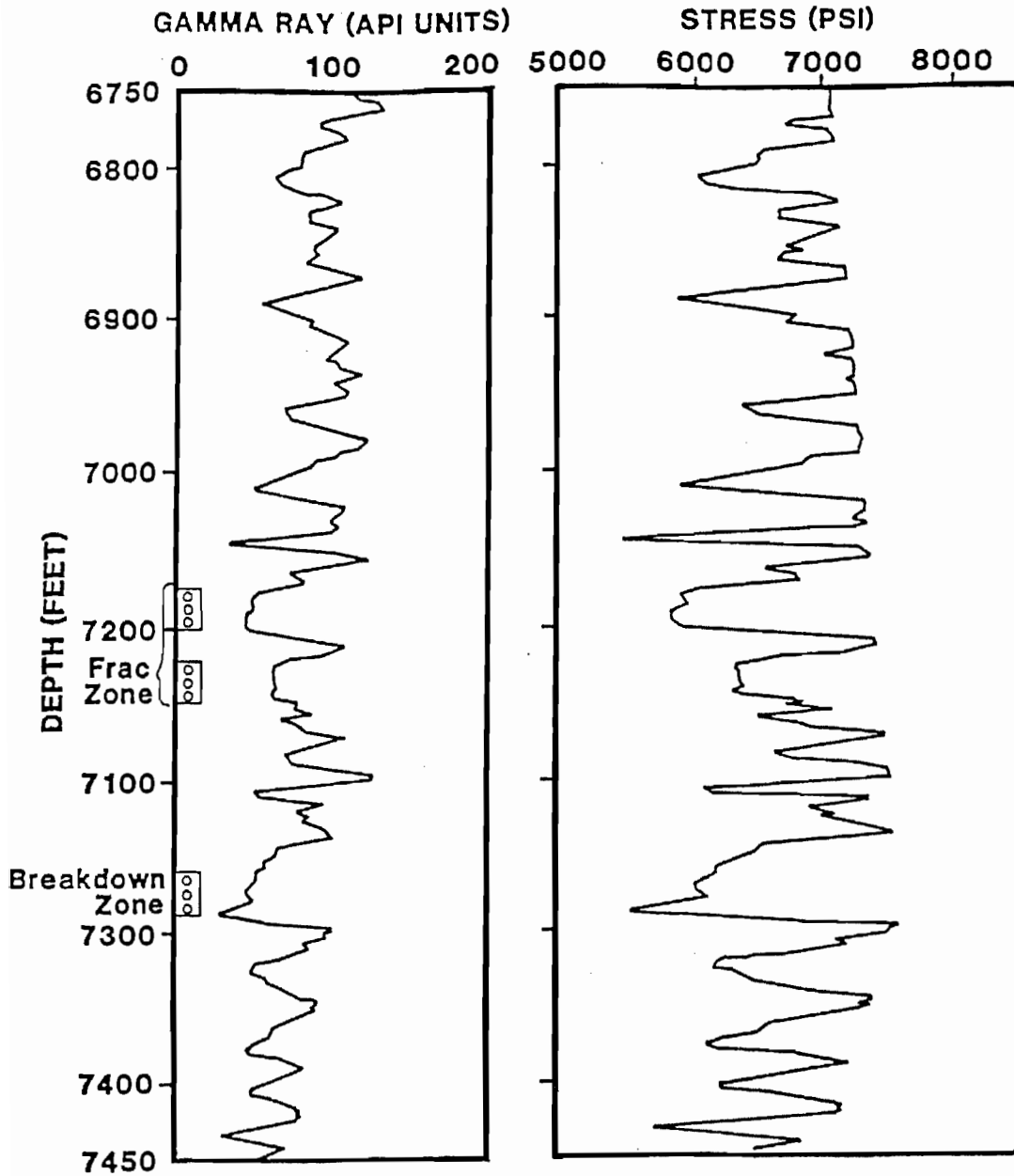


FIGURE 19: Stress Profile Through the Paludal Zone in MWX-1 Using the Bilinear K Factor/Gamma Ray Correlation.

MWX-1, MINIFRAC #1, PALUDAL

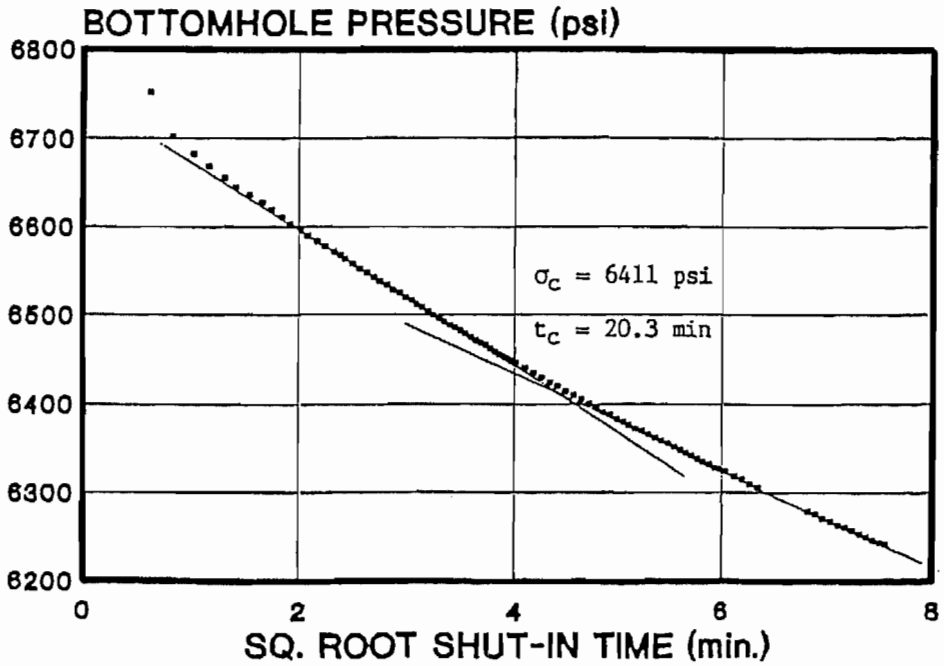
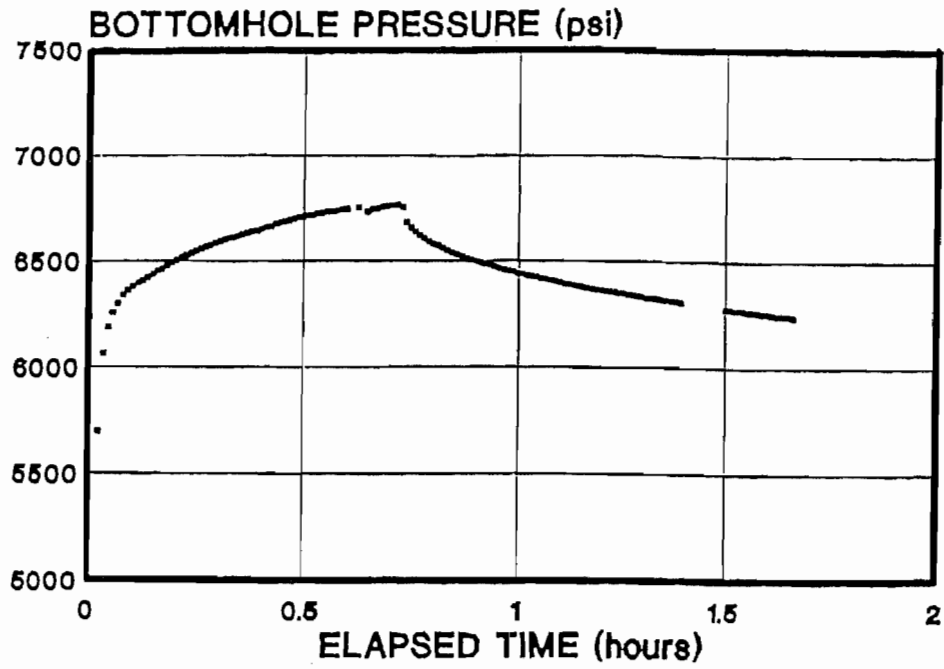


FIGURE 20: BHP Versus Time and Square Root Time for MWX-1, Paludal Minifrac No. 1.

MWX-1 STRESS PROFILE LINEAR CORRELATION

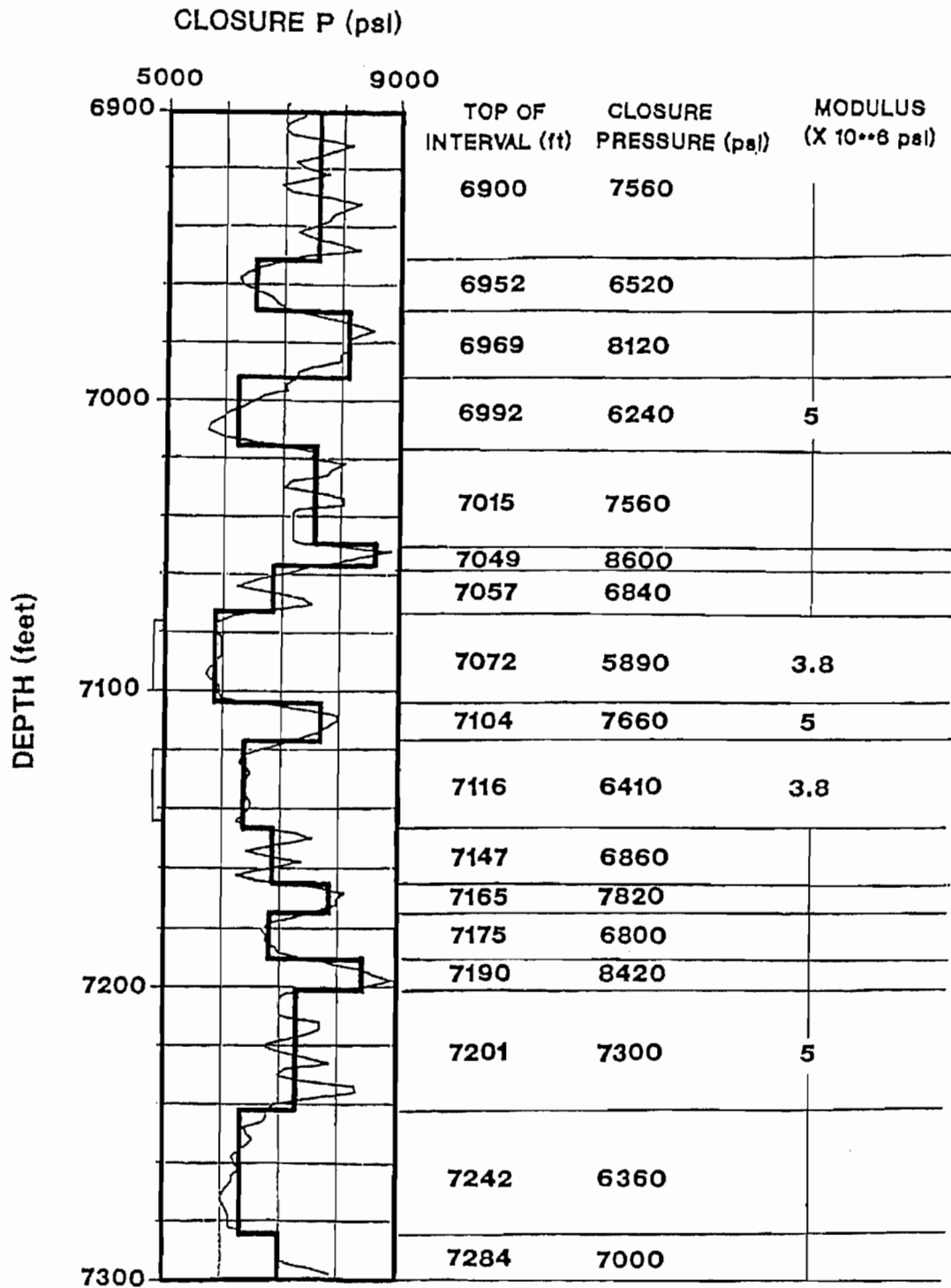
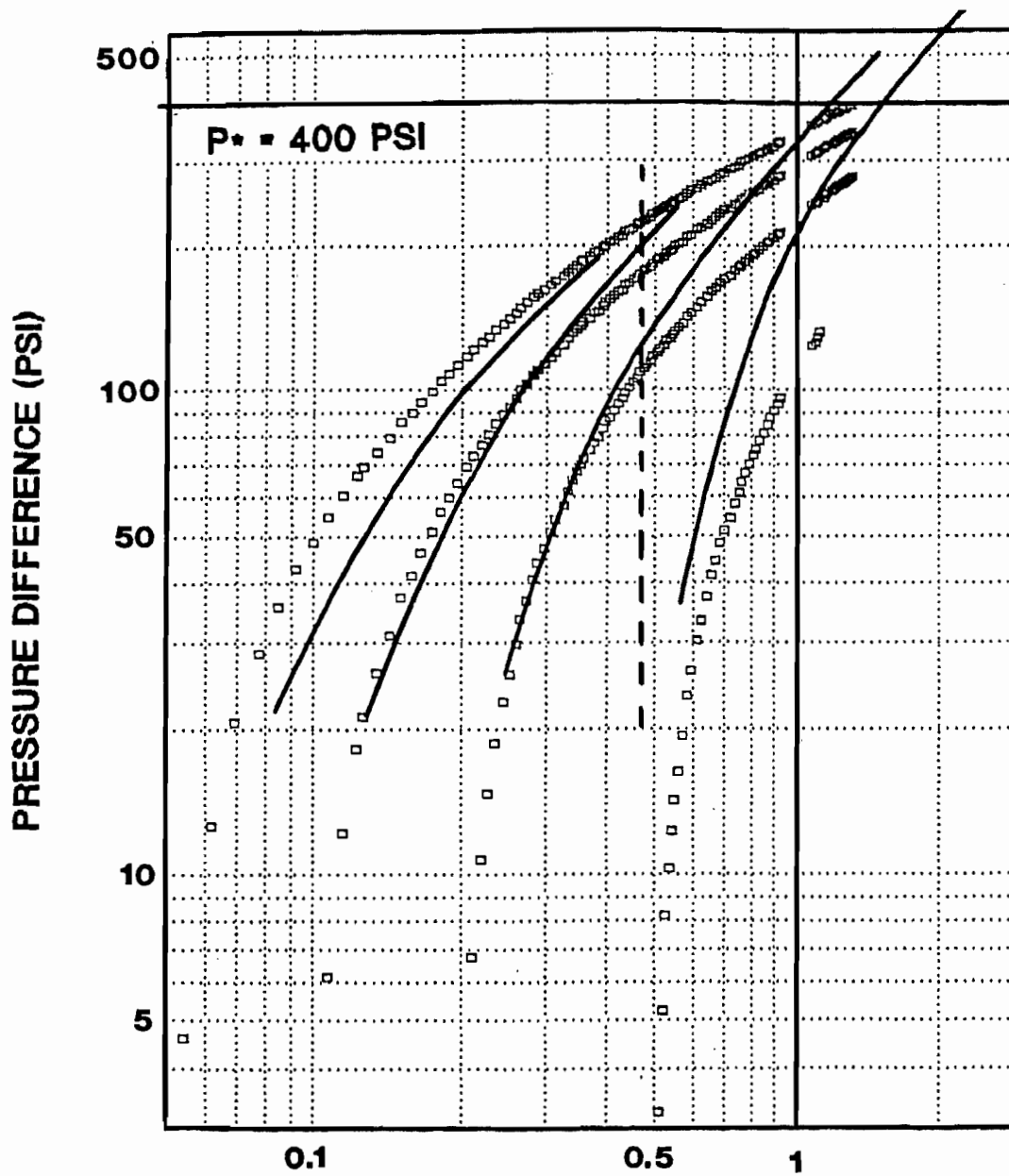


FIGURE 21: Smoothed Stress Profile Through Paludal Zone in MWX-1.

MWX-1, MINIFRAC #1 INJ./DECLINE



SHUT-IN TIME/PUMP TIME, PUMP TIME = 43.1 MIN.

FIGURE 22: Minifrac No. 1 Pressure Decline Type Curve Match,
 $P_c = 5890$ psi, $t_0 = 43.1$ minutes.

Bounds:
 --- Upper
 — Interpolated
 --- Lower

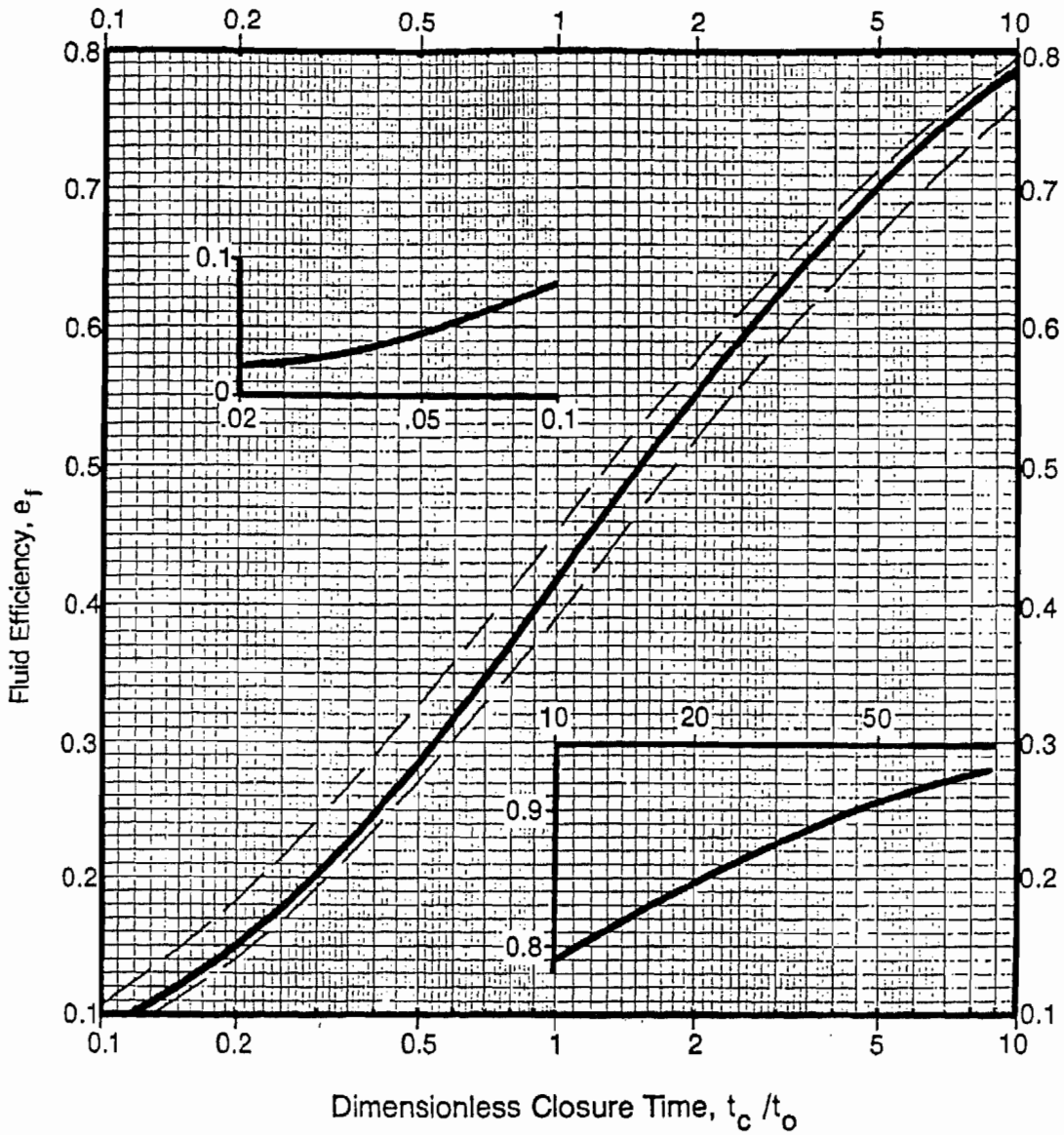


FIGURE 23: Fluid Efficiency Versus Dimensionless Closure Time.

MWX-1, MINIFRAC #1 INJ./DECLINE

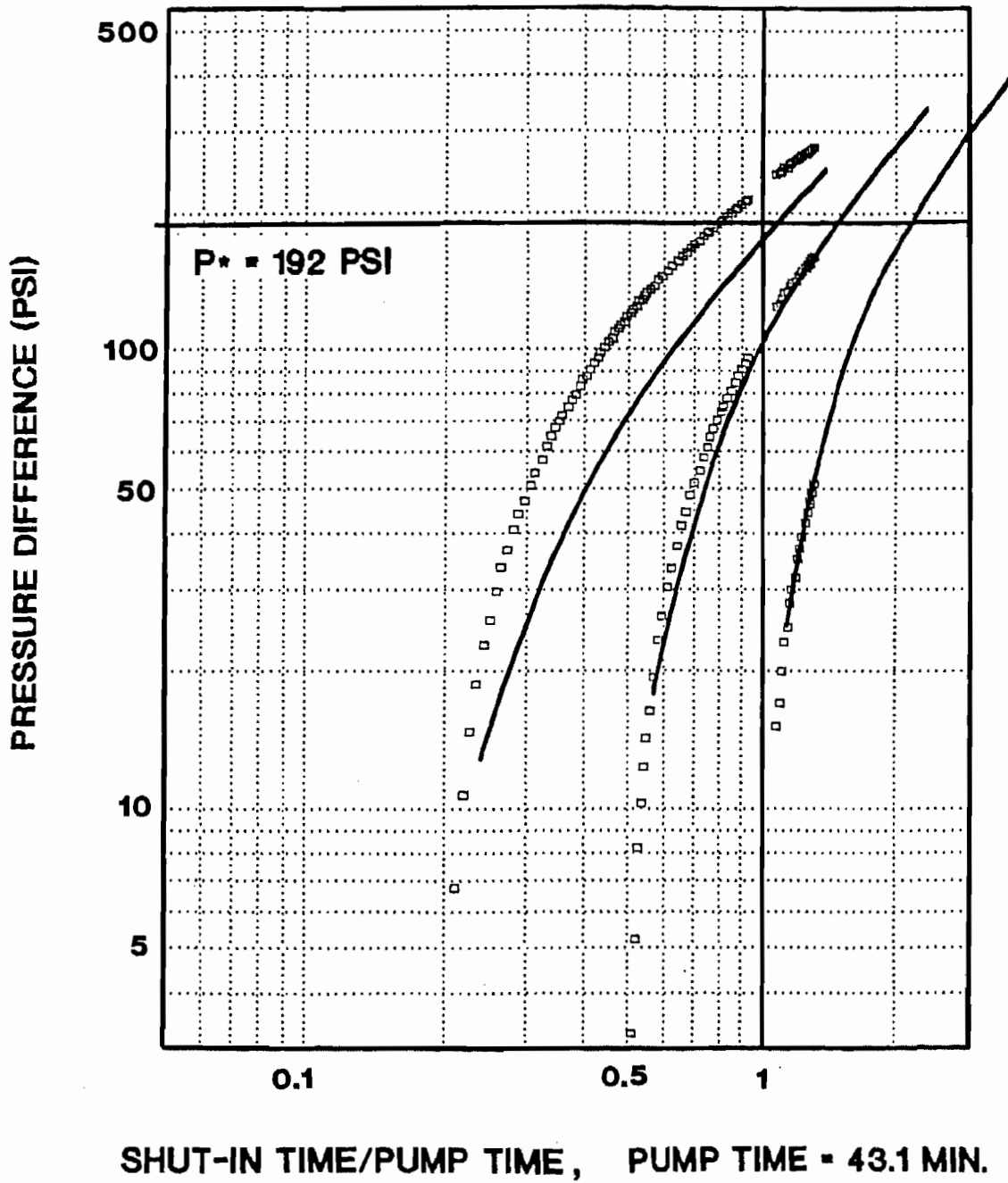
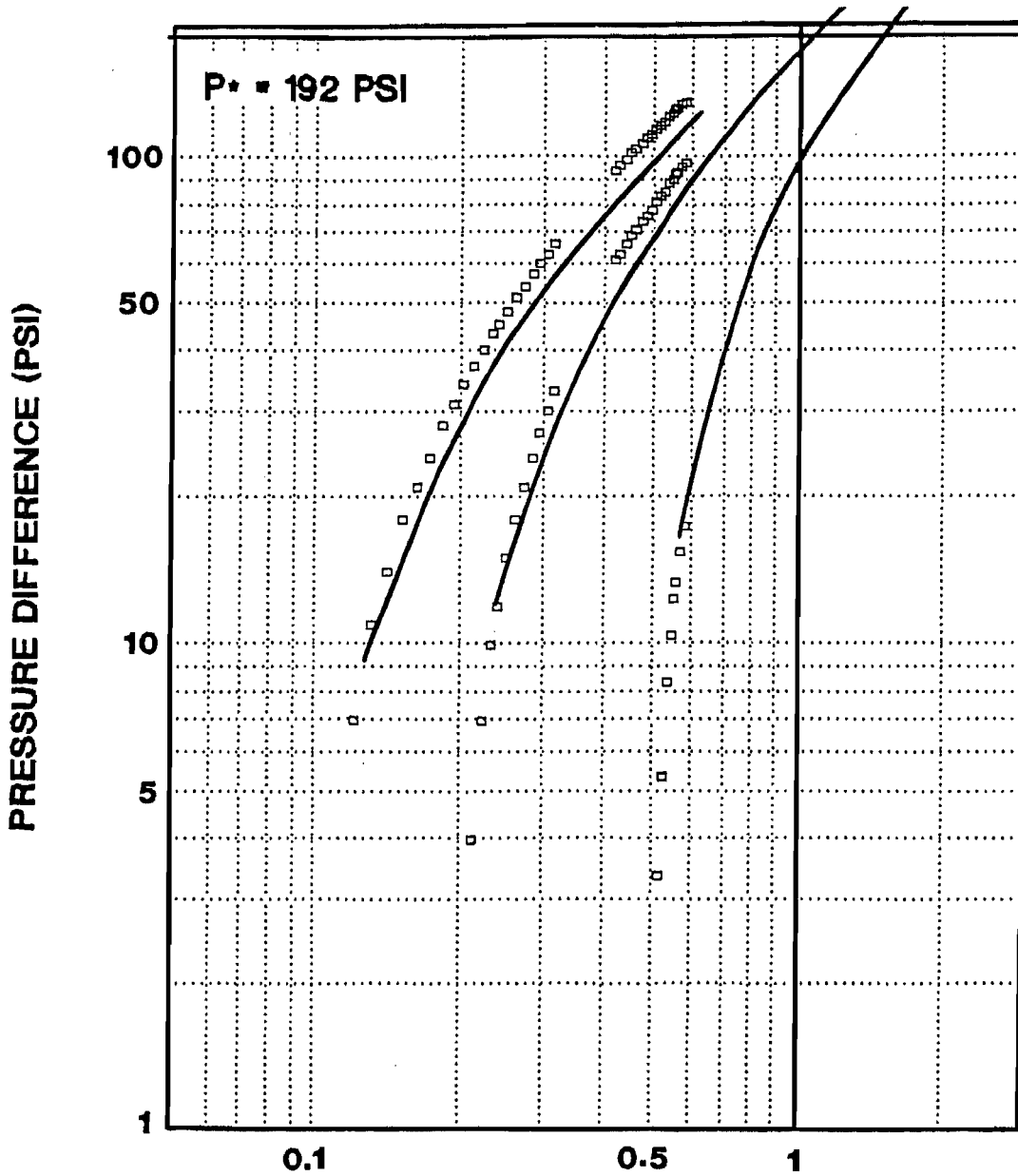


FIGURE 24: Minifrac No. 1 Pressure Decline Type Curve Match,
 $P_c = 5890 \text{ psi}$, $t_0 = 43.1 \text{ minutes}$.

MWX-1, MINIFRAC #1 INJ./DECLINE



SHUT-IN TIME/PUMP TIME, PUMP TIME = 63.4 MIN.

FIGURE 25: Minifrac No. 1 Pressure Decline Type Curve Match, $P_c = 5890$ psi, $t_0 = 63.4$ minutes.

MWX-1 STRESS PROFILE LINEAR CORRELATION

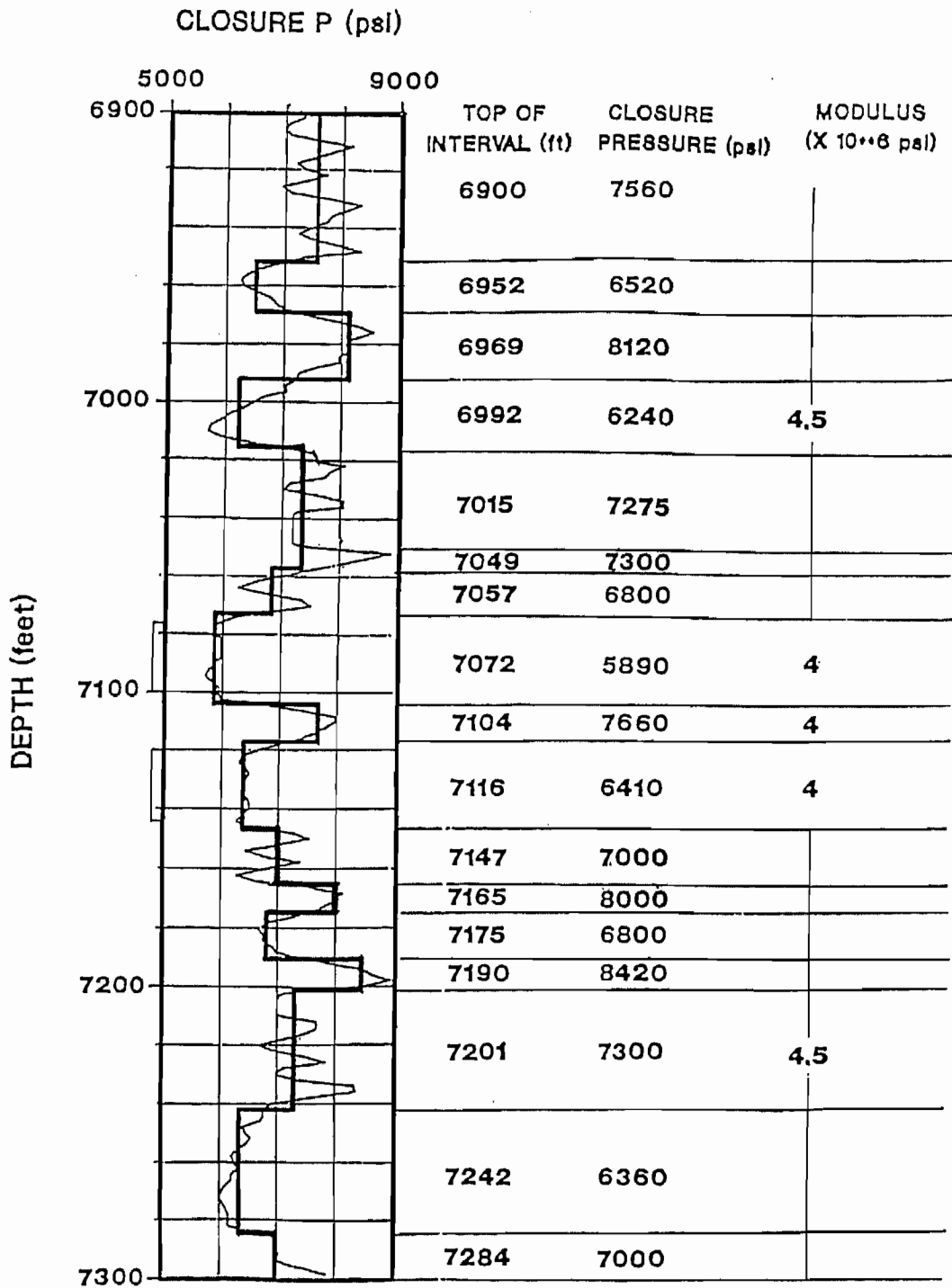


FIGURE 26: Revised Smoothed Stress Profile Through MWX-1 Paludal Zone.

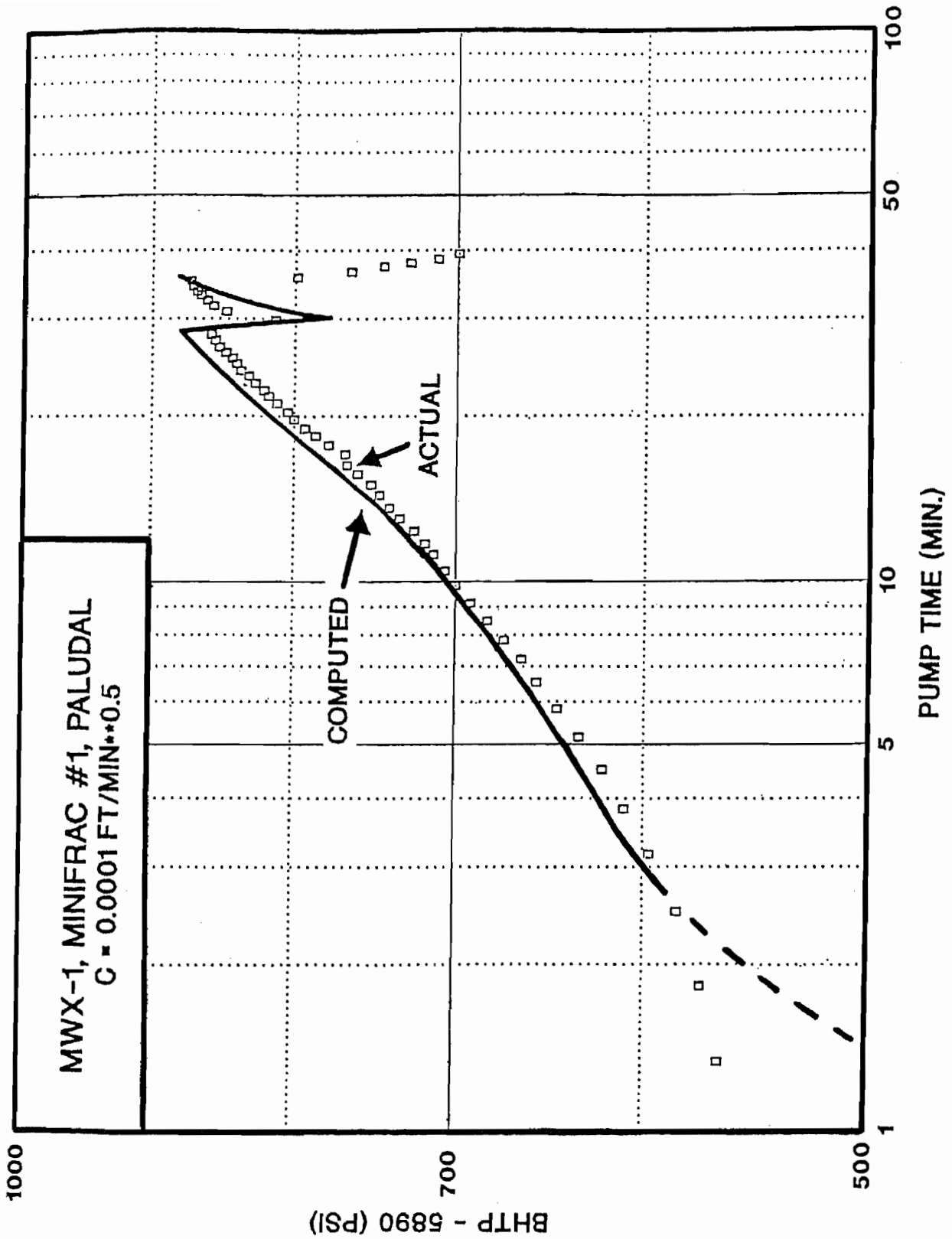


FIGURE 27: Pressure History Match of MWX-1, Minifrac No. 1 Injection.

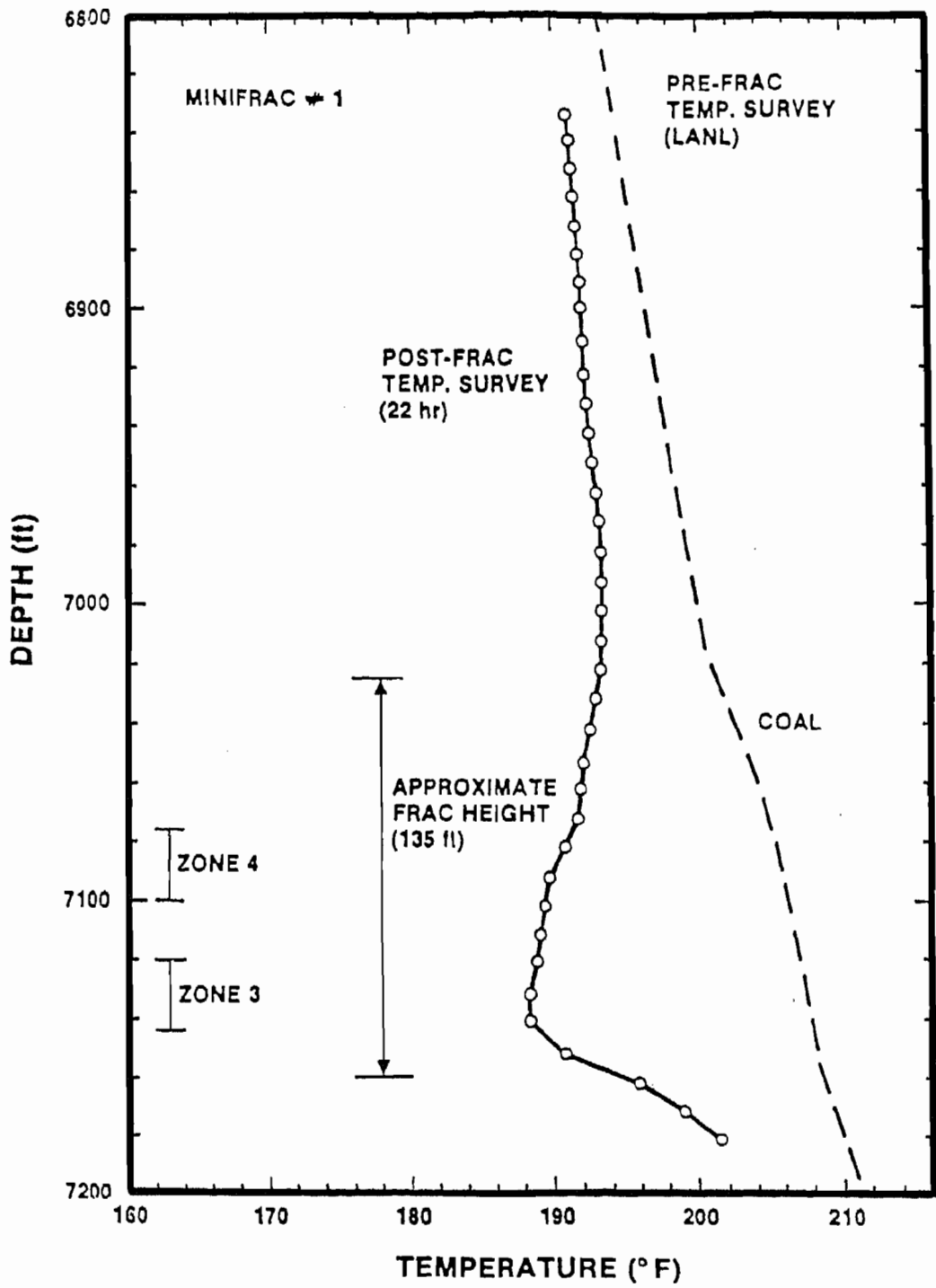


FIGURE 28: Post-Minifrac No. 1 Temperature Log and Estimated Fracture Height.

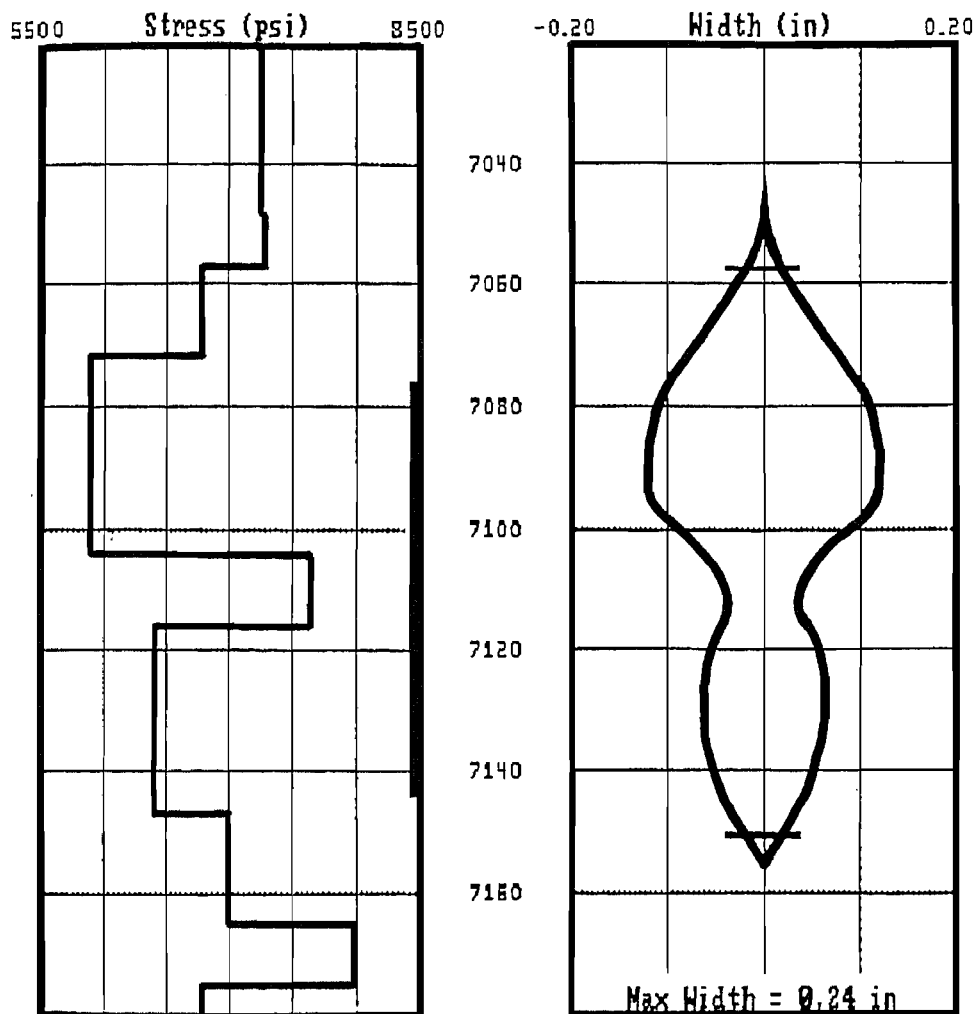


FIGURE 29: Computed Fracture Width-Height Profile for MWX-1, Minifrac No. 1 Pressure History Match.

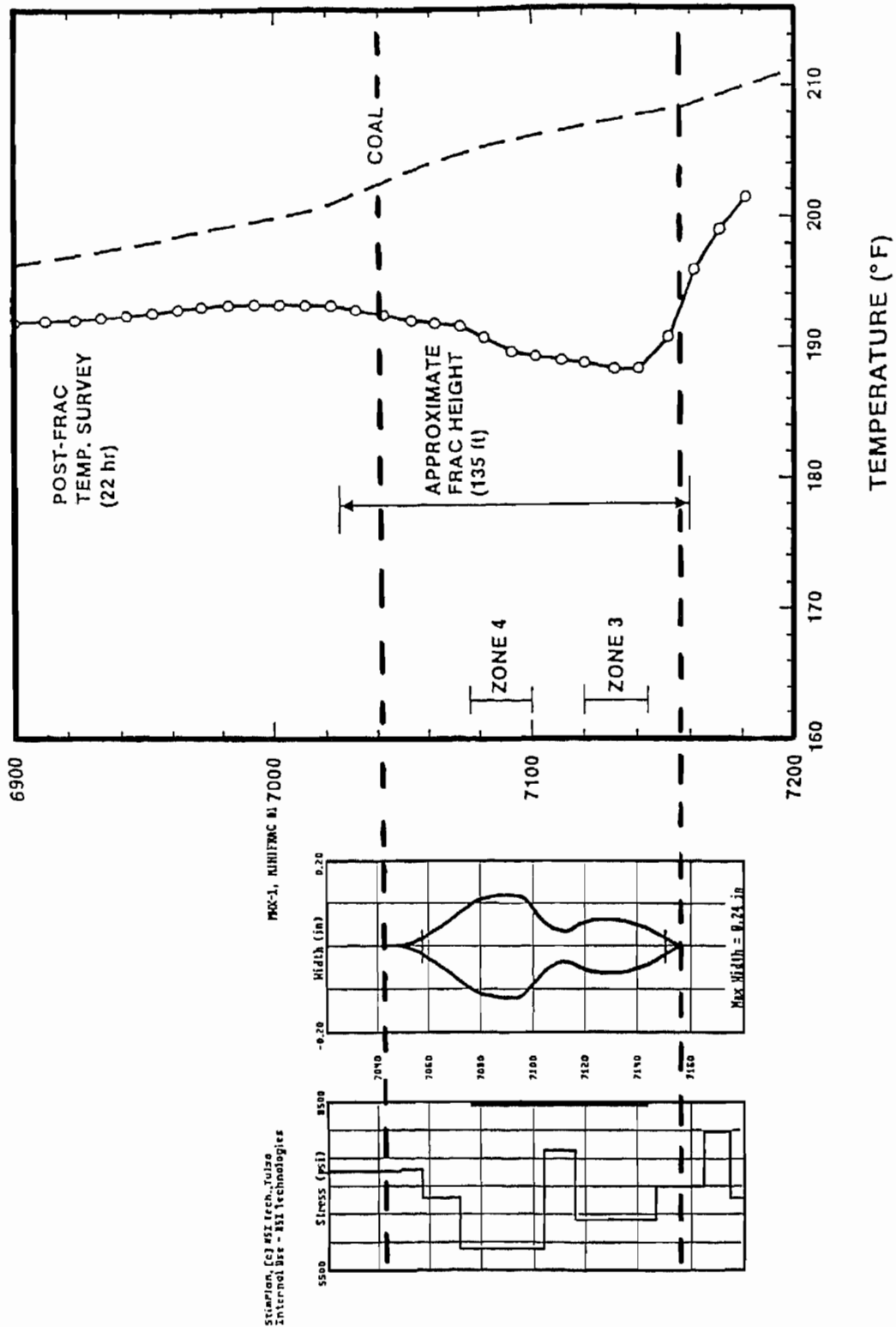


FIGURE 30: Comparison of Created Fracture Height From Temperature Log and Predicted Height From Pressure History Match, MWX-1, Minifrac No. 1.

MWX-1, MINIFRAC #1, PALUDAL ZONE PRESSURE DECLINE HISTORY MATCH

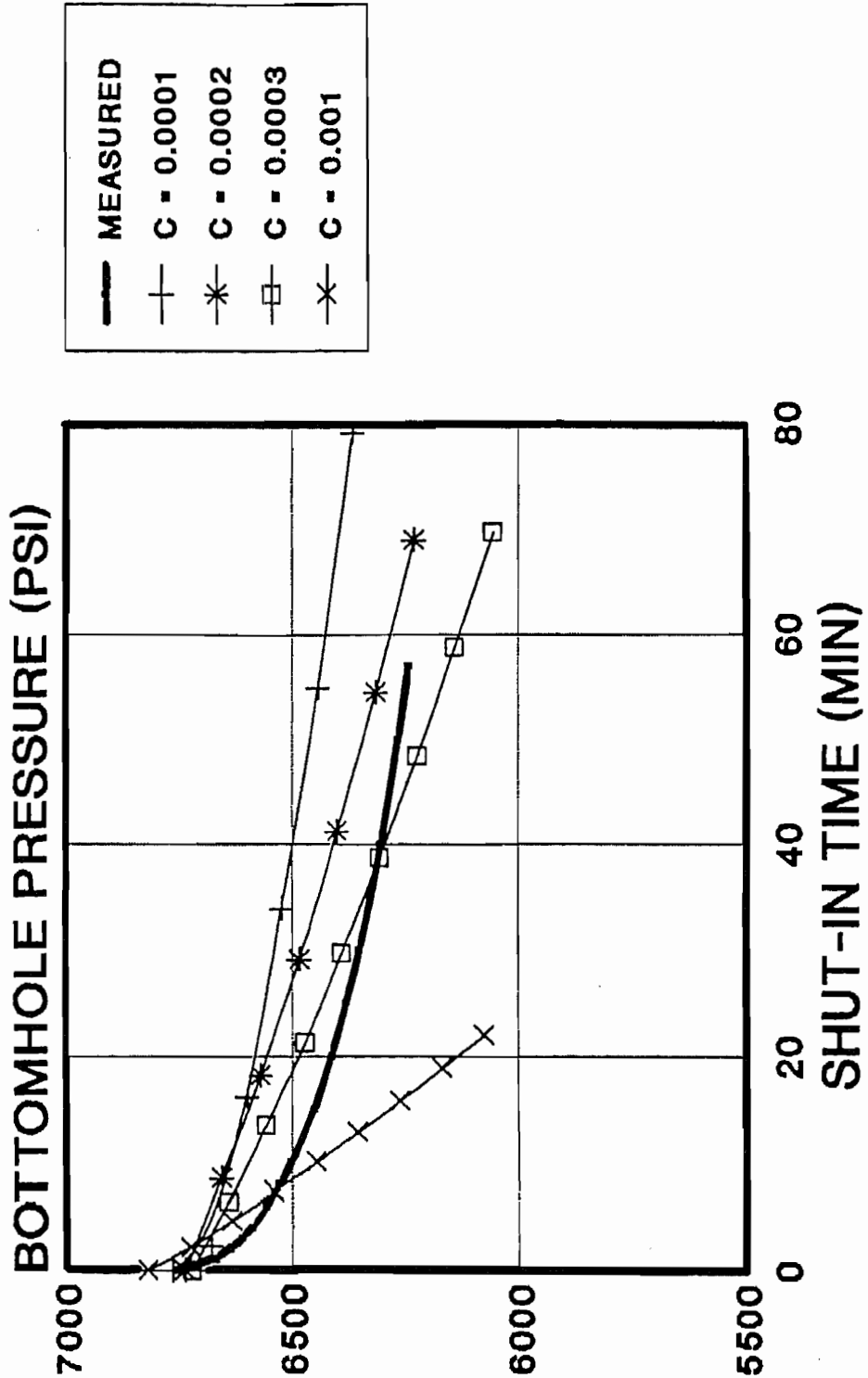


FIGURE 31: Pressure Decline History Match for MWX-1, Minifrac No. 1.

MWX-1, MINIFRAC #2 INJECTION/DECLINE

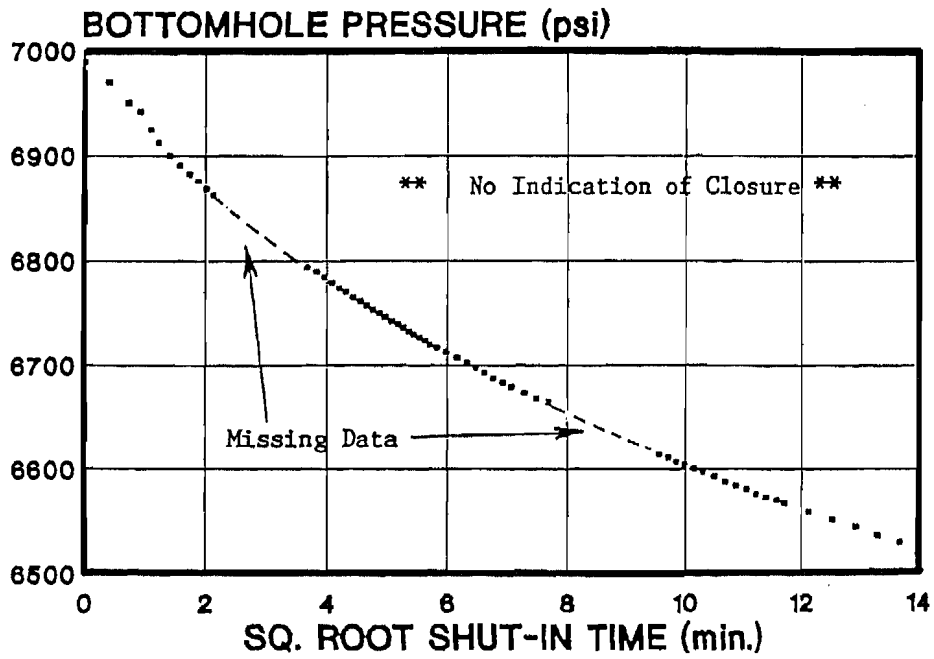
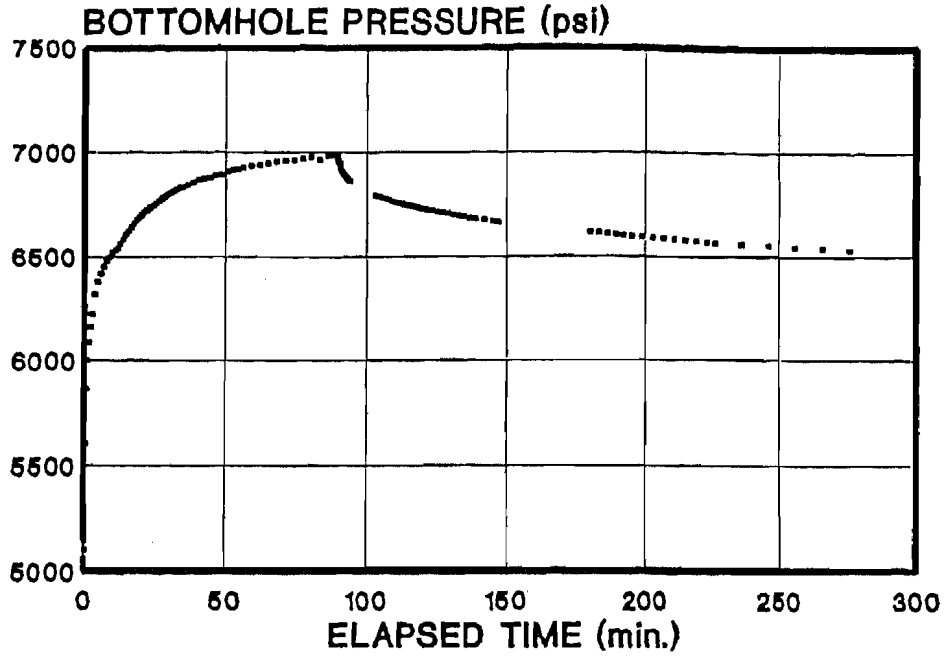


FIGURE 32: BHP Versus Time and Square-Root Time for MWX-1 Paludal Zone, Minifrac No. 2.

MWX-1, MINIFRAC #2 INJ./DECLINE

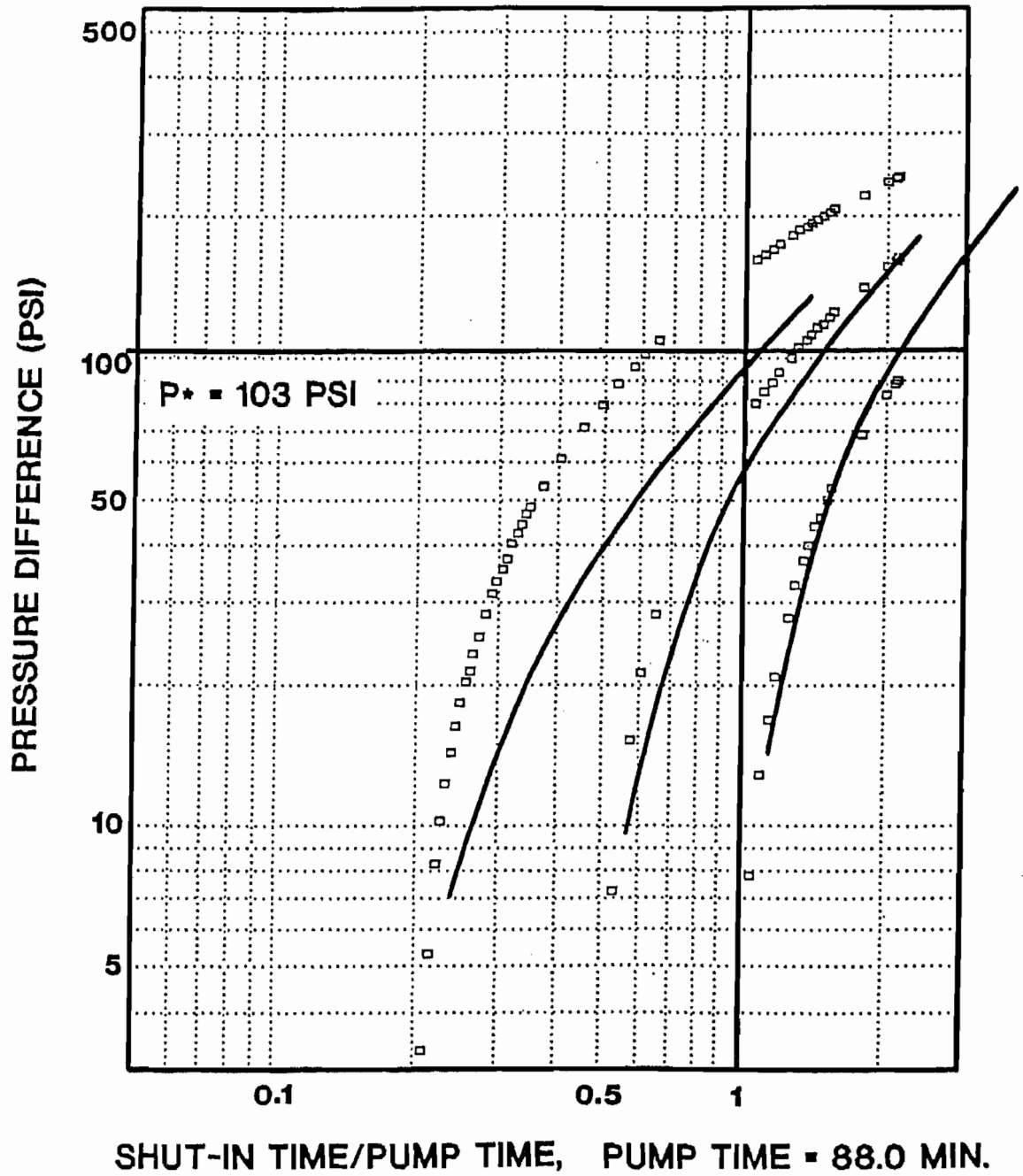


FIGURE 33: Minifrac No. 2 Pressure Decline Type Curve Match, MWX-1 Paludal Zone.

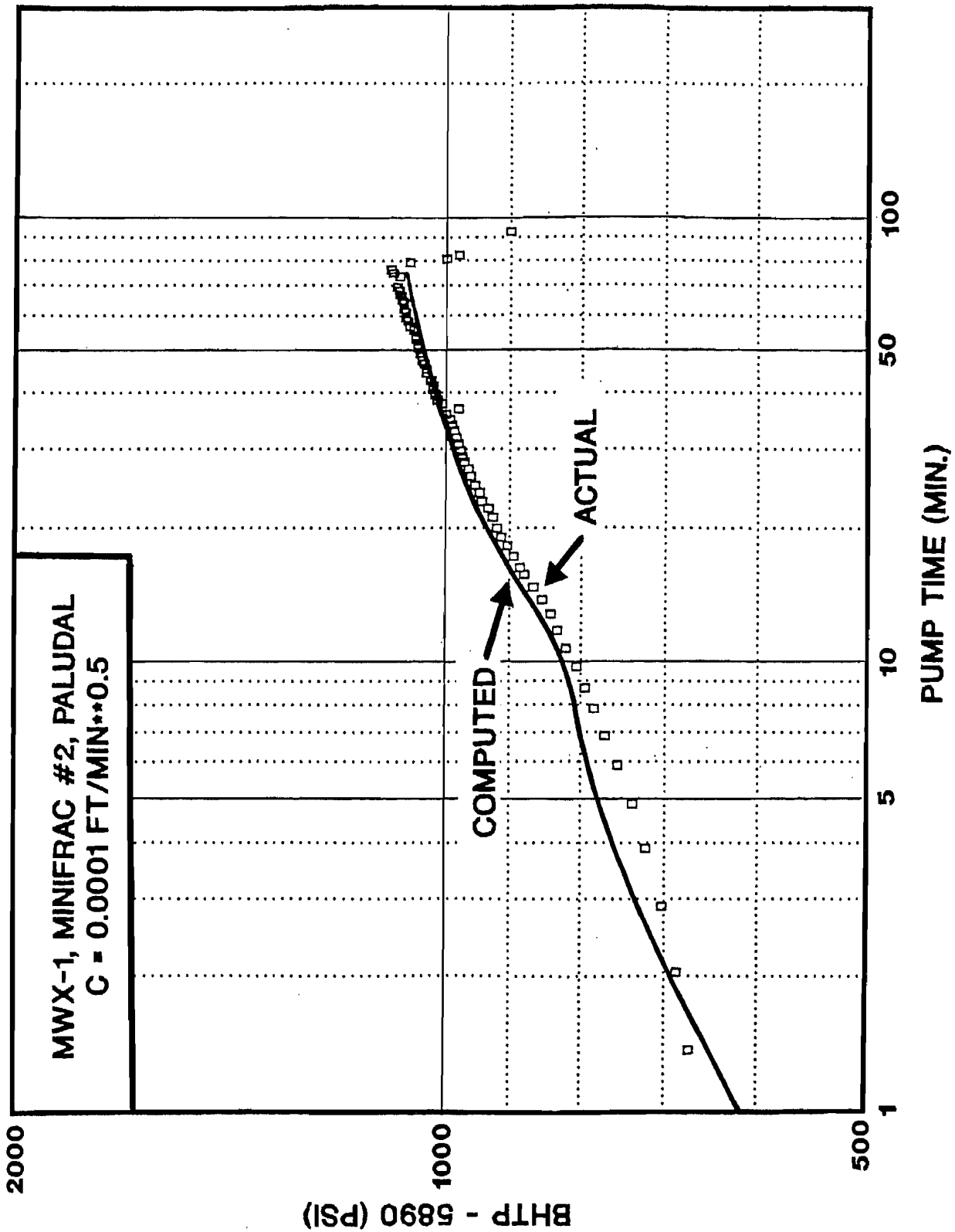


FIGURE 34: Pressure History Match of MWX-1, Paludal Minifrac #2 Injection.

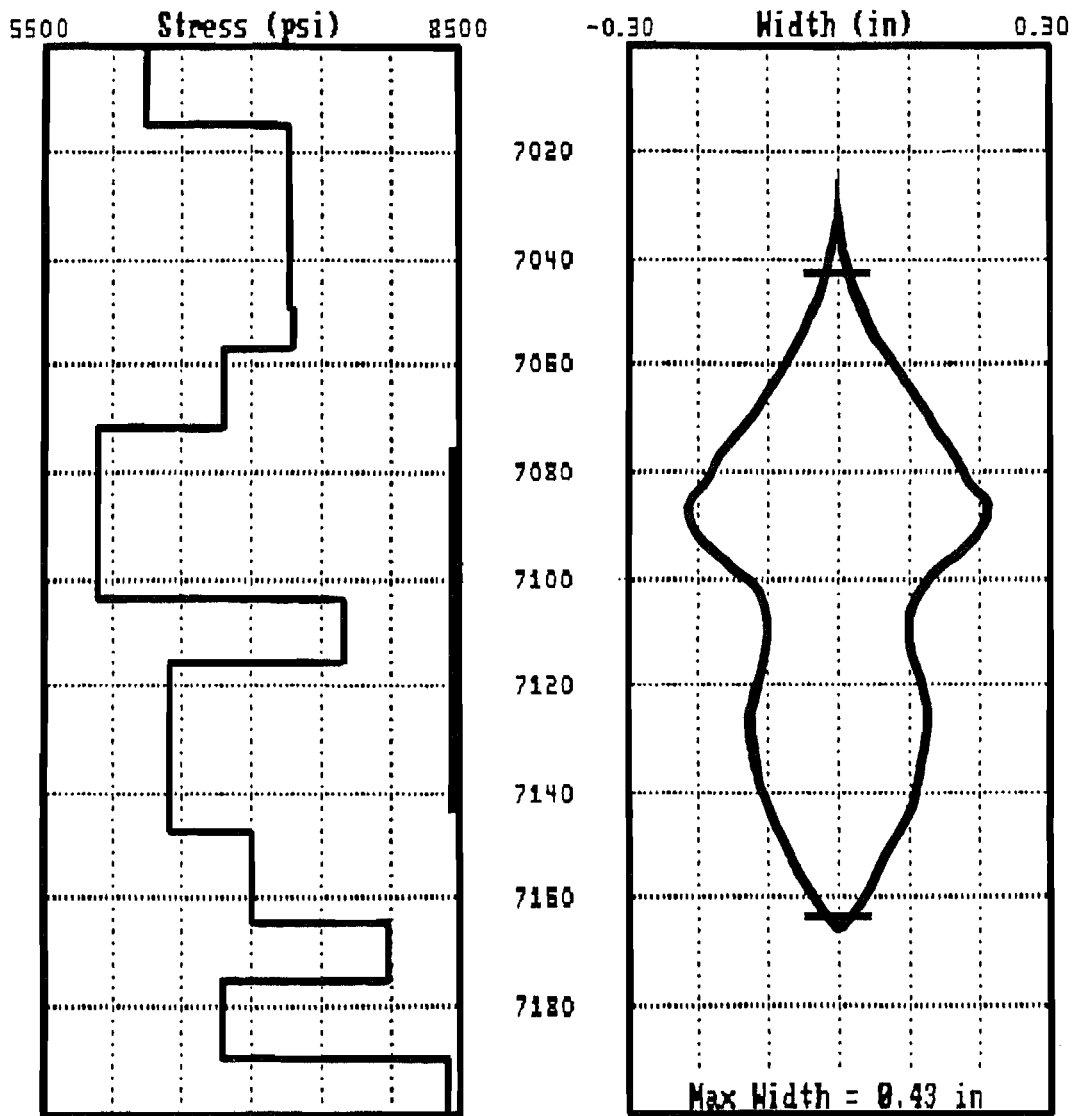


FIGURE 35: Computed Fracture Width-Height Profile for Minifrac No. 2
Pressure History Match, MWX-1 Paludal Zone.

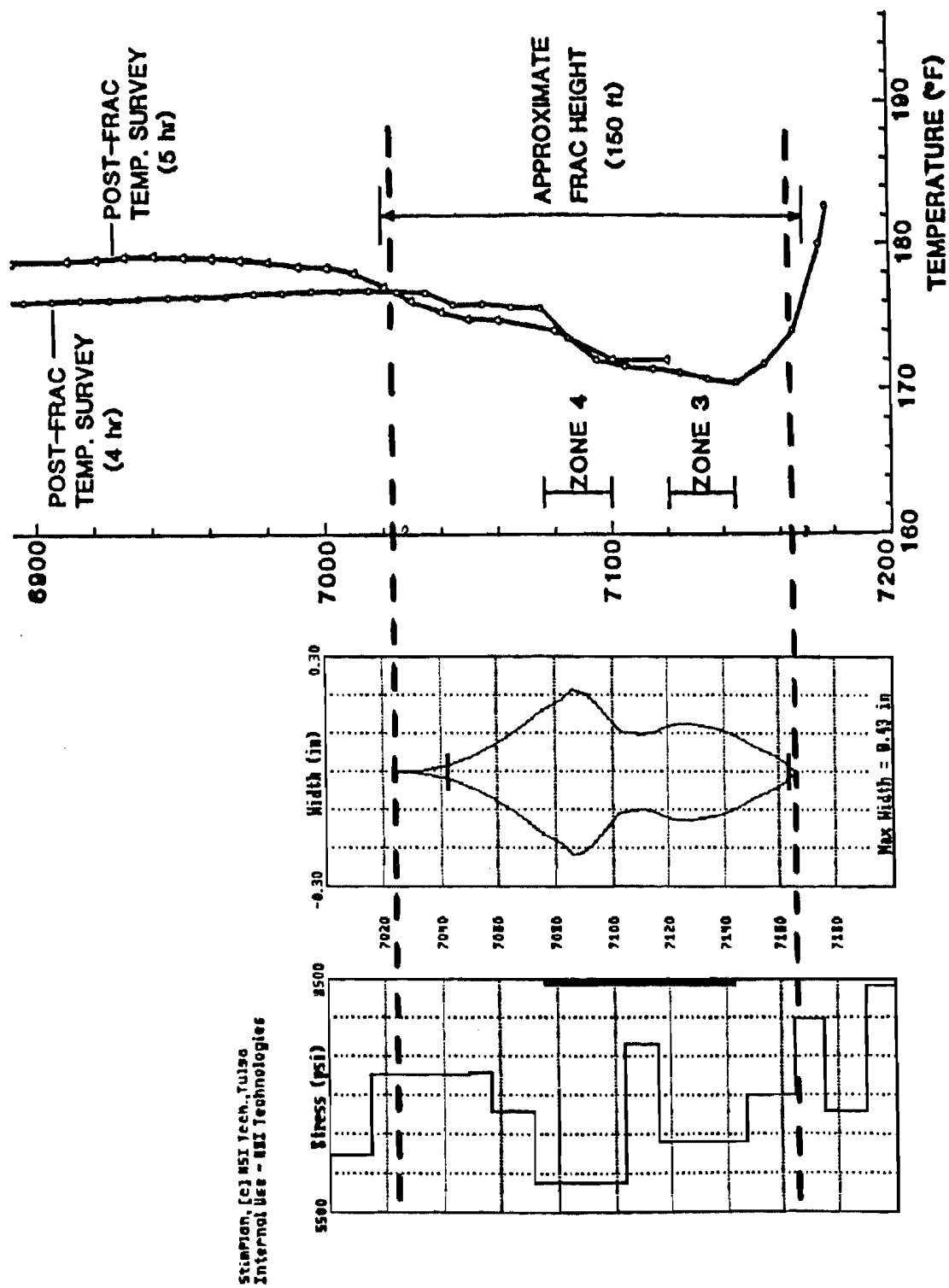


FIGURE 36: Comparison of Created Fracture Height From Temperature Log and Predicted Height From Pressure History Match, Minifrac #2.

MWX-1, MINIFRAC #2, PALUDAL ZONE PRESSURE DECLINE HISTORY MATCH

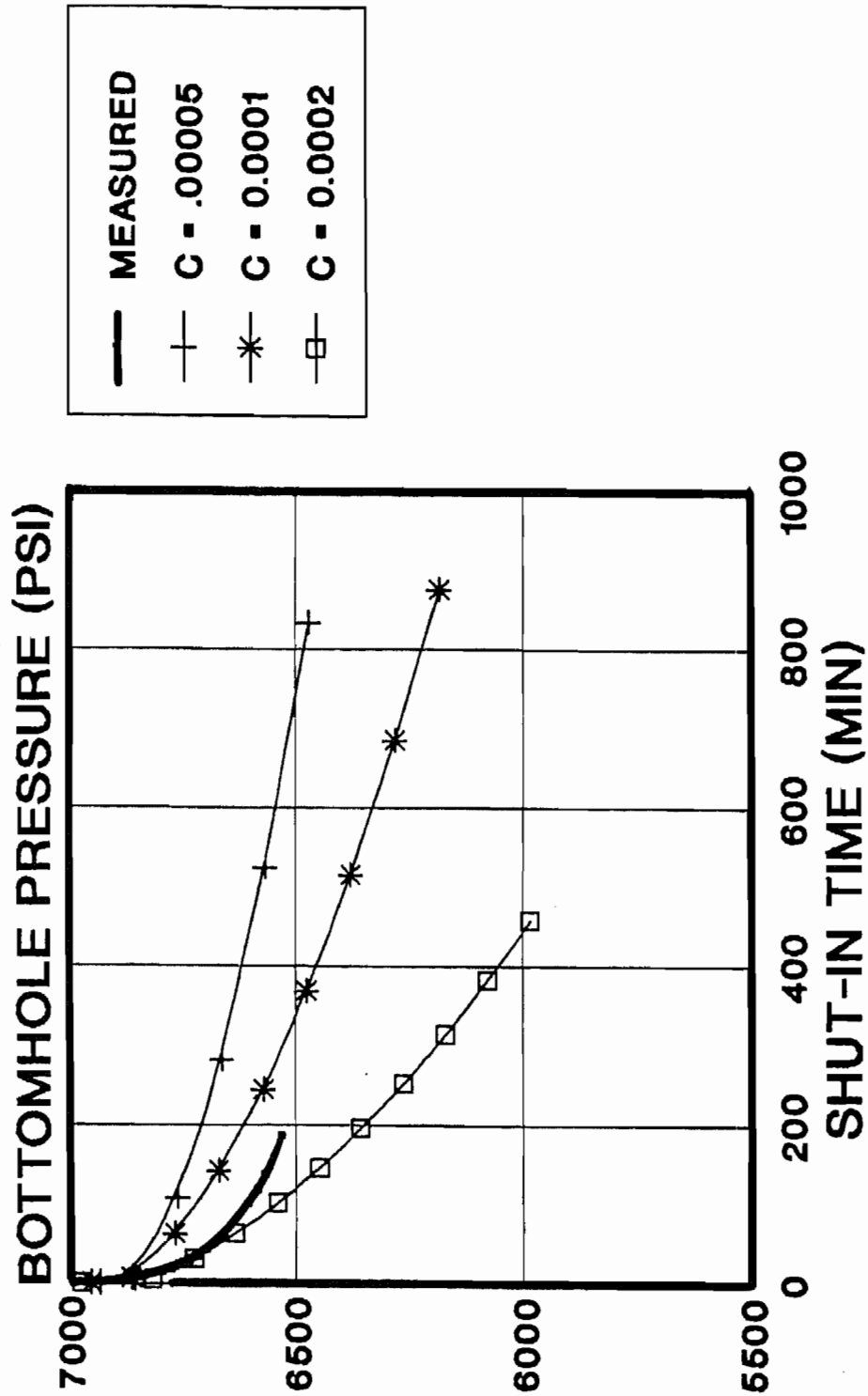


FIGURE 37: Pressure Decline History Match for MWX-1, Minifrac #2.

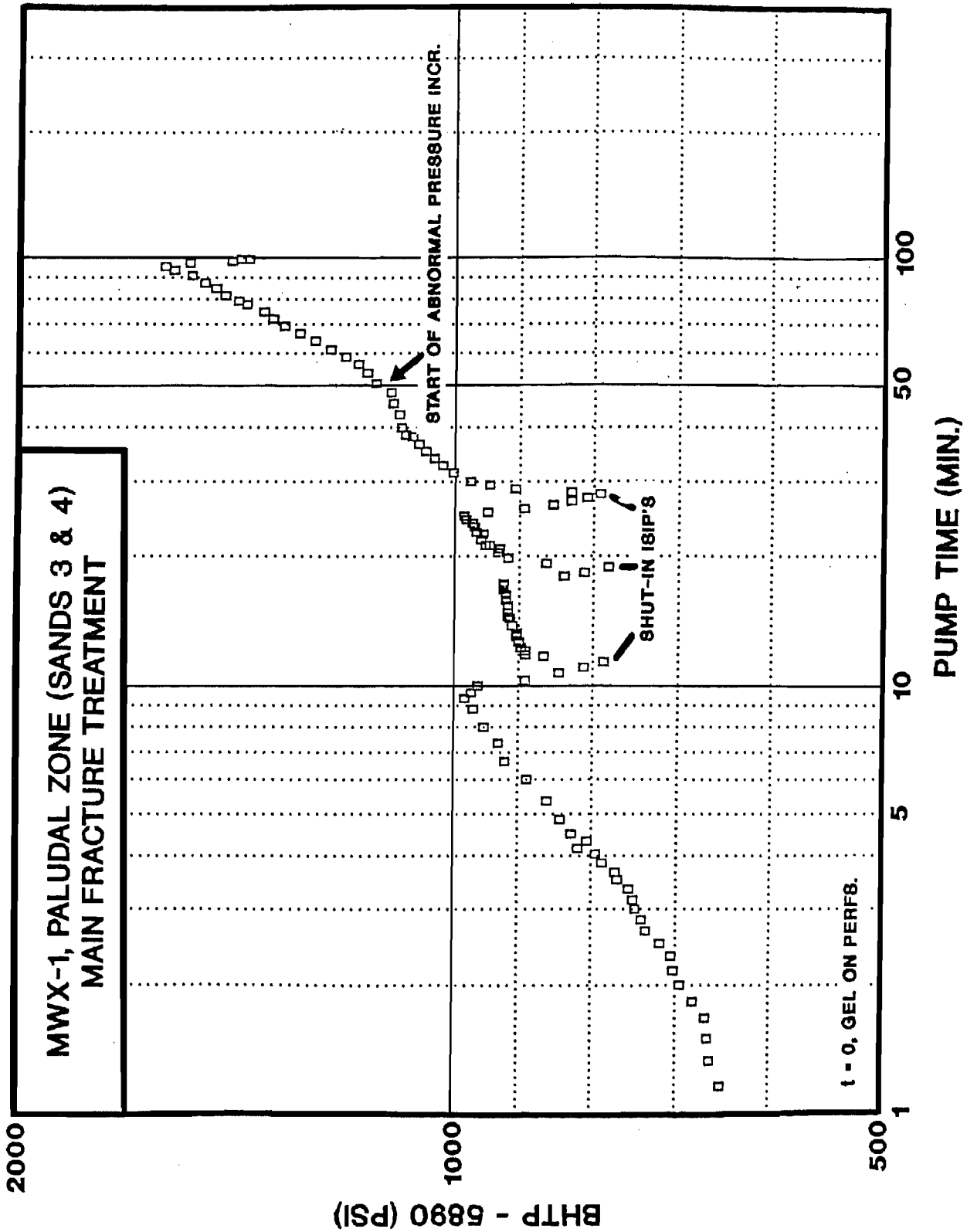


FIGURE 38: Nolte-Smith Log-Log Plot of Net BHTP During MWX-1 Paludal Fracturing Treatment.

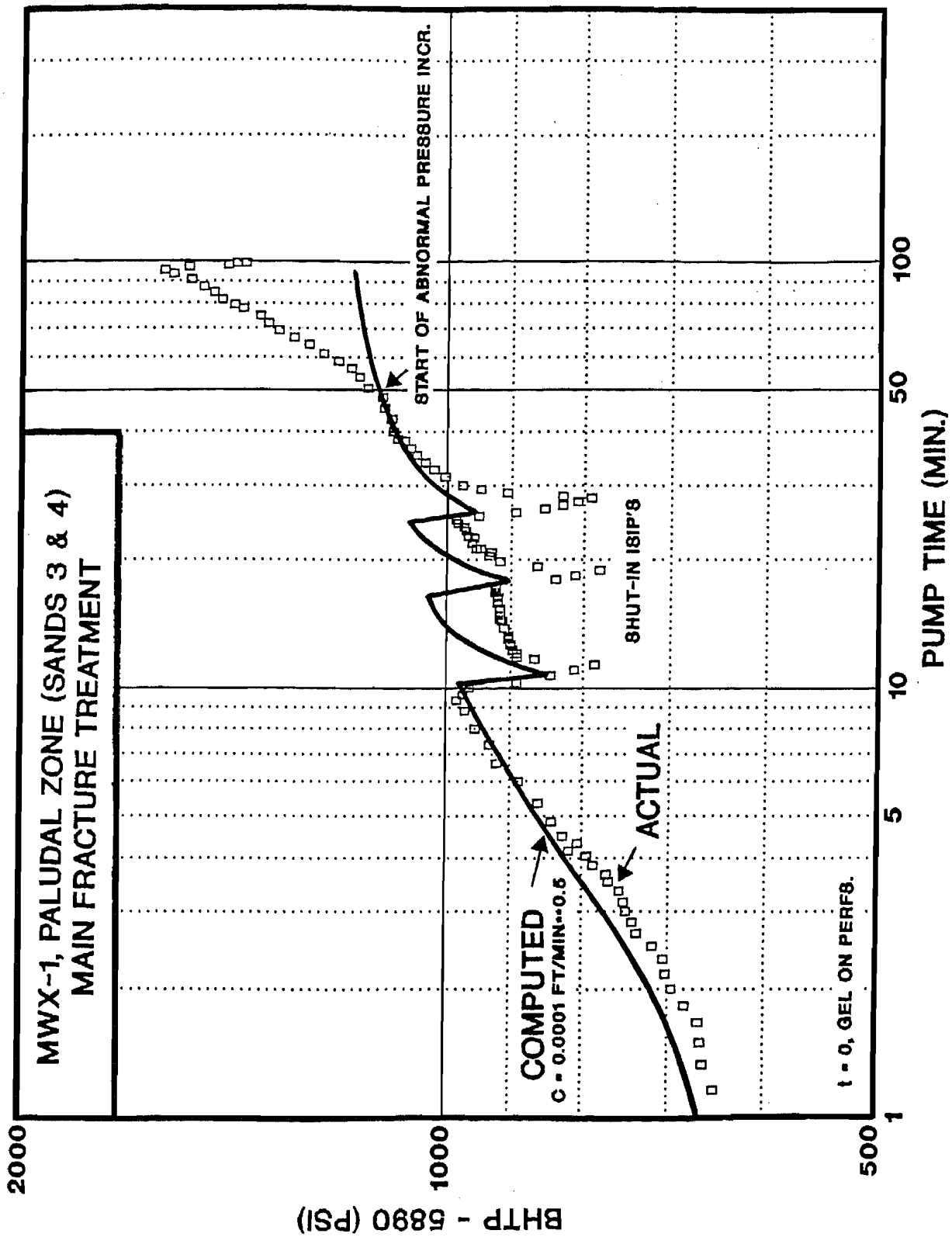


FIGURE 39: Pressure History Match of Paludal Fracture Treatment Using a Leak-Off Coefficient of 0.0001 ft/min**0.5.

MWX-1 COMPARISON OF MINIFRACS AND MAIN FRAC TREATMENT NET PRESSURES

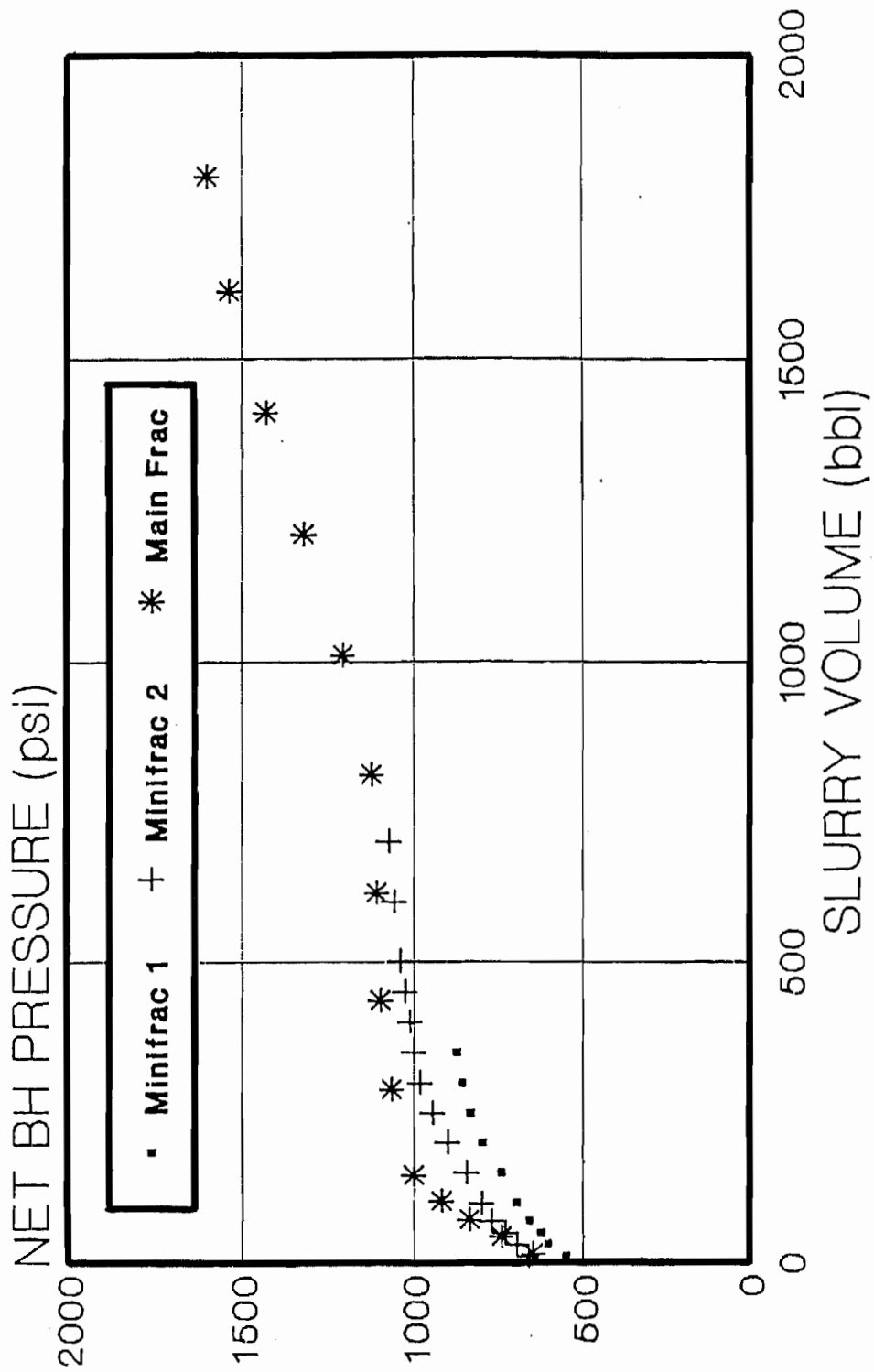


FIGURE 40: Comparison of Minifracs and Main Fracture Treatment Net BHTP's Versus Injected Volume, MWX-1 Paludal Zone.

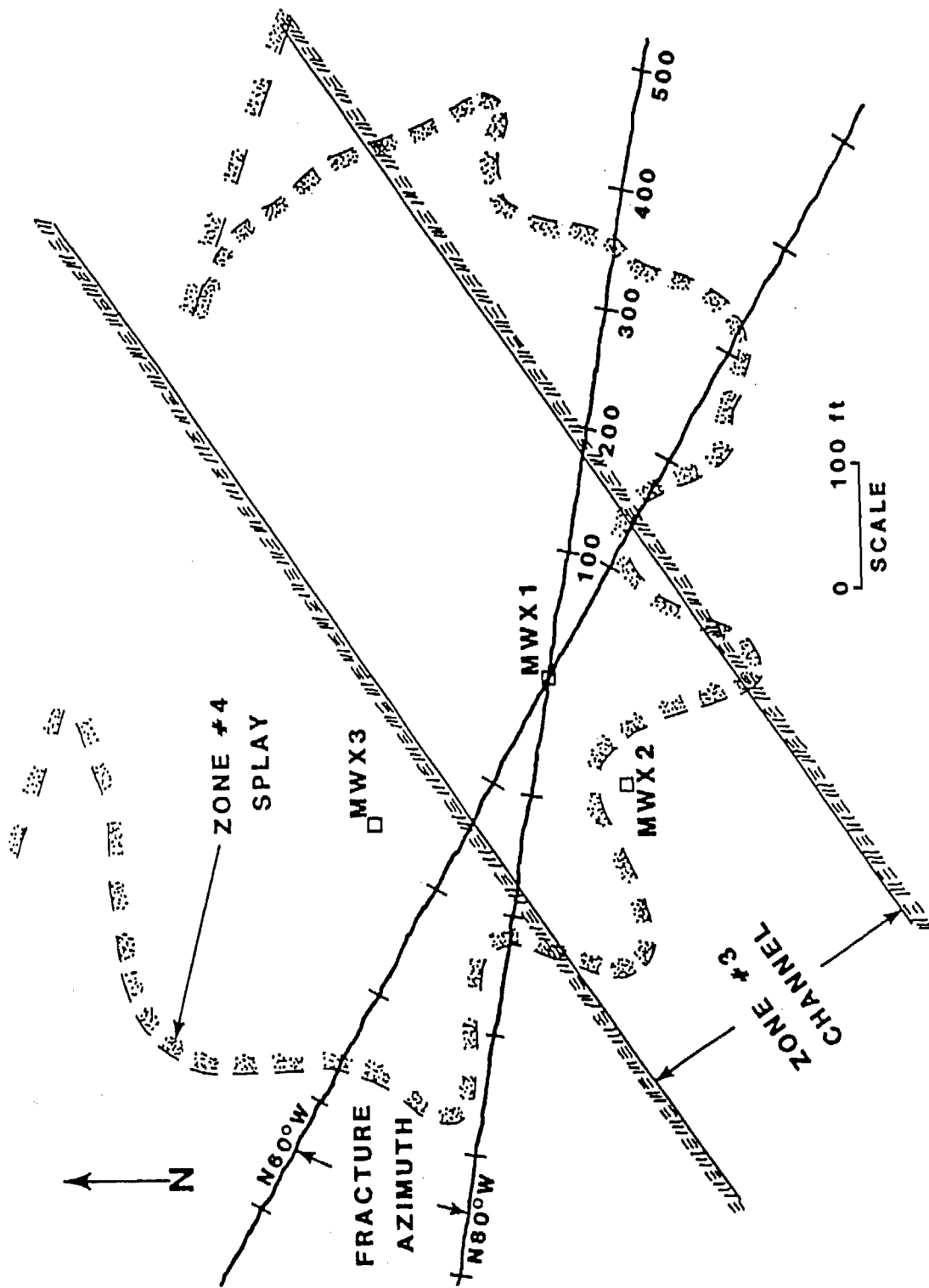


FIGURE 41: Estimated Sand Geometry for Paludal Sands 3 and 4.

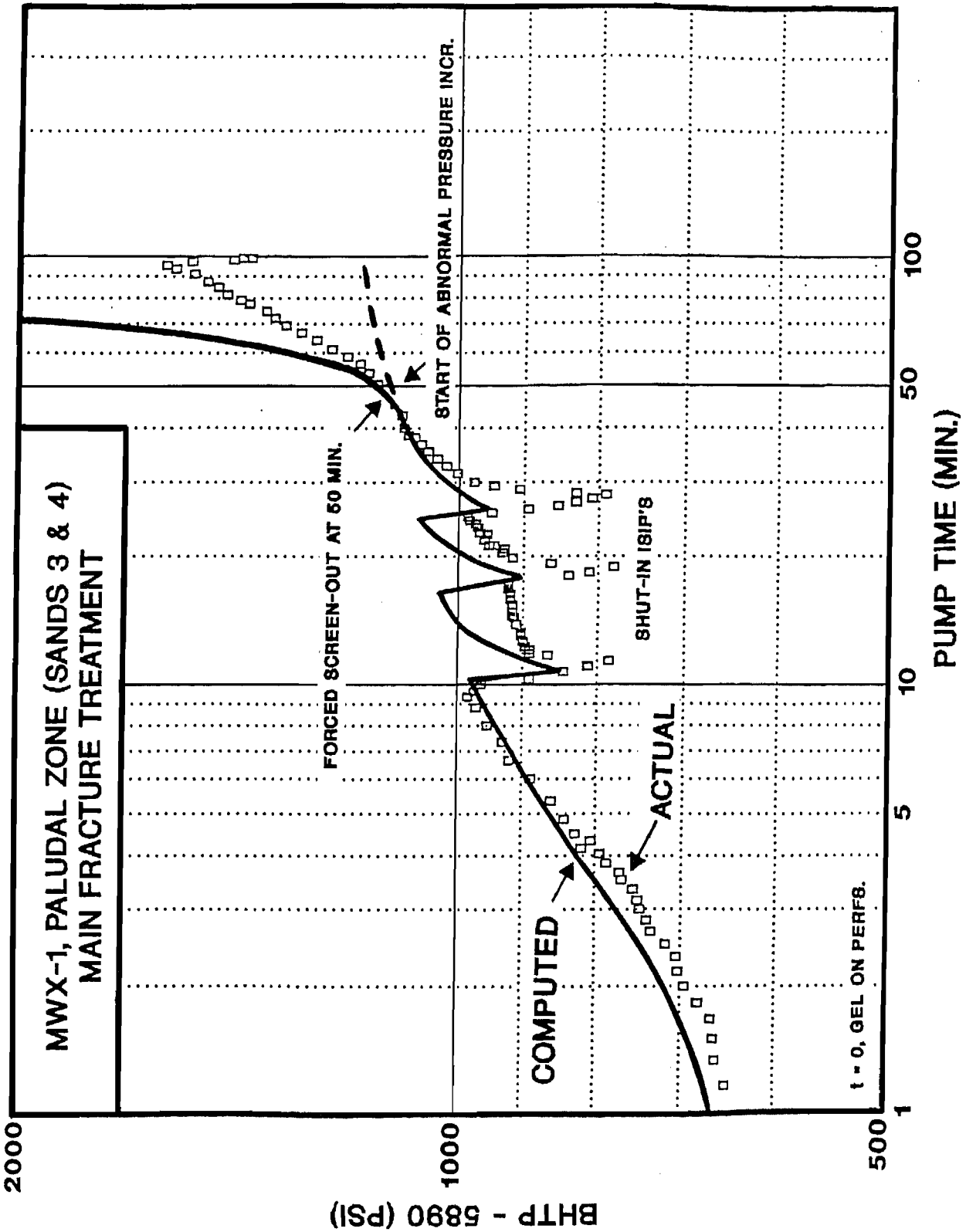


FIGURE 42: Simulated Pressure History for Paludal Fracture Treatment Assuming a Tip Screen-Out at 50 Minutes.

PALUDAL POST-FRAC TEMPERATURE LOG

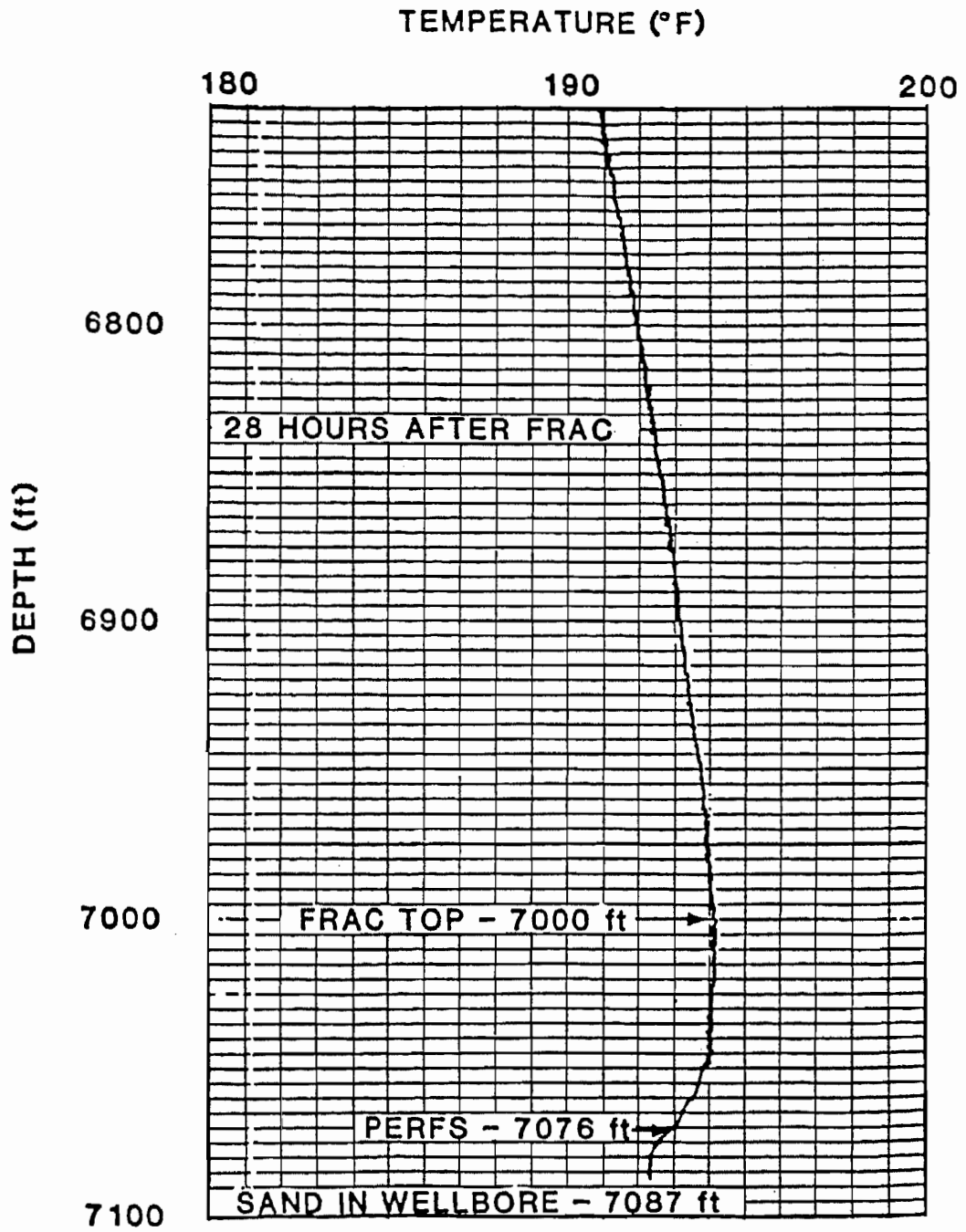


FIGURE 43: Post-Frac Temperature Log, MWX-1 Paludal Frac Treatment.

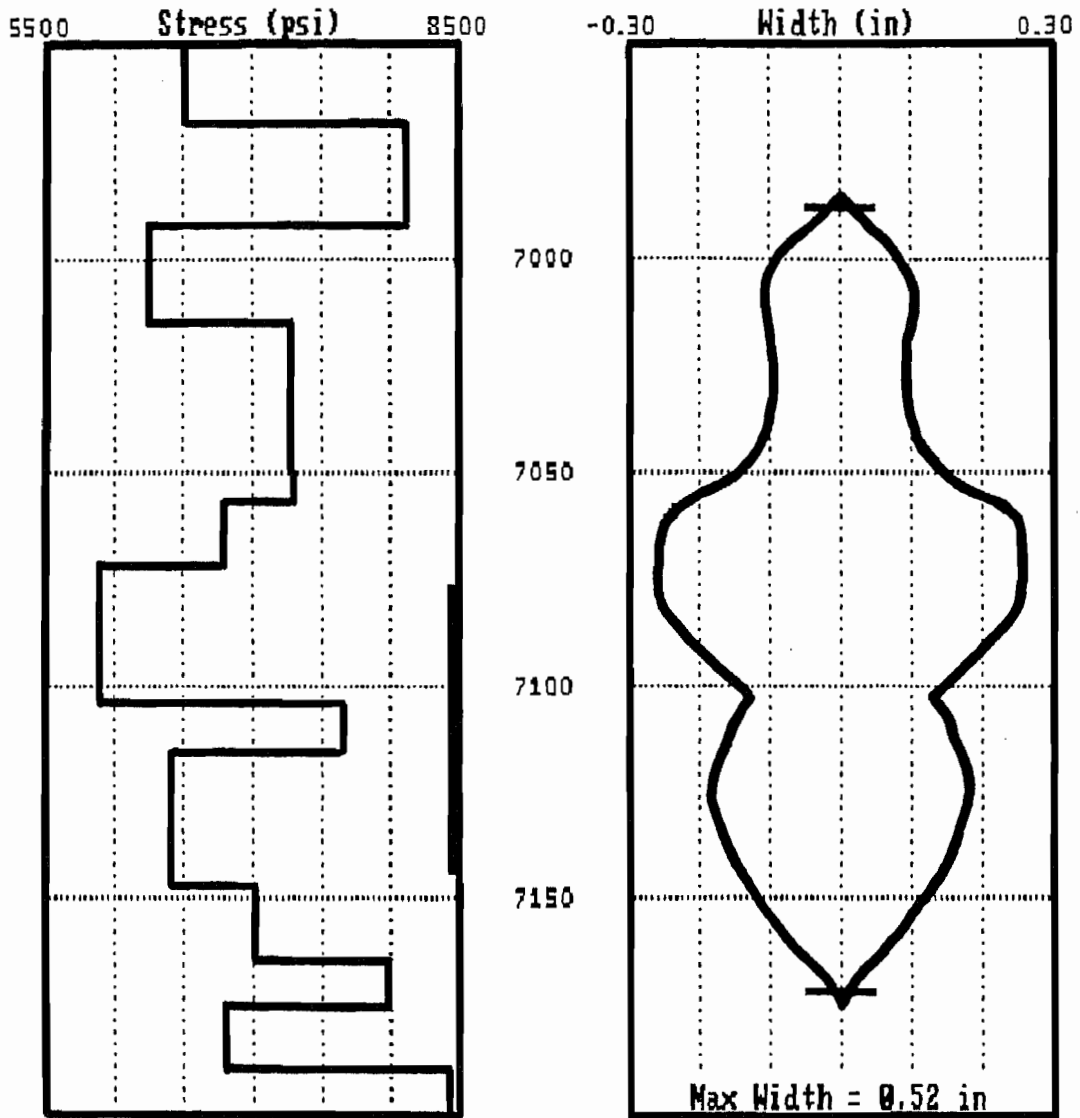


FIGURE 44: Computed Fracture Width-Height Profile for Main Fracture Treatment Pressure History Match, MMX-1 Paludal Zone.

TABLE 1: Summary of Sandia Stress Test Results.

TEST ZONE	DEPTH	GAMMA RAY	CLOSURE STRESS	FRAC GRADIENT	PORE PRES	OB PRES	K FACTOR
2F1	5851	90	5925	1.01	3400	6144	0.92
2F2	5941	115	5750	0.97	3465	6238	0.82
2F3	5963	65	4600	0.77	3480	6261	0.40
2F4	6007	110	6200	1.03	3500	6307	0.96
3C1	6375	125	6540	1.03	4300	6694	0.94
3C2	6399	140	6445	1.01	4300	6719	0.89
3C3	6421	140	6805	1.06	4400	6742	1.03
3C4	6443	55	5720	0.89	4400	6765	0.56
3C5	6461	65	5670	0.88	4400	6784	0.53
3C6	6513	75	5845	0.90	4400	6839	0.59
3C7	6528	145	6665	1.02	4400	6854	0.92
3C8	6549	53	5640	0.86	4400	6876	0.50
3C9	6566	120	6980	1.06	4400	6894	1.03
3C10	6607	120	7130	1.08	4500	6937	1.08
3C11U*	6707	90	7100	1.06	4600	7042	1.02
3C11L*	6766	90	7100	1.05	4600	7104	1.00
2P1 +	6929	115	5830	0.84	4950	7275	0.38
2P2 +	6964	70	5745	0.82	5030	7312	0.31
2P3 +	7011	90	6325	0.90	5140	7362	0.53
3P1 +	7033	160	6800	0.97	5190	7385	0.73
3P2 +	7049	30	7200	1.02	5230	7401	0.91
3P3 +	7069	115	5780	0.82	5300	7422	0.23
2P4	7170	80	7000	0.98	5300	7529	0.76
2P5 +	7207	75	6900	0.96	5450	7567	0.68
2P6	7264	50	6755	0.93	5500	7627	0.59
2P7	7304	110	6430	0.88	5550	7669	0.42
2P8	7395	65	6720	0.91	5600	7765	0.52
2P9	7424	30	6865	0.92	5600	7795	0.58
2M1 #	7467	50	6800	0.91	5800	7840	0.49
2M2 #	7531	55	6590	0.88	5850	7908	0.36
2M3 #	7601	85	7610	1.00	5900	7981	0.82
2M4	7665	105	8150	1.06	6300	8048	1.06
2M5	7766	105	8590	1.11	6300	8154	1.23
2M6 &	7850	50	6645	0.85	6150	8243	0.24
2M7	7895	80	6830	0.87	6300	8290	0.27
2M8	7924	90	7800	0.98	6300	8320	0.74
2M9	7971	60	6885	0.86	6300	8370	0.28
2M10	8015	110	8150	1.02	6800	8416	0.84
2M11	8061	90	8230	1.02	6800	8464	0.86

- * - ZONES IN COMMUNICATION
- + - ZONES WITH AVAILABLE BOTTOMHOLE PRESSURE DATA
- # - ESTIMATED PORE PRESSURE
- & - 3 TEN FOOT PERFORATED ZONES OPEN; 3 MONTH DRAWDOWN (PORE PRESSURE)

TEST	DEPTH	SANDIA CLOSURE	NSI CLOSURE	PORE PRES	OB PRES	SANDIA GRADIENT	NSI GRADIENT	SANDIA K	NSI K
2P1TST3	6929	5830	6015	4950	7275	0.84	0.87	0.38	0.46
2P1TST4	6929	5830	6200	4950	7275	0.84	0.89	0.38	0.54
2P2TST1	6964	5745	5750	5030	7312	0.82	0.83	0.31	0.32
2P2TST2	6964	5745	5835	5030	7312	0.82	0.84	0.31	0.35
2P2TST4	6964	5745	6000	5030	7312	0.82	0.86	0.31	0.43
2P3TST3	7011	6325	6295	5140	7362	0.90	0.90	0.53	0.52
2P3TST4	7011	6325	6200	5140	7362	0.90	0.90	0.53	0.51
2P3TST5	7011	6325	6300	5140	7362	0.90	0.90	0.53	0.52
3P1TST4	7033	6800	6710	5190	7385	0.97	0.95	0.73	0.69
3P1TST5	7033	6800	6675	5190	7385	0.97	0.95	0.73	0.68
3P1TST7	7033	6800	6795	5190	7385	0.97	0.97	0.73	0.73
3P1TST8	7033	6800	6710	5190	7385	0.97	0.95	0.73	0.69
3P2TST3	7049	7200	7125	5230	7401	1.02	1.01	0.91	0.87
3P2TST4	7049	7200	7235	5230	7401	1.02	1.03	0.91	0.92
3P2TST5	7049	7200	7135	5230	7401	1.02	1.01	0.91	0.88
3P3TST4	7069	5780	5700	5300	7422	0.82	0.81	0.23	0.19
3P3TST5	7069	5780	5690	5300	7422	0.82	0.80	0.23	0.18
2P5TST1	7207	6900	6820	5450	7567	0.96	0.95	0.68	0.65
2P5TST2	7207	6900	6820	5450	7567	0.96	0.95	0.68	0.65
2P5TST3	7207	6900	6865	5450	7567	0.96	0.95	0.68	0.67
2P5TST4	7207	6900	6845	5450	7567	0.96	0.95	0.68	0.66

TABLE 2: Summary of Paludal Zone Stress Data Re-analysis Results.

TEST ZONE	DEPTH	GAMMA RAY	MEAN GAMMA	STD DEV	FRAC GRADIENT	K (STRESS)	K (SONIC)
2F1	5851	90	100	10	1.01	0.92	0.353
2F2	5941	115	112	11	0.97	0.82	0.345
2F3	5963	65	63	4	0.77	0.40	0.269
2F4	6007	110	108	9	1.03	0.96	0.326
3C1	6375	125	121	18	1.03	0.94	-
3C2	6399	140	125	20	1.01	0.89	-
3C3	6421	140	132	15	1.06	1.03	-
3C4	6443	55	60	7	0.89	0.56	-
3C5	6461	65	65	2	0.88	0.53	-
3C6	6513	75	74	8	0.90	0.59	-
3C7	6528	145	118	21	1.02	0.92	-
3C8	6549	53	57	4	0.86	0.50	-
3C9	6566	120	113	15	1.06	1.03	-
3C10	6607	120	119	18	1.08	1.08	-
3C11U	6707	90	89	7	1.06	1.02	-
3C11L	6766	90	112	23	1.05	1.00	-
2P1	6929	115	101	8	0.84	0.38	*
2P2	6964	70	77	17	0.82	0.31	*
2P3	7011	90	94	13	0.90	0.53	0.416
3P1	7033	160	109	36	0.97	0.73	-
3P2	7049	30	56	30	1.02	0.91	-
3P3	7069	115	115	18	0.82	0.23	-
2P4	7170	80	85	5	0.98	0.76	0.300
2P5	7207	75	72	10	0.96	0.68	0.410
2P6	7264	50	60	11	0.93	0.59	0.230
2P7	7304	110	103	9	0.88	0.42	0.387
2P8	7395	65	68	7	0.91	0.52	0.341
2P9	7424	30	35	13	0.92	0.58	*
2M1	7467	50	53	4	0.91	0.49	0.239
2M2	7531	55	56	2	0.88	0.36	0.291
2M3	7601	85	81	2	1.00	0.82	0.290
2M4	7665	105	102	3	1.06	1.06	0.364
2M5	7766	105	105	2	1.11	1.23	0.354
2M6	7850	50	50	8	0.85	0.24	0.178
2M7	7895	80	87	8	0.87	0.27	0.279
2M8	7924	90	90	2	0.98	0.74	0.300
2M9	7971	60	60	1	0.86	0.28	0.233
2M10	8015	110	110	7	1.02	0.84	0.330
2M11	8061	90	92	2	1.02	0.86	0.298

* - NO USABLE SONIC LOG INFORMATION IN ZONE

TABLE 3: Summary of Stress, Sonic Log, and Mean Gamma Ray Data Considered for Correlation Analysis.

TABLE NO. 4

WORKSHEET FOR PRESSURE DECLINE ANALYSIS - PERKINS & KERN GEOMETRY

Input Data:

Young's Modulus = E' = 4.5×10^6 psi (Source - Sandia)
 Pump Time = t_p = 43.1 min (Source - Minifrac Data)
 Volume Pumped = V = 15,000 gal (Source - Minifrac Data)
 ISIP = 6701 psi (Source - NSI)
 Closure Pressure = σ_c = 6411 psi (Source - NSI)
 Closure time = Δt_c = 20.3 min (Source - NSI)
 Net $p = p_s = \text{ISIP} - \text{Closure Pressure} = 290$ psi
 Match $p = P^*$ (from Type Curves) = 400 psi

Geometry Parameters:

$g_o = 1.45$, $g_c = 1.00$, $\beta' = 0.638$, $K = 1.00$

EFFICIENCY ANALYSIS

from time-to-close and graph * from pressures
 efficiency = $e_f = 0.275$ * $\rho = \pi p_s / 4 K g_o P^* = 0.393$
 * $e_f = \rho / (1 + \rho) = 0.282$
 use efficiency $e_f = 0.28$

LEAK-OFF COEFFICIENT

Leak-Off Coefficient (ft/min**0.5) = $C = P^* \beta' h / r_p t_p^{**0.5} E'$; $r_p = h_p/h$

CASE 1: $h = 135'$, $h_p = 55'$ $C = [(400)(.638)(135)]/[(0.41)(6.57)(4.5 \times 10^6)]$
 $C = 0.0028$ ft/min**0.5

CASE 2: $h = 55'$, $h_p = 55'$ $C = [(400)(.638)(55)]/[(1.00)(6.57)(4.5 \times 10^6)]$
 $C = 0.00047$ ft/min**0.5

TABLE NO. 5

WORKSHEET FOR PRESSURE DECLINE ANALYSIS - PERKINS & KERN GEOMETRY

Input Data:

Young's Modulus = E' = 4.5×10^6 psi (Source - Sandia)
 Pump Time = t_p = 43.1 min (Source - Minifrac Data)
 Volume Pumped = V = 15,000 gal (Source - Minifrac Data)
 ISIP = 6701 psi (Source - NSI)
 Closure Pressure = σ_c = 5890 psi (Source - NSI)
 Closure time = Δt_c = 148.5 min (Source - NSI)
 Net $p = p_s =$ ISIP - Closure Pressure = 811 psi
 Match $p = P^*$ (from Type Curves) = 192 psi

Geometry Parameters:

$g_o = 1.45$, $g_c = 1.00$, $\beta' = 0.638$, $K = 1.00$

EFFICIENCY ANALYSIS

from time-to-close and graph * from pressures
 efficiency = $e_f = 0.630$ * $\rho = \pi p_s / 4 K g_o P^* = 2.290$
 * $e_f = \rho / (1 + \rho) = 0.690$
 use efficiency $e_f = 0.660$

LEAK-OFF COEFFICIENT

Leak-Off Coefficient (ft/min**0.5) = $C = P^* \beta' h / r_p t_p^{**0.5} E'$; $r_p = h_p/h$

CASE 3: $h = 135'$, $h_p = 55'$ $C = [(192)(.638)(135)]/[(.185)(6.57)(4.5 \times 10^6)]$
 $C = 0.0030$ ft/min**0.5

CASE 4: $h = 135'$, $h_p = 55'$ $C = [(192)(.638)(135)]/[(0.41)(6.57)(4.5 \times 10^6)]$
 $C = 0.0014$ ft/min**0.5

CASE 5: $h = 25'$, $h_p = 25'$ $C = [(192)(.638)(25)]/[(1.00)(6.57)(4.5 \times 10^6)]$
 $C = 0.0001$ ft/min**0.5

CASE 6: $h = 55'$, $h_p = 55'$ $C = [(192)(.638)(55)]/[(1.00)(6.57)(4.5 \times 10^6)]$
 $C = 0.00022$ ft/min**0.5

TABLE NO. 6
WORKSHEET FOR PRESSURE DECLINE ANALYSIS - PERKINS & KERN GEOMETRY

Input Data:

Young's Modulus = E' = 4.5×10^6 psi (Source - Sandia)
 Pump Time = t_p = 63.4 min (Source - Minifrac Data)
 Volume Pumped = V = 15,000 gal (Source - Minifrac Data)
 ISIP = 6411 psi (Source - NSI)
 Closure Pressure = σ_c = 5890 psi (Source - NSI)
 Closure time = Δt_c = 128.2 min (Source - NSI)
 Net $p = p_s = \text{ISIP} - \text{Closure Pressure} = 521$ psi
 Match $p = P^*$ (from Type Curves) = 192 psi

Geometry Parameters:

$g_o = 1.45$, $g_c = 1.00$, $\beta' = 0.638$, $K = 1.00$

EFFICIENCY ANALYSIS

from time-to-close and graph * from pressures
 efficiency = $e_f = 0.550$ * $\rho = \pi p_s / 4 K g_o P^* = 1.470$
 * $e_f = \rho / (1 + \rho) = 0.590$
 use efficiency $e_f = 0.570$

LEAK-OFF COEFFICIENT

Leak-Off Coefficient (ft/min**0.5) = $C = P^* \beta' h / r_p t_p^{**0.5} E'$; $r_p = h_p/h$

CASE 7: $h = 135'$, $h_p = 25'$ $C = [(192)(.638)(135)] / [(.185)(7.96)(4.5 \times 10^6)]$
 $C = 0.0025$ ft/min**0.5

CASE 8: $h = 25'$, $h_p = 25'$ $C = [(192)(.638)(25)] / [(1.00)(7.96)(4.5 \times 10^6)]$
 $C = 0.00009$ ft/min**0.5

TABLE NO. 7
 MWX-1, MINIFRAC #1, PALUDAL ZONE
 RESULTS OF PRESSURE DECLINE ANALYSIS

<u>CASE</u>	<u>t(o)</u> (min)	<u>P(c)</u> (psi)	<u>t(c)</u> (min)	<u>Eff.</u>	<u>h</u> (ft)	<u>h(p)</u> (ft)	<u>P*</u> (psi)	<u>C</u> (ft/min**.5)
1	43.1	6411	20.3	0.28	135	55	400	0.0028
2	43.1	6411	20.3	0.28	55	55	400	0.00047
3	43.1	5890	148.5	0.66	135	25	192	0.0030
4	43.1	5890	148.5	0.66	135	55	192	0.0014
5	43.1	5890	148.5	0.66	25	25	192	0.00010
6	43.1	5890	148.5	0.66	55	55	192	0.00022
7	63.4	5890	128.2	0.57	135	25	192	0.0025
8	63.4	5890	128.2	0.57	25	25	192	0.00009
<u>SANDIA</u>								
	43.0	5805	180.0	-	135	55	180	0.0013

TABLE NO. 8

WORKSHEET FOR PRESSURE DECLINE ANALYSIS - PERKINS & KERN GEOMETRY

Input Data:

Young's Modulus = E' = 4.5×10^6 psi (Source - Sandia)
 Pump Time = t_p = 88.0 min (Source - Minifrac Data)
 Volume Pumped = V = 30,000 gal (Source - Minifrac Data)
 ISIP = psi (Source - NSI)
 Closure Pressure = σ_c = psi (Source - NSI)
 Closure time = Δt_c = min (Source - NSI)
 Net $p = p_s = \text{ISIP} - \text{Closure Pressure} =$ psi
 Match $p = P^*$ (from Type Curves) = 103 psi

Geometry Parameters:

$g_o = 1.45$, $g_c = 1.00$, $\beta' = 0.594$, $K = 1.00$

EFFICIENCY ANALYSIS

from time-to-close and graph * from pressures
 efficiency = $e_f =$ * $\rho = \pi p_s / 4 K g_o P^* =$
 * $e_f = \rho / (1 + \rho) =$
 use efficiency $e_f =$

LEAK-OFF COEFFICIENT

Leak-Off Coefficient (ft/min**0.5) = $C = P^* \beta' h / r_p t_p^{**0.5} E'$; $r_p = h_p/h$

CASE 1: $h = 150'$, $h_p = 55'$ $C = [(103)(.594)(150)] / [(0.37)(9.38)(4.5 \times 10^6)]$
 $C = 0.0006 \text{ ft/min}^{**0.5}$

CASE 2: $h = 55'$, $h_p = 55'$ $C = [(103)(.594)(55)] / [(1.00)(9.38)(4.5 \times 10^6)]$
 $C = 0.00008 \text{ ft/min}^{**0.5}$

CASE 3: $h = 25'$, $h_p = 25'$ $C = [(103)(.594)(25)] / [(1.00)(9.38)(4.5 \times 10^6)]$
 $C = 0.00004 \text{ ft/min}^{**0.5}$

TABLE NO. 9
MWX-1 PALUDAL ZONE FRACTURE TREATMENT SCHEDULE

<u>Stage</u>	<u>Fluid Type</u>	<u>Fluid Volume</u> (gals)	<u>Sand Mesh</u>	<u>Sand Conc.</u> (lbs/gal)
1	Methanol	7,700	Prepad	Prepad
2	Apollo 40	18,000	Pad	Pad
3	Apollo 35	3,000	20/40	1.5
4	Apollo 35	5,000	20/40	2.0
5	Apollo 35	6,000	20/40	3.0
6	Apollo 35	14,000	20/40	4.0
7	Apollo 25	18,000	20/40	5.5
8	Apollo 25	1,000	12/20	5.5
9	Water	8,764	Flush	Flush

Total Volume : 81,464 gals of which 65,000 gals was gel.

Total Sand : 193,000 lbs.

APPENDIX

COMPUTER SIMULATIONS OF MWX-1, PALUDAL MINIFRACS
AND MAIN FRACTURE TREATMENT

CONTENTS	PAGE

A.1 Minifrac No. 1, C = 0.0001 ft/min**0.5	86
A.2 Minifrac No. 1, C = 0.0002 ft/min**0.5	93
A.3 Minifrac No. 1, C = 0.0003 ft/min**0.5	100
A.4 Minifrac No. 1, C = 0.0010 ft/min**0.5	107
A.5 Minifrac No. 2, C = 0.00005 ft/min**0.5	114
A.6 Minifrac No. 2, C = 0.0001 ft/min**0.5	120
A.7 Minifrac No. 2, C = 0.0002 ft/min**0.5	126
A.8 Main Frac Treatment, C = 0.0001 ft/min**0.5	132
A.9 Main Frac Treatment, Forcing Screen-Out @ 50 min. ...	143
A.10 Main Frac Treatment, Simulating Propped Length at 50 minutes	152

A.1

MINIFRAC NO. 1, C = 0.0001 ft/min**0.5

Frac Summary * MWX-1, MINIFRAC #1

Design Data					
FLUID LOSS:	Coefficient (ft/sqrt(min))	0.0001		
	Spurt Loss (gal/100 sq ft)	0.00		
FORMATION:	Modulus (MM psi)	4.50		
	Fracture Height (ft)	72.0		
	Fluid Loss Height (ft)	55.0		
	Perforated Height (ft)	68.0		
TEMPERATURE:	Bottom Hole (deg F)	180		
PRESSURE:	Reservoir Pressure (psi)	5200.0		
	Closure Pressure (psi)	5890.0		
DEPTH:	Well Depth (ft)	7076		
FROMATION LAYER DATA:					
Depth	Stress at Top	Stres Grad	Modulus	Toughnesss	
6952	6520.0	0.000	4.50	1.00	
6969	8120.0	0.000	4.50	1.00	
6992	6240.0	0.000	4.50	1.00	
7015	7275.0	0.000	4.50	1.00	
7049	7300.0	0.000	4.50	1.00	
7057	6800.0	0.000	4.50	1.00	
7072	5890.0	0.000	4.00	1.00	
7104	7660.0	0.000	4.00	1.00	
7116	6410.0	0.000	4.00	1.00	
7147	7000.0	0.000	4.50	1.00	
7165	8000.0	0.000	4.50	1.00	
7175	6800.0	0.000	4.50	1.00	
7190	8420.0	0.000	4.50	1.00	
7201	7300.0	0.000	4.50	1.00	
7242	6360.0	0.433	4.50	1.00	
	Fluid Pressure Gradient (psi/ft)	0.433		
	Fracture Top (ft)	7076		
	Fracture Bottom (ft)	7144		

Calculated Results from 3-D Simulator	
STIMPLAN (TM) , NSI , Tulsa,OK	
Licensed To: Internal Use - NSI Technologies	
1/2 LENGTH:	'Hydraulic' length (ft) 2409
	Propped length (ft) 0
PRESSURE:	Max Net Pressure (psi) 880
TIME:	Max Exposure to Form. Temp. (min) .. 28.1
	Time to Close (min) 205.3
RATE:	Fluid Loss Rate during pad (bpm) ... 0.0
EFFICIENCY:	at end of pumping schedule 0.67
PROPPANT:	Average In Situ Conc. (#/sq ft) 0.0
	Average Conductivity (md-ft) 0
HEIGHT:	Max Fracture Height (ft) 114
WIDTH:	Avg width at end of pumping (in) ... 0.03

Fluid ID No.	2						30#

Specific Gravity						1.04	
	@Welbor	@FormTmp	@1Hr	@2Hr	@4Hr	@8Hr	
vis (cp @ 170 1/sec)	32	20	10	5	5	5	
non-Newtonian n'	0.58	0.67	0.80	0.90	0.90	0.90	

Time History * NSI STIMPLAN 3-D Fracture Simulation
MWX-1, MINIFRAC #1

Time (min)	Pen (ft)	Pres (psi)	Rate (bpm)	Prop (PPG)	Sl Vol (MGal)	Eff- ciency	Loss (bpm)	Hght (ft)	W-Avg (in)
0.5	140	421	10.0	0.0	0.2	0.67	1.3	72	0.01
0.7	210	437	10.0	0.0	0.3	0.60	1.7	72	0.01
1.0	280	465	10.0	0.0	0.4	0.59	2.0	72	0.01
1.5	350	496	10.0	0.0	0.6	0.60	2.0	72	0.01
1.9	420	528	10.0	0.0	0.8	0.61	2.1	72	0.01
2.4	490	562	10.0	0.0	1.0	0.61	2.2	72	0.01
2.9	560	588	10.0	0.0	1.2	0.62	2.3	72	0.01
3.3	630	609	10.0	0.0	1.4	0.62	2.4	72	0.02
3.9	700	626	10.0	0.0	1.6	0.62	2.5	73	0.02
4.4	770	635	10.0	0.0	1.9	0.62	2.5	74	0.02
5.0	840	649	10.0	0.0	2.1	0.62	2.6	75	0.02
5.6	910	651	10.0	0.0	2.3	0.62	2.7	76	0.02
6.2	980	660	10.0	0.0	2.6	0.62	2.7	76	0.02
6.9	1050	670	10.0	0.0	2.9	0.62	2.8	77	0.02
7.6	1120	685	10.0	0.0	3.2	0.62	2.8	78	0.02
8.3	1190	690	10.0	0.0	3.5	0.62	2.8	79	0.02
9.1	1260	700	10.0	0.0	3.8	0.62	2.8	79	0.02
10.0	1330	700	10.0	0.0	4.2	0.62	2.8	79	0.02
10.8	1400	713	10.0	0.0	4.6	0.63	2.8	88	0.02
11.8	1470	693	10.0	0.0	4.9	0.63	2.8	88	0.02
12.7	1540	724	10.0	0.0	5.3	0.63	2.9	90	0.02
13.7	1610	715	10.0	0.0	5.8	0.63	2.9	90	0.02
14.7	1680	764	10.0	0.0	6.2	0.63	2.9	94	0.02
15.7	1750	768	10.0	0.0	6.6	0.63	2.9	96	0.02
16.8	1820	793	10.0	0.0	7.1	0.63	2.9	99	0.02
18.0	1890	783	10.0	0.0	7.6	0.63	2.9	99	0.03
19.2	1960	817	10.0	0.0	8.1	0.64	2.9	103	0.03
20.7	2030	810	10.0	0.0	8.7	0.64	2.8	103	0.03
22.5	2100	849	10.0	0.0	9.5	0.64	2.8	108	0.03
24.9	2170	834	10.0	0.0	10.5	0.65	2.6	108	0.03
27.3	2240	878	10.0	0.0	11.5	0.66	2.5	113	0.03
29.3	2286	834	10.0	0.0	12.3	0.66	2.3	113	0.03
30.5	2301	797	0.2	0.0	12.3	0.65	2.2	113	0.03
32.8	2336	860	10.0	0.0	13.3	0.66	2.3	113	0.03
35.3	2371	880	10.0	0.0	14.4	0.67	2.2	113	0.03
36.9	2391	877	10.0	0.0	15.0	0.67	2.0	114	0.03
39.1	2409	796	0.0	0.0	15.0	0.66	2.0	114	0.03
53.0	2409	717	0.0	0.0	15.0	0.60	1.5	114	0.03
70.6	2409	637	0.0	0.0	15.0	0.53	1.3	114	0.03
91.3	2409	557	0.0	0.0	15.0	0.46	1.1	114	0.02
115.2	2409	478	0.0	0.0	15.0	0.40	1.0	114	0.02
142.2	2409	398	0.0	0.0	15.0	0.33	0.9	114	0.02
172.4	2409	319	0.0	0.0	15.0	0.26	0.8	114	0.01
205.8	2409	239	0.0	0.0	15.0	0.20	0.7	114	0.01
242.2	2409	159	0.0	0.0	15.0	0.13	0.6	114	0.01

GEOMETRY SUMMARY * At End of Pumping Schedule
MWX-1, MINIFRAC #1

Dstnce (ft)	Press (psi)	W-Avg (in)	Q (bpm)	Sh-Rate (1/sec)	-----Hght (ft)-----			Bank Prop Fraction	Prop (PSF)	
					Total	Up	Dn			
35	871	0.09	5.0	210	114	34	12	107	0.00	0.00
105	859	0.09	4.9	222	112	32	12	105	0.00	0.00
175	847	0.08	4.8	233	110	31	11	104	0.00	0.00
245	833	0.08	4.7	246	109	30	10	103	0.00	0.00
315	818	0.08	4.5	259	107	29	10	101	0.00	0.00
385	802	0.07	4.3	273	105	28	9	100	0.00	0.00
455	787	0.07	4.1	286	103	26	8	98	0.00	0.00
525	771	0.07	3.8	301	100	25	8	95	0.00	0.00
595	753	0.07	3.6	321	98	23	7	93	0.00	0.00
665	740	0.06	3.3	332	95	21	6	91	0.00	0.00
735	721	0.06	3.0	357	91	19	5	87	0.00	0.00
805	644	0.05	2.7	433	89	17	4	85	0.00	0.00
875	644	0.03	2.0	911	76	11	0	71	0.00	0.00
945	621	0.03	1.7	830	76	9	0	73	0.00	0.00
1015	631	0.03	1.4	1067	74	7	0	72	0.00	0.00
1085	615	0.02	1.3	1174	73	6	0	72	0.00	0.00
1155	568	0.02	1.2	1264	72	4	0	72	0.00	0.00
1225	511	0.02	1.1	1430	72	4	0	72	0.00	0.00
1295	472	0.02	0.9	1491	72	4	0	72	0.00	0.00
1365	429	0.02	0.8	1575	72	4	0	72	0.00	0.00
1435	400	0.02	0.8	1768	72	4	0	72	0.00	0.00
1505	389	0.02	0.7	1835	72	4	0	72	0.00	0.00
1575	377	0.01	0.7	1880	72	4	0	72	0.00	0.00
1645	365	0.01	0.7	1930	72	4	0	72	0.00	0.00
1715	352	0.01	0.7	1988	72	4	0	72	0.00	0.00
1785	338	0.01	0.6	2057	72	4	0	72	0.00	0.00
1855	323	0.01	0.6	2139	72	4	0	72	0.00	0.00
1925	306	0.01	0.6	2241	72	4	0	72	0.00	0.00
1995	287	0.01	0.5	2373	72	4	0	72	0.00	0.00
2065	267	0.01	0.5	2554	72	4	0	72	0.00	0.00
2135	242	0.01	0.4	2828	72	4	0	72	0.00	0.00
2205	210	0.01	0.4	3328	72	4	0	72	0.00	0.00
2271	172	0.01	0.3	4212	72	4	0	72	0.00	0.00
2319	138	0.01	0.3	5350	72	4	0	72	0.00	0.00
2354	112	0.00	0.2	6655	72	4	0	72	0.00	0.00
2381	58	0.00	0.2	9999	72	4	0	72	0.00	0.00

FLUID SUMMARY * At End of Pumping Schedule
MWX-1, MINIFRAC #1

Stage	Fluid	Prop	Pos	Concentration			Fl Vol	Ex Tim	Temp	Visc	Fall	
No	Gone	ID	ID	(ft)	In	Now	Desgn	(MGal)	(min)	(deg F)	(cp)	Frac
1	1	3	1	2391	0.0	0.0	0.0	0.2	5.3	180	2	0.00
1	1	3	1	2391	0.0	0.0	0.0	0.3	6.4	180	2	0.00
1	1	3	1	2391	0.0	0.0	0.0	0.4	8.3	180	2	0.00
1	1	3	1	2391	0.0	0.0	0.0	0.6	9.2	180	2	0.00
1	1	3	1	2391	0.0	0.0	0.0	0.8	11.6	180	2	0.00
1	1	3	1	2391	0.0	0.0	0.0	1.0	13.2	180	2	0.00
1	1	3	1	2391	0.0	0.0	0.0	1.2	14.4	180	2	0.00
1	1	3	1	2391	0.0	0.0	0.0	1.4	16.9	180	2	0.00
1	1	3	1	2391	0.0	0.0	0.0	1.6	18.4	180	2	0.00
1	1	3	1	2391	0.0	0.0	0.0	1.9	22.4	180	2	0.00
1	1	3	1	2391	0.0	0.0	0.0	2.1	25.1	180	2	0.00
1	1	3	1	2391	0.0	0.0	0.0	2.3	26.8	180	2	0.00
1	0	3	1	2366	0.0	0.0	0.0	2.5	28.1	180	2	0.00
2	0	1	1	2343	0.0	0.0	0.1	2.6	27.4	180	2	0.00
2	0	1	1	2287	0.0	0.0	0.2	2.9	26.6	180	2	0.00
2	0	1	1	2192	0.0	0.0	0.3	3.2	25.7	180	2	0.00
2	0	1	1	2082	0.0	0.0	0.3	3.5	23.9	180	2	0.00
2	0	1	1	1960	0.0	0.0	0.4	3.8	21.9	180	2	0.00
2	0	1	1	1826	0.0	0.0	0.4	4.2	20.9	180	2	0.00
2	0	1	1	1680	0.0	0.0	0.5	4.5	18.7	180	2	0.00
2	0	1	1	1524	0.0	0.0	0.6	4.9	17.5	180	2	0.00
2	0	1	1	1431	0.0	0.0	0.6	5.0	17.5	180	2	0.00
3	0	2	1	1353	0.0	0.0	0.6	5.3	14.5	180	7	0.00
3	0	2	1	1209	0.0	0.0	0.7	5.7	10.0	180	7	0.00
3	0	2	1	1061	0.0	0.0	0.7	6.1	10.0	180	8	0.00
3	0	2	1	931	0.0	0.0	0.8	6.5	7.8	180	9	0.00
3	0	2	1	830	0.0	0.0	0.9	7.0	4.5	180	10	0.00
3	0	2	1	756	0.0	0.0	0.9	7.4	2.1	180	11	0.00
3	0	2	1	689	0.0	0.0	0.9	7.9	2.1	180	12	0.00
3	0	2	1	618	0.0	0.0	0.9	8.6	0.0	124	14	0.00
3	0	2	1	539	0.0	0.0	0.9	9.3	0.0	95	15	0.00
3	0	2	1	447	0.0	0.0	0.9	10.2	0.0	90	16	0.00
3	0	2	1	348	0.0	0.0	1.0	11.2	0.0	86	17	0.00
3	0	2	1	261	0.0	0.0	1.0	12.0	0.0	82	17	0.00
4	0	2	1	223	0.0	0.0	1.0	12.0	0.0	81	17	0.00
5	0	2	1	182	0.0	0.0	1.0	12.9	0.0	79	18	0.00
5	0	2	1	96	0.0	0.0	1.0	14.0	0.0	74	19	0.00
5	0	2	1	26	0.0	0.0	1.0	14.6	0.0	72	19	0.00

A.2

MINIFRAC NO. 1, C = 0.0002 ft/min**0.5

Frac Summary * MWX-1, MINIFRAC #1

Design Data					
FLUID LOSS:	Coefficient (ft/sqrt(min))	0.0002		
	Spurt Loss (gal/100 sq ft)	0.00		
FORMATION:	Modulus (MM psi)	4.50		
	Fracture Height (ft)	72.0		
	Fluid Loss Height (ft)	55.0		
	Perforated Height (ft)	68.0		
TEMPERATURE:	Bottom Hole (deg F)	180		
PRESSURE:	Reservoir Pressure (psi)	5200.0		
	Closure Pressure (psi)	5890.0		
DEPTH:	Well Depth (ft)	7076		
FROMATION LAYER DATA:					
Depth	Stress at Top	Stres Grad	Modulus	Toughnesss	
6952	6520.0	0.000	4.50	1.00	
6969	8120.0	0.000	4.50	1.00	
6992	6240.0	0.000	4.50	1.00	
7015	7275.0	0.000	4.50	1.00	
7049	7300.0	0.000	4.50	1.00	
7057	6800.0	0.000	4.50	1.00	
7072	5890.0	0.000	4.00	1.00	
7104	7660.0	0.000	4.00	1.00	
7116	6410.0	0.000	4.00	1.00	
7147	7000.0	0.000	4.50	1.00	
7165	8000.0	0.000	4.50	1.00	
7175	6800.0	0.000	4.50	1.00	
7190	8420.0	0.000	4.50	1.00	
7201	7300.0	0.000	4.50	1.00	
7242	6360.0	0.433	4.50	1.00	
	Fluid Pressure Gradient (psi/ft)		0.433	
	Fracture Top (ft)		7076	
	Fracture Bottom (ft)		7144	

Calculated Results from 3-D Simulator	
STIMPLAN (TM) , NSI , Tulsa,OK	
Licensed To: Internal Use - NSI Technologies	
1/2 LENGTH:	'Hydraulic' length (ft) 1682
	Propped length (ft) 0
PRESSURE:	Max Net Pressure (psi) 862
TIME:	Max Exposure to Form. Temp. (min) .. 24.0
	Time to Close (min) 101.1
RATE:	Fluid Loss Rate during pad (bpm) ... 0.0
EFFICIENCY:	at end of pumping schedule 0.56
PROPPANT:	Average In Situ Conc. (#/sq ft) 0.0
	Average Conductivity (md-ft) 0
HEIGHT:	Max Fracture Height (ft) 111
WIDTH:	Avg width at end of pumping (in) ... 0.04

Fluid ID No. 2		30#				
Specific Gravity						1.04
	@Welbor	@FormTmp	@1Hr	@2Hr	@4Hr	@8Hr
vis (cp @ 170 l/sec)	32	20	10	5	5	5
non-Newtonian n'	0.58	0.67	0.80	0.90	0.90	0.90

Time History * NSI STIMPLAN 3-D Fracture Simulation
MWX-1, MINIFRAC #1

Time (min)	Pen (ft)	Pres (psi)	Rate (bpm)	Prop (PPG)	Sl Vol (MGal)	Eff- ciency	Loss (bpm)	Hght (ft)	W-Avg (in)
0.4	120	396	10.0	0.0	0.2	0.59	2.4	72	0.01
0.7	180	419	10.0	0.0	0.3	0.52	3.0	72	0.01
1.0	240	446	10.0	0.0	0.4	0.50	3.4	72	0.01
1.4	300	477	10.0	0.0	0.6	0.51	3.4	72	0.01
1.9	360	504	10.0	0.0	0.8	0.51	3.5	72	0.01
2.3	420	539	10.0	0.0	1.0	0.51	3.7	72	0.01
2.8	480	563	10.0	0.0	1.2	0.51	3.9	72	0.01
3.4	540	583	10.0	0.0	1.4	0.50	4.0	72	0.01
3.9	600	599	10.0	0.0	1.6	0.50	4.2	72	0.02
4.5	660	617	10.0	0.0	1.9	0.49	4.3	73	0.02
5.1	720	626	10.0	0.0	2.1	0.49	4.4	74	0.02
5.7	780	636	10.0	0.0	2.4	0.49	4.5	75	0.02
6.4	840	642	10.0	0.0	2.7	0.49	4.6	75	0.02
7.1	900	662	10.0	0.0	3.0	0.48	4.6	76	0.02
7.8	960	675	10.0	0.0	3.3	0.48	4.6	77	0.02
8.7	1020	681	10.0	0.0	3.7	0.48	4.6	78	0.02
9.5	1080	690	10.0	0.0	4.0	0.48	4.7	79	0.02
10.5	1140	693	10.0	0.0	4.4	0.48	4.7	79	0.02
11.4	1200	699	10.0	0.0	4.8	0.48	4.7	79	0.02
12.4	1260	697	10.0	0.0	5.2	0.48	4.7	79	0.02
13.4	1320	727	10.0	0.0	5.6	0.48	4.8	89	0.02
14.5	1380	731	10.0	0.0	6.1	0.48	4.7	90	0.02
15.7	1440	785	10.0	0.0	6.6	0.48	4.7	97	0.02
17.2	1500	778	10.0	0.0	7.3	0.48	4.6	98	0.02
19.2	1560	832	10.0	0.0	8.1	0.49	4.4	105	0.02
22.3	1620	830	10.0	0.0	9.4	0.50	4.0	106	0.03
25.0	1650	862	10.0	0.0	10.5	0.52	3.7	110	0.03
27.7	1665	830	10.0	0.0	11.6	0.53	3.3	110	0.03
29.3	1682	860	10.0	0.0	12.3	0.54	3.1	111	0.03
30.5	1682	788	0.2	0.0	12.3	0.52	3.0	111	0.03
32.0	1682	814	10.0	0.0	13.0	0.53	2.9	111	0.03
33.5	1682	817	10.0	0.0	13.6	0.54	2.8	111	0.04
35.0	1682	822	10.0	0.0	14.2	0.55	2.7	111	0.04
36.9	1682	848	10.0	0.0	15.0	0.56	2.6	111	0.04
45.4	1682	764	0.0	0.0	15.0	0.50	2.2	111	0.04
55.1	1682	679	0.0	0.0	15.0	0.45	2.0	111	0.04
66.0	1682	594	0.0	0.0	15.0	0.39	1.8	111	0.03
78.1	1682	509	0.0	0.0	15.0	0.34	1.6	111	0.03
91.4	1682	424	0.0	0.0	15.0	0.28	1.5	111	0.02
105.8	1682	339	0.0	0.0	15.0	0.22	1.4	111	0.02
121.3	1682	255	0.0	0.0	15.0	0.17	1.3	111	0.01
138.0	1682	170	0.0	0.0	15.0	0.11	1.2	111	0.01

GEOMETRY SUMMARY * At End of Pumping Schedule
MWX-1, MINIFRAC #1

Dstnce (ft)	Press (psi)	W-Avg (in)	Q (bpm)	Sh-Rate (1/sec)	-----Hght (ft)-----			Bank Prop Fraction	Prop (PSF)	
					Total	Up	Dn			
30	846	0.08	5.0	240	111	31	11	104	0.00	0.00
90	842	0.08	4.8	245	109	31	11	103	0.00	0.00
150	837	0.08	4.6	250	107	29	10	102	0.00	0.00
210	833	0.08	4.5	257	106	28	9	100	0.00	0.00
270	828	0.08	4.3	263	104	27	9	99	0.00	0.00
330	824	0.07	4.1	272	102	26	8	97	0.00	0.00
390	819	0.07	3.9	282	99	24	7	95	0.00	0.00
450	816	0.07	3.7	337	93	22	6	86	0.00	0.00
510	811	0.06	3.6	375	88	16	3	84	0.00	0.00
570	806	0.04	3.4	1072	75	11	0	71	0.00	0.00
630	801	0.04	3.3	1051	75	8	0	73	0.00	0.00
690	796	0.04	3.2	1033	75	8	0	73	0.00	0.00
750	790	0.03	3.0	1464	73	7	0	71	0.00	0.00
810	784	0.03	2.9	1489	73	5	0	72	0.00	0.00
870	778	0.03	2.8	1610	72	4	0	72	0.00	0.00
930	772	0.03	2.7	1558	72	4	0	72	0.00	0.00
990	767	0.03	2.5	1496	72	4	0	72	0.00	0.00
1050	761	0.03	2.4	1424	72	4	0	72	0.00	0.00
1110	756	0.03	2.2	1342	72	4	0	72	0.00	0.00
1170	752	0.03	2.0	1250	72	4	0	72	0.00	0.00
1230	747	0.03	1.8	1149	72	4	0	72	0.00	0.00
1290	743	0.03	1.6	1035	72	4	0	72	0.00	0.00
1350	740	0.03	1.4	909	72	4	0	72	0.00	0.00
1410	737	0.03	1.2	774	72	4	0	72	0.00	0.00
1470	735	0.03	1.0	634	72	4	0	72	0.00	0.00
1530	732	0.03	0.7	487	72	4	0	72	0.00	0.00
1590	729	0.03	0.5	342	72	4	0	72	0.00	0.00
1635	728	0.03	0.3	186	72	4	0	72	0.00	0.00
1658	728	0.03	0.1	98	72	4	0	72	0.00	0.00
1673	728	0.03	0.1	53	72	4	0	72	0.00	0.00

FLUID SUMMARY * At End of Pumping Schedule
MWX-1, MINIFRAC #1

Stage No	Fluid Gone	Prop ID	Pos (ft)	Concentration In	Concentration Now	Concentration Desgn	Fl Vol (MGal)	Ex Tim (min)	Temp (deg F)	Visc (cp)	Fall Frac
1	1	3	1	1682	0.0	0.0	0.0	0.2	2.5	180	2 0.00
1	1	3	1	1682	0.0	0.0	0.0	0.3	3.4	180	2 0.00
1	1	3	1	1682	0.0	0.0	0.0	0.4	3.6	180	2 0.00
1	1	3	1	1682	0.0	0.0	0.0	0.6	3.9	180	2 0.00
1	1	3	1	1682	0.0	0.0	0.0	0.8	4.9	180	2 0.00
1	1	3	1	1682	0.0	0.0	0.0	1.0	6.0	180	2 0.00
1	1	3	1	1682	0.0	0.0	0.0	1.2	6.4	180	2 0.00
1	1	3	1	1682	0.0	0.0	0.0	1.4	7.7	180	2 0.00
1	1	3	1	1682	0.0	0.0	0.0	1.6	8.1	180	2 0.00
1	1	3	1	1682	0.0	0.0	0.0	1.9	9.7	180	2 0.00
1	1	3	1	1682	0.0	0.0	0.0	2.1	9.7	180	2 0.00
1	1	3	1	1682	0.0	0.0	0.0	2.4	10.8	180	2 0.00
1	1	3	1	1682	0.0	0.0	0.0	2.5	13.3	180	2 0.00
2	1	1	1	1682	0.0	0.0	0.0	2.7	12.5	180	2 0.00
2	1	1	1	1682	0.0	0.0	0.0	3.0	14.5	180	2 0.00
2	1	1	1	1682	0.0	0.0	0.0	3.3	18.5	180	2 0.00
2	1	1	1	1682	0.0	0.0	0.0	3.7	23.3	180	2 0.00
2	0	1	1	1676	0.0	0.0	0.1	4.0	24.0	180	2 0.00
2	0	1	1	1662	0.0	0.0	0.1	4.4	22.0	180	2 0.00
2	0	1	1	1636	0.0	0.0	0.2	4.8	20.9	180	2 0.00
2	0	1	1	1610	0.0	0.0	0.2	5.0	19.5	180	2 0.00
3	0	2	1	1588	0.0	0.0	0.3	5.2	19.5	180	11 0.00
3	0	2	1	1547	0.0	0.0	0.3	5.6	15.2	180	10 0.00
3	0	2	1	1476	0.0	0.0	0.4	6.1	15.2	180	9 0.00
3	0	2	1	1382	0.0	0.0	0.6	6.6	12.3	180	9 0.00
3	0	2	1	1244	0.0	0.0	0.7	7.2	9.6	180	8 0.00
3	0	2	1	1038	0.0	0.0	0.8	8.0	6.1	180	7 0.00
3	0	2	1	751	0.0	0.0	0.8	9.2	1.7	180	8 0.00
3	0	2	1	503	0.0	0.0	0.9	10.4	0.0	180	11 0.00
3	0	2	1	365	0.0	0.0	0.9	11.4	0.0	94	16 0.00
3	0	2	1	275	0.0	0.0	0.9	12.1	0.0	88	17 0.00
4	0	2	1	242	0.0	0.0	1.0	12.1	0.0	88	17 0.00
5	0	2	1	212	0.0	0.0	1.0	12.7	0.0	84	17 0.00
5	0	2	1	154	0.0	0.0	1.0	13.3	0.0	80	17 0.00
5	0	2	1	97	0.0	0.0	1.0	13.9	0.0	76	18 0.00
5	0	2	1	34	0.0	0.0	1.0	14.7	0.0	72	18 0.00

A.3

MINIFRAC NO. 1, C = 0.0003 ft/min**0.5

Frac Summary * MWX-1, MINIFRAC #1

Design Data				
FLUID LOSS:	Coefficient (ft/sqrt(min)) 0.0003			
	Spurt Loss (gal/100 sq ft) 0.00			
FORMATION:	Modulus (MM psi) 4.50			
	Fracture Height (ft) 72.0			
	Fluid Loss Height (ft) 55.0			
	Perforated Height (ft) 68.0			
TEMPERATURE:	Bottom Hole (deg F) 180			
PRESSURE:	Reservoir Pressure (psi) 5200.0			
	Closure Pressure (psi) 5890.0			
DEPTH:	Well Depth (ft) 7076			
FROMATION LAYER DATA:				
Depth	Stress at Top	Stres Grad	Modulus	Toughnesss
6952	6520.0	0.000	4.50	1.00
6969	8120.0	0.000	4.50	1.00
6992	6240.0	0.000	4.50	1.00
7015	7275.0	0.000	4.50	1.00
7049	7300.0	0.000	4.50	1.00
7057	6800.0	0.000	4.50	1.00
7072	5890.0	0.000	4.00	1.00
7104	7660.0	0.000	4.00	1.00
7116	6410.0	0.000	4.00	1.00
7147	7000.0	0.000	4.50	1.00
7165	8000.0	0.000	4.50	1.00
7175	6800.0	0.000	4.50	1.00
7190	8420.0	0.000	4.50	1.00
7201	7300.0	0.000	4.50	1.00
7242	6360.0	0.433	4.50	1.00
Fluid Pressure Gradient (psi/ft)				0.433
Fracture Top (ft)				7076
Fracture Bottom (ft)				7144

Calculated Results from 3-D Simulator	
STIMPLAN (TM) , NSI , Tulsa,OK	
Licensed To: Internal Use - NSI Technologies	
1/2 LENGTH:	'Hydraulic' length (ft) 1318
	Propped length (ft) 0
PRESSURE:	Max Net Pressure (psi) 863
TIME:	Max Exposure to Form. Temp. (min) .. 21.5
	Time to Close (min) 69.7
RATE:	Fluid Loss Rate during pad (bpm) ... 0.0
EFFICIENCY:	at end of pumping schedule 0.49
PROPPANT:	Average In Situ Conc. (#/sq ft) 0.0
	Average Conductivity (md-ft) 0
HEIGHT:	Max Fracture Height (ft) 110
WIDTH:	Avg width at end of pumping (in) ... 0.05

STIMPLAN (TM). NSI Technologies, Tulsa, OK
 Licensed To: Internal Use - NSI Technologies

WELL ID:
 MWX-1, MINIFRAC #1
 DEPTH: Well Depth (ft) 7076
 PRESSURE: Reservoir Pressure (psi) 5200
 Closure Pressure (psi) 5890
 TEMPERATURE: Bottom Hole Temperature (deg F) 180

**** Pumping Schedule ****

Sl Vol (Mgal)	Fl Vol (Mgal)	Conc (ppg)	Rate (bpm)	Fluid Type	Prop Type	Pump Time (min)
2.5	2.5	0.0	10.0	3	1	6.0
2.5	2.5	0.0	10.0	1	1	6.0
7.3	7.3	0.0	10.0	2	1	17.4
0.0	0.0	0.0	0.2	2	1	1.2
2.7	2.7	0.0	10.0	2	1	6.4
Total Slurry		15.0	Total Fluid		15.0	
Total Proppant ...		0.0	Avg. Conc		0.0	
Total Pump Time ..		36.9	min			

Proppant ID No. 1 20- 40 Ottawa_Snd

Specific Gravity 2.65
 'Damage Factor' 0.70
 Closure Pres (Mpsi) 0 2 4 8 16
 KfW @ 2 #/sq ft (md-ft) 2000 2000 2000 2000 2000

Fluid ID No. 3 nonXL

Specific Gravity 1.04
 @Wellbor @FormTmp @1Hr @2Hr @4Hr @8Hr
 vis (cp @ 170 l/sec) . 5 2 2 2 2 2
 non-Newtonian n' 0.90 1.00 1.00 1.00 1.00 1.00

Fluid ID No. 1 20#

Specific Gravity 1.04
 @Wellbor @FormTmp @1Hr @2Hr @4Hr @8Hr
 vis (cp @ 170 l/sec) . 14 5 2 2 2 2
 non-Newtonian n' 0.80 0.90 1.00 1.00 1.00 1.00

Fluid ID No. 2	30#					
Specific Gravity	1.04					
	@Welbor	@FormTmp	@1Hr	@2Hr	@4Hr	@8Hr
vis (cp @ 170 1/sec) .	32	20	10	5	5	5
non-Newtonian n'	0.58	0.67	0.80	0.90	0.90	0.90

Time History * NSI STIMPLAN 3-D Fracture Simulation
MWX-1, MINIFRAC #1

Time (min)	Pen (ft)	Pres (psi)	Rate (bpm)	Prop (PPG)	Sl Vol (MGal)	Eff- ciency	Loss (bpm)	Hght (ft)	W-Avg (in)
0.5	120	388	10.0	0.0	0.2	0.51	3.4	72	0.01
0.8	180	417	10.0	0.0	0.3	0.45	4.2	72	0.01
1.2	240	445	10.0	0.0	0.5	0.43	4.6	72	0.01
1.7	300	474	10.0	0.0	0.7	0.43	4.6	72	0.01
2.2	360	502	10.0	0.0	0.9	0.43	4.8	72	0.01
2.8	420	537	10.0	0.0	1.2	0.42	5.0	72	0.01
3.5	480	561	10.0	0.0	1.5	0.41	5.2	72	0.01
4.1	540	580	10.0	0.0	1.7	0.41	5.4	72	0.01
4.8	600	595	10.0	0.0	2.0	0.40	5.6	72	0.02
5.6	660	614	10.0	0.0	2.3	0.40	5.7	73	0.02
6.3	720	626	10.0	0.0	2.7	0.39	5.8	74	0.02
7.2	780	651	10.0	0.0	3.0	0.39	5.9	75	0.02
8.1	840	670	10.0	0.0	3.4	0.38	5.9	77	0.02
9.2	900	675	10.0	0.0	3.8	0.38	5.9	77	0.02
10.3	960	683	10.0	0.0	4.3	0.38	5.9	78	0.02
11.4	1020	685	10.0	0.0	4.8	0.38	5.9	78	0.02
12.5	1080	688	10.0	0.0	5.3	0.37	6.0	79	0.02
13.7	1140	720	10.0	0.0	5.8	0.37	6.1	88	0.02
15.3	1200	746	10.0	0.0	6.4	0.37	5.9	92	0.02
17.3	1260	805	10.0	0.0	7.3	0.38	5.6	100	0.02
20.1	1290	802	10.0	0.0	8.5	0.40	5.0	102	0.02
23.0	1305	849	10.0	0.0	9.7	0.42	4.4	108	0.03
26.0	1309	815	10.0	0.0	10.9	0.44	3.9	108	0.03
28.2	1316	863	10.0	0.0	11.9	0.45	3.6	110	0.03
29.3	1318	826	10.0	0.0	12.3	0.46	3.3	110	0.03
30.5	1318	735	0.2	0.0	12.3	0.45	3.3	110	0.03
32.0	1318	758	10.0	0.0	13.0	0.46	3.2	110	0.04
33.5	1318	767	10.0	0.0	13.6	0.47	3.1	110	0.04
35.0	1318	788	10.0	0.0	14.2	0.48	3.0	110	0.04
36.9	1318	831	10.0	0.0	15.0	0.49	2.9	110	0.05
43.3	1318	748	0.0	0.0	15.0	0.44	2.6	110	0.04
50.4	1318	665	0.0	0.0	15.0	0.39	2.5	110	0.04
58.2	1318	582	0.0	0.0	15.0	0.34	2.3	110	0.03
66.6	1318	499	0.0	0.0	15.0	0.29	2.1	110	0.03
75.6	1318	416	0.0	0.0	15.0	0.25	1.9	110	0.02
85.3	1318	332	0.0	0.0	15.0	0.20	1.8	110	0.02
95.7	1318	249	0.0	0.0	15.0	0.15	1.7	110	0.01
106.6	1318	166	0.0	0.0	15.0	0.10	1.6	110	0.01

GEOMETRY SUMMARY * At End of Pumping Schedule
MWX-1, MINIFRAC #1

Dstnce (ft)	Press (psi)	W-Avg (in)	Q (bpm)	Sh-Rate (l/sec)	-----Hght (ft)-----			Bank Prop Fraction	Prop (PSF)	
					Total	Up	Dn			
30	829	0.08	5.0	251	110	31	11	104	0.00	0.00
90	824	0.08	4.7	252	109	30	10	103	0.00	0.00
150	820	0.08	4.4	253	107	29	10	101	0.00	0.00
210	815	0.08	4.1	253	105	28	9	100	0.00	0.00
270	811	0.07	3.9	256	103	26	8	98	0.00	0.00
330	807	0.07	3.6	259	101	25	8	96	0.00	0.00
390	804	0.07	3.3	261	98	24	7	93	0.00	0.00
450	801	0.06	3.0	300	91	21	6	83	0.00	0.00
510	798	0.06	2.8	291	89	19	4	84	0.00	0.00
570	794	0.05	2.5	501	78	11	0	74	0.00	0.00
630	791	0.05	2.3	551	77	9	0	75	0.00	0.00
690	786	0.03	2.2	1050	73	7	0	71	0.00	0.00
750	782	0.03	2.0	984	73	5	0	72	0.00	0.00
810	777	0.03	1.8	1061	72	4	0	72	0.00	0.00
870	773	0.03	1.7	973	72	4	0	72	0.00	0.00
930	769	0.03	1.5	878	72	4	0	72	0.00	0.00
990	766	0.03	1.3	775	72	4	0	72	0.00	0.00
1050	763	0.03	1.1	664	72	4	0	72	0.00	0.00
1110	760	0.03	0.9	545	72	4	0	72	0.00	0.00
1170	758	0.03	0.7	418	72	4	0	72	0.00	0.00
1230	756	0.03	0.5	285	72	4	0	72	0.00	0.00
1275	756	0.03	0.2	145	72	4	0	72	0.00	0.00
1298	756	0.03	0.1	72	72	4	0	72	0.00	0.00
1307	755	0.03	0.1	34	72	4	0	72	0.00	0.00
1313	755	0.03	0.0	26	72	4	0	72	0.00	0.00

FLUID SUMMARY * At End of Pumping Schedule
MWX-1, MINIFRAC #1

Stage No	Fluid Gone	Prop ID	Pos ID	Pos (ft)	Concentration In	Concentration Now	Concentration Design	Fl Vol (MGal)	Ex Tim (min)	Temp (deg F)	Visc (cp)	Fall Frac
1	1	3	1	1318	0.0	0.0	0.0	0.2	1.9	180	2	0.00
1	1	3	1	1318	0.0	0.0	0.0	0.3	2.2	180	2	0.00
1	1	3	1	1318	0.0	0.0	0.0	0.5	3.0	180	2	0.00
1	1	3	1	1318	0.0	0.0	0.0	0.7	3.2	180	2	0.00
1	1	3	1	1318	0.0	0.0	0.0	0.9	4.2	180	2	0.00
1	1	3	1	1318	0.0	0.0	0.0	1.2	4.5	180	2	0.00
1	1	3	1	1318	0.0	0.0	0.0	1.5	5.9	180	2	0.00
1	1	3	1	1318	0.0	0.0	0.0	1.7	5.6	180	2	0.00
1	1	3	1	1318	0.0	0.0	0.0	2.0	6.0	180	2	0.00
1	1	3	1	1318	0.0	0.0	0.0	2.3	6.3	180	2	0.00
1	1	3	1	1318	0.0	0.0	0.0	2.5	7.7	180	2	0.00
2	1	1	1	1318	0.0	0.0	0.0	2.7	8.6	180	2	0.00
2	1	1	1	1318	0.0	0.0	0.0	3.0	7.7	180	2	0.00
2	1	1	1	1318	0.0	0.0	0.0	3.4	9.0	180	2	0.00
2	1	1	1	1318	0.0	0.0	0.0	3.8	13.7	180	2	0.00
2	1	1	1	1318	0.0	0.0	0.0	4.3	16.8	180	2	0.00
2	1	1	1	1318	0.0	0.0	0.0	4.8	19.8	180	2	0.00
2	0	1	1	1312	0.0	0.0	0.0	5.0	21.5	180	2	0.00
3	0	2	1	1306	0.0	0.0	0.1	5.3	19.6	180	21	0.00
3	0	2	1	1288	0.0	0.0	0.2	5.8	17.2	180	16	0.00
3	0	2	1	1238	0.0	0.0	0.3	6.4	14.4	180	12	0.00
3	0	2	1	1128	0.0	0.0	0.4	7.3	11.4	180	10	0.00
3	0	2	1	912	0.0	0.0	0.6	8.4	8.8	180	8	0.00
3	0	2	1	649	0.0	0.0	0.8	9.6	4.7	180	10	0.00
3	0	2	1	455	0.0	0.0	0.9	10.8	1.7	180	12	0.00
3	0	2	1	338	0.0	0.0	0.9	11.7	0.0	172	13	0.00
3	0	2	1	270	0.0	0.0	0.9	12.1	0.0	93	17	0.00
4	0	2	1	246	0.0	0.0	0.9	12.1	0.0	93	17	0.00
5	0	2	1	216	0.0	0.0	0.9	12.7	0.0	88	17	0.00
5	0	2	1	157	0.0	0.0	1.0	13.3	0.0	83	17	0.00
5	0	2	1	99	0.0	0.0	1.0	13.9	0.0	78	17	0.00
5	0	2	1	35	0.0	0.0	1.0	14.7	0.0	73	18	0.00

A.4

MINIFRAC NO. 1, C = 0.001 ft/min**0.5

Frac Summary * MWX-1, MINIFRAC #1

Design Data					
FLUID LOSS:	Coefficient (ft/sqrt(min))	0.0010		
	Spurt Loss (gal/100 sq ft)	0.00		
FORMATION:	Modulus (MM psi)	4.50		
	Fracture Height (ft)	72.0		
	Fluid Loss Height (ft)	55.0		
	Perforated Height (ft)	68.0		
TEMPERATURE:	Bottom Hole (deg F)	180		
PRESSURE:	Reservoir Pressure (psi)	5200.0		
	Closure Pressure (psi)	5890.0		
DEPTH:	Well Depth (ft)	7076		
FROMATION LAYER DATA:					
Depth	Stress at Top	Stres Grad	Modulus	Toughnesss	
6952	6520.0	0.000	4.50	1.00	
6969	8120.0	0.000	4.50	1.00	
6992	6240.0	0.000	4.50	1.00	
7015	7275.0	0.000	4.50	1.00	
7049	7300.0	0.000	4.50	1.00	
7057	6800.0	0.000	4.50	1.00	
7072	5890.0	0.000	4.00	1.00	
7104	7660.0	0.000	4.00	1.00	
7116	6410.0	0.000	4.00	1.00	
7147	7000.0	0.000	4.50	1.00	
7165	8000.0	0.000	4.50	1.00	
7175	6800.0	0.000	4.50	1.00	
7190	8420.0	0.000	4.50	1.00	
7201	7300.0	0.000	4.50	1.00	
7242	6360.0	0.433	4.50	1.00	
	Fluid Pressure Gradient (psi/ft)		0.433	
	Fracture Top (ft)		7076	
	Fracture Bottom (ft)		7144	

Calculated Results from 3-D Simulator	
STIMPLAN (TM) , NSI , Tulsa,OK	
Licensed To: Internal Use - NSI Technologies	
1/2 LENGTH:	'Hydraulic' length (ft) 626
	Propped length (ft) 0
PRESSURE:	Max Net Pressure (psi) 921
TIME:	Max Exposure to Form. Temp. (min) .. 12.6
	Time to Close (min) 20.6
RATE:	Fluid Loss Rate during pad (bpm) ... 0.0
EFFICIENCY:	at end of pumping schedule 0.27
PROPPANT:	Average In Situ Conc. (#/sq ft) 0.0
	Average Conductivity (md-ft) 0
HEIGHT:	Max Fracture Height (ft) 105
WIDTH:	Avg width at end of pumping (in) ... 0.05

Fluid ID No. 2	30#					
Specific Gravity	1.04					
	@Welbor	@FormTmp	@1Hr	@2Hr	@4Hr	@8Hr
vis (cp @ 170 1/sec) .	40	32	20	10	5	5
non-Newtonian n'	0.53	0.58	0.67	0.80	0.90	0.90

Time History * NSI STIMPLAN 3-D Fracture Simulation
MWX-1, MINIFRAC #1

Time (min)	Pen (ft)	Pres (psi)	Rate (bpm)	Prop (PPG)	Sl Vol (MGal)	Eff- ciency	Loss (bpm)	Hght (ft)	W-Avg (in)
0.5	70	398	10.0	0.0	0.2	0.27	6.7	70	0.01
0.8	105	443	10.0	0.0	0.3	0.21	7.8	70	0.01
1.3	140	459	10.0	0.0	0.6	0.19	8.0	70	0.01
2.1	175	495	10.0	0.0	0.9	0.19	7.8	71	0.01
2.8	210	530	10.0	0.0	1.2	0.18	8.0	71	0.01
3.7	245	566	10.0	0.0	1.6	0.18	8.2	72	0.01
4.7	280	592	10.0	0.0	2.0	0.17	8.3	72	0.01
5.8	315	610	10.0	0.0	2.4	0.16	8.5	73	0.01
7.0	350	624	10.0	0.0	3.0	0.16	8.5	74	0.01
8.5	385	685	10.0	0.0	3.6	0.16	8.4	77	0.02
10.4	420	706	10.0	0.0	4.4	0.16	8.1	79	0.02
12.4	455	712	10.0	0.0	5.2	0.17	7.9	88	0.02
14.5	490	726	10.0	0.0	6.1	0.17	7.9	89	0.02
16.9	525	812	10.0	0.0	7.1	0.18	7.8	101	0.02
20.5	527	788	10.0	0.0	8.6	0.21	6.3	101	0.03
21.9	532	796	10.0	0.0	9.2	0.23	5.8	101	0.03
23.1	540	797	10.0	0.0	9.7	0.24	5.9	102	0.03
24.5	558	808	10.0	0.0	10.3	0.24	6.3	103	0.03
26.9	593	813	10.0	0.0	11.3	0.25	6.9	104	0.04
29.3	626	817	10.0	0.0	12.3	0.25	7.1	105	0.04
30.5	626	706	0.2	0.0	12.3	0.23	6.3	105	0.04
32.0	626	748	10.0	0.0	13.0	0.24	5.9	105	0.04
33.5	626	787	10.0	0.0	13.6	0.25	5.5	105	0.04
35.0	626	841	10.0	0.0	14.2	0.26	5.3	105	0.05
36.9	626	921	10.0	0.0	15.0	0.27	5.0	105	0.05
38.9	626	829	0.0	0.0	15.0	0.24	4.8	105	0.05
41.3	626	737	0.0	0.0	15.0	0.22	4.6	105	0.04
43.7	626	645	0.0	0.0	15.0	0.19	4.4	105	0.04
46.3	626	553	0.0	0.0	15.0	0.16	4.2	105	0.03
49.0	626	460	0.0	0.0	15.0	0.14	4.0	105	0.03
51.7	626	368	0.0	0.0	15.0	0.11	3.9	105	0.02
54.6	626	276	0.0	0.0	15.0	0.08	3.8	105	0.02
57.5	626	184	0.0	0.0	15.0	0.06	3.6	105	0.01

GEOMETRY SUMMARY * At End of Pumping Schedule
MWX-1, MINIFRAC #1

Dstance (ft)	Press (psi)	W-Avg (in)	Q (bpm)	Sh-Rate (1/sec)	-----Hght (ft)-----			Bank Prop Fraction	Prop (PSF)	
					Total	Up	Dn			
18	919	0.09	5.0	238	105	28	9	99	0.00	0.00
53	916	0.08	4.6	250	101	27	9	94	0.00	0.00
88	913	0.08	4.3	235	101	25	8	96	0.00	0.00
123	911	0.08	4.0	228	100	24	7	94	0.00	0.00
158	908	0.08	3.7	222	98	23	7	93	0.00	0.00
193	906	0.08	3.4	213	97	22	6	92	0.00	0.00
228	903	0.08	3.0	209	94	21	6	89	0.00	0.00
263	901	0.07	2.8	203	92	20	5	86	0.00	0.00
298	899	0.07	2.4	203	88	17	4	83	0.00	0.00
333	897	0.06	2.2	249	79	11	0	76	0.00	0.00
368	895	0.05	1.9	318	77	10	0	75	0.00	0.00
403	892	0.04	1.6	426	75	7	0	74	0.00	0.00
438	889	0.03	1.4	612	72	4	0	72	0.00	0.00
473	887	0.03	1.2	670	70	2	0	70	0.00	0.00
508	884	0.03	1.0	555	70	2	0	70	0.00	0.00
526	883	0.03	0.8	432	70	2	0	70	0.00	0.00
529	883	0.03	0.8	424	70	2	0	70	0.00	0.00
536	883	0.03	0.7	407	70	2	0	70	0.00	0.00
549	882	0.03	0.6	371	70	2	0	70	0.00	0.00
575	881	0.03	0.5	296	70	2	0	70	0.00	0.00
609	104	0.00	0.2	572	70	2	0	70	0.00	0.00

FLUID SUMMARY * At End of Pumping Schedule
MWX-1, MINIFRAC #1

Stage No	Fluid Gone	Prop ID	Pos ID	Pos (ft)	Concentration			Fl Vol (MGal)	Ex Tim (min)	Temp (deg F)	Visc (cp)	Fall Frac
					In	Now	Desgn					
1	1	3	1	626	0.0	0.0	0.0	0.2	0.4	180	3	0.00
1	1	3	1	626	0.0	0.0	0.0	0.3	0.6	180	3	0.00
1	1	3	1	626	0.0	0.0	0.0	0.6	0.8	180	3	0.00
1	1	3	1	626	0.0	0.0	0.0	0.9	0.8	180	3	0.00
1	1	3	1	626	0.0	0.0	0.0	1.2	0.9	180	3	0.00
1	1	3	1	626	0.0	0.0	0.0	1.6	1.0	180	3	0.00
1	1	3	1	626	0.0	0.0	0.0	2.0	1.1	180	3	0.00
1	1	3	1	626	0.0	0.0	0.0	2.4	1.3	180	3	0.00
1	1	3	1	626	0.0	0.0	0.0	2.5	3.0	180	3	0.00
2	1	1	1	626	0.0	0.0	0.0	3.0	1.7	180	4	0.00
2	1	1	1	626	0.0	0.0	0.0	3.6	4.0	180	4	0.00
2	1	1	1	626	0.0	0.0	0.0	4.4	4.3	180	6	0.00
2	1	1	1	626	0.0	0.0	0.0	5.0	5.2	180	4	0.00
3	1	2	1	626	0.0	0.0	0.0	5.2	7.8	180	6	0.00
3	1	2	1	626	0.0	0.0	0.0	6.1	8.1	180	4	0.00
3	1	2	1	626	0.0	0.0	0.0	7.1	12.6	180	11	0.00
3	1	2	1	626	0.0	0.0	0.0	8.6	10.4	180	16	0.00
3	0	2	1	570	0.0	0.0	0.1	9.2	10.3	180	16	0.00
3	0	2	1	531	0.0	0.0	0.3	9.7	10.3	180	13	0.00
3	0	2	1	467	0.0	0.0	0.4	10.3	7.8	180	12	0.00
3	0	2	1	372	0.0	0.0	0.5	11.3	4.7	180	16	0.00
3	0	2	1	276	0.0	0.0	0.7	12.3	1.7	180	19	0.00
4	0	2	1	234	0.0	0.0	0.7	12.3	1.7	180	19	0.00
5	0	2	1	207	0.0	0.0	0.8	12.9	0.0	180	19	0.00
5	0	2	1	153	0.0	0.0	0.8	13.5	0.0	157	19	0.00
5	0	2	1	98	0.0	0.0	0.9	14.1	0.0	89	21	0.00
5	0	2	1	35	0.0	0.0	0.9	14.9	0.0	76	20	0.00

A.5

MINIFRAC NO. 2, C = 0.00005 ft/min**0.5

Frac Summary * MWX-1, MINIFRAC #2

Design Data				
FLUID LOSS:	Coefficient (ft/sqrt(min))	0.00005	
	Spurt Loss (gal/100 sq ft)	0.00	
FORMATION:	Modulus (MM psi)	4.50	
	Fracture Height (ft)	72.0	
	Fluid Loss Height (ft)	55.0	
	Perforated Height (ft)	68.0	
TEMPERATURE:	Bottom Hole (deg F)	180	
PRESSURE:	Reservoir Pressure (psi)	5200.0	
	Closure Pressure (psi)	5890.0	
DEPTH:	Well Depth (ft)	7076	
FROMATION LAYER DATA:				
Depth	Stress at Top	Stres Grad	Modulus	Toughnesss
6952	6520.0	0.000	4.50	1.00
6969	8120.0	0.000	4.50	1.00
6992	6240.0	0.000	4.50	1.00
7015	7275.0	0.000	4.50	1.00
7049	7300.0	0.000	4.50	1.00
7057	6800.0	0.000	4.50	1.00
7072	5890.0	0.000	4.00	1.00
7104	7660.0	0.000	4.00	1.00
7116	6410.0	0.000	4.00	1.00
7147	7000.0	0.000	4.50	1.00
7165	8000.0	0.000	4.50	1.00
7175	6800.0	0.000	4.50	1.00
7190	8420.0	0.000	4.50	1.00
7201	7300.0	0.000	4.50	1.00
7242	6360.0	0.433	4.50	1.00
	Fluid Pressure Gradient (psi/ft)	0.433	
	Fracture Top (ft)	7076	
	Fracture Bottom (ft)	7144	

Calculated Results from 3-D Simulator	
STIMPLAN (TM) , NSI , Tulsa,OK	
Licensed To: Internal Use - NSI Technologies	
1/2 LENGTH:	'Hydraulic' length (ft) 2696
	Propped length (ft) 0
PRESSURE:	Max Net Pressure (psi) 1118
TIME:	Max Exposure to Form. Temp. (min) .. 63.6
	Time to Close (min) 2730.7
RATE:	Fluid Loss Rate during pad (bpm) ... 0.0
EFFICIENCY:	at end of pumping schedule 0.86
PROPPANT:	Average In Situ Conc. (#/sq ft) 0.0
	Average Conductivity (md-ft) 0
HEIGHT:	Max Fracture Height (ft) 143
WIDTH:	Avg width at end of pumping (in) ... 0.06

Time History * NSI STIMPLAN 3-D Fracture Simulation
MWX-1, MINIFRAC #2

Time (min)	Pen (ft)	Pres (psi)	Rate (bpm)	Prop (PPG)	Sl Vol (MGal)	Eff- ciency	Loss (bpm)	Hght (ft)	W-Avg (in)
0.7	168	614	9.9	0.0	0.3	0.81	0.7	72	0.01
1.2	288	596	9.9	0.0	0.5	0.68	0.9	72	0.01
1.8	408	676	9.9	0.0	0.8	0.66	1.1	72	0.01
2.8	528	770	9.9	0.0	1.2	0.69	1.1	73	0.02
3.9	648	829	9.9	0.0	1.6	0.70	1.1	92	0.02
5.8	768	780	9.9	0.0	2.4	0.74	1.0	92	0.02
7.4	888	870	9.9	0.0	3.1	0.75	1.0	101	0.03
10.0	1008	783	9.9	0.0	4.2	0.78	1.0	101	0.03
12.1	1128	892	9.9	0.0	5.0	0.78	1.0	106	0.03
14.8	1248	878	9.9	0.0	6.2	0.80	1.0	106	0.04
17.2	1368	966	9.9	0.0	7.2	0.80	1.0	116	0.04
21.0	1488	922	9.9	0.0	8.8	0.81	1.0	116	0.04
24.2	1608	1011	9.9	0.0	10.1	0.82	1.0	124	0.04
28.5	1728	981	9.9	0.0	11.9	0.83	1.0	124	0.05
32.0	1848	1044	9.9	0.0	13.3	0.83	1.0	130	0.05
37.0	1968	996	9.9	0.0	15.4	0.84	1.0	130	0.05
41.2	2088	1064	9.9	0.0	17.2	0.84	1.0	134	0.05
46.8	2208	1040	9.9	0.0	19.5	0.84	1.0	134	0.06
51.5	2328	1093	9.9	0.0	21.4	0.85	1.0	139	0.06
56.5	2388	1018	9.9	0.0	23.5	0.85	0.9	139	0.06
62.3	2508	1078	9.9	0.0	26.0	0.85	1.0	139	0.06
68.4	2628	1118	9.9	0.0	28.5	0.86	1.0	143	0.06
72.2	2666	1042	9.9	0.0	30.1	0.86	0.9	143	0.06
76.7	2696	967	0.0	0.0	30.1	0.85	0.9	143	0.06
179.9	2696	870	0.0	0.0	30.1	0.77	0.4	143	0.06
354.6	2696	773	0.0	0.0	30.1	0.68	0.3	143	0.05
596.2	2696	677	0.0	0.0	30.1	0.60	0.2	143	0.04
904.6	2696	580	0.0	0.0	30.1	0.51	0.2	143	0.04
1279.4	2696	483	0.0	0.0	30.1	0.43	0.2	143	0.03
1720.8	2696	387	0.0	0.0	30.1	0.34	0.1	143	0.02
2228.6	2696	290	0.0	0.0	30.1	0.26	0.1	143	0.02
2802.9	2696	193	0.0	0.0	30.1	0.17	0.1	143	0.01

GEOMETRY SUMMARY * At End of Pumping Schedule
MWX-1, MINIFRAC #2

Dstnce (ft)	Press (psi)	W-Avg (in)	Q (bpm)	Sh-Rate (1/sec)	-----Hght (ft)-----			Bank Prop Fraction	Prop (PSF)	
					Total	Up	Dn			
54	1032	0.15	5.0	51	143	57	24	127	0.00	0.00
138	1012	0.15	4.8	54	141	55	23	126	0.00	0.00
228	994	0.14	4.7	55	141	51	21	131	0.00	0.00
348	959	0.13	4.4	66	137	50	21	125	0.00	0.00
468	924	0.11	4.1	84	130	47	19	117	0.00	0.00
588	891	0.11	3.8	83	130	44	18	121	0.00	0.00
708	864	0.10	3.4	106	122	41	16	111	0.00	0.00
828	839	0.09	3.1	106	121	39	15	114	0.00	0.00
948	816	0.09	2.8	116	117	36	13	110	0.00	0.00
1068	788	0.08	2.6	139	111	33	12	102	0.00	0.00
1188	758	0.07	2.3	145	109	30	10	103	0.00	0.00
1308	721	0.07	2.0	169	102	27	9	97	0.00	0.00
1428	589	0.05	1.7	291	92	21	6	86	0.00	0.00
1548	572	0.04	0.9	272	79	11	0	76	0.00	0.00
1668	604	0.03	0.4	365	73	6	0	72	0.00	0.00
1788	559	0.02	0.4	426	72	4	0	72	0.00	0.00
1908	510	0.02	0.4	525	72	4	0	72	0.00	0.00
2028	473	0.02	0.4	624	72	4	0	72	0.00	0.00
2148	430	0.02	0.4	749	72	4	0	72	0.00	0.00
2268	377	0.01	0.4	935	72	4	0	72	0.00	0.00
2358	328	0.01	0.3	1123	72	4	0	72	0.00	0.00
2448	268	0.01	0.3	1547	72	4	0	72	0.00	0.00
2568	170	0.01	0.2	2889	72	4	0	72	0.00	0.00
2647	69	0.00	0.1	9544	72	4	0	72	0.00	0.00

FLUID SUMMARY * At End of Pumping Schedule
MWX-1, MINIFRAC #2

Stage No	Fluid Gone	Prop ID	Pos ID	Pos (ft)	Concentration			Fl Vol (MGal)	Ex Tim (min)	Temp (deg F)	Visc (cp)	Fall Frac
					In	Now	Desgn					
1	1	2	1	2666	0.0	0.0	0.0	0.3	25.9	180	4	0.00
1	1	2	1	2666	0.0	0.0	0.0	0.5	33.0	180	4	0.00
1	1	2	1	2666	0.0	0.0	0.0	0.8	46.8	180	5	0.00
1	1	2	1	2666	0.0	0.0	0.0	1.2	60.5	180	4	0.00
1	0	2	1	2635	0.0	0.0	0.0	1.6	63.6	180	4	0.00
1	0	2	1	2490	0.0	0.0	0.2	2.4	59.3	180	5	0.00
1	0	2	1	2244	0.0	0.0	0.5	3.1	56.8	180	6	0.00
1	0	2	1	1990	0.0	0.0	0.6	3.8	54.2	180	6	0.00
2	0	1	1	1798	0.0	0.0	0.7	4.1	51.1	180	17	0.00
2	0	1	1	1625	0.0	0.0	0.8	4.9	47.6	180	20	0.00
2	0	1	1	1429	0.0	0.0	0.8	6.1	40.0	180	22	0.00
2	0	1	1	1294	0.0	0.0	0.9	7.0	31.2	180	29	0.00
2	0	1	1	1172	0.0	0.0	0.9	8.5	26.3	180	32	0.00
2	0	1	1	1046	0.0	0.0	0.9	9.8	21.2	180	34	0.00
2	0	1	1	927	0.0	0.0	0.9	11.5	10.9	180	39	0.00
2	0	1	1	814	0.0	0.0	0.9	12.9	4.9	180	42	0.00
2	0	1	1	700	0.0	0.0	0.9	14.9	0.0	169	47	0.00
2	0	1	1	587	0.0	0.0	1.0	16.6	0.0	94	77	0.00
2	0	1	1	479	0.0	0.0	1.0	18.8	0.0	90	79	0.00
2	0	1	1	375	0.0	0.0	1.0	20.7	0.0	85	91	0.00
2	0	1	1	288	0.0	0.0	1.0	22.7	0.0	82	100	0.00
2	0	1	1	197	0.0	0.0	1.0	25.0	0.0	79	106	0.00
2	0	1	1	104	0.0	0.0	1.0	27.4	0.0	74	113	0.00
2	0	1	1	29	0.0	0.0	1.0	28.9	0.0	72	116	0.00

A.6

MINIFRAC NO. 2, C = 0.0001 ft/min**0.5

Frac Summary * MWX-1, MINIFRAC #2

Design Data				
FLUID LOSS:	Coefficient (ft/sqrt(min))	0.0001	
	Spurt Loss (gal/100 sq ft)	0.00	
FORMATION:	Modulus (MM psi)	4.50	
	Fracture Height (ft)	72.0	
	Fluid Loss Height (ft)	55.0	
	Perforated Height (ft)	68.0	
TEMPERATURE:	Bottom Hole (deg F)	180	
PRESSURE:	Reservoir Pressure (psi)	5200.0	
	Closure Pressure (psi)	5890.0	
DEPTH:	Well Depth (ft)	7076	
FROMATION LAYER DATA:				
Depth	Stress at Top	Stres Grad	Modulus	Toughnesss
6952	6520.0	0.000	4.50	1.00
6969	8120.0	0.000	4.50	1.00
6992	6240.0	0.000	4.50	1.00
7015	7275.0	0.000	4.50	1.00
7049	7300.0	0.000	4.50	1.00
7057	6800.0	0.000	4.50	1.00
7072	5890.0	0.000	4.00	1.00
7104	7660.0	0.000	4.00	1.00
7116	6410.0	0.000	4.00	1.00
7147	7000.0	0.000	4.50	1.00
7165	8000.0	0.000	4.50	1.00
7175	6800.0	0.000	4.50	1.00
7190	8420.0	0.000	4.50	1.00
7201	7300.0	0.000	4.50	1.00
7242	6360.0	0.433	4.50	1.00
	Fluid Pressure Gradient (psi/ft)	0.433	
	Fracture Top (ft)	7076	
	Fracture Bottom (ft)	7144	

Calculated Results from 3-D Simulator	
STIMPLAN (TM) , NSI , Tulsa,OK	
Licensed To: Internal Use - NSI Technologies	
1/2 LENGTH:	'Hydraulic' length (ft) 2183
	Propped length (ft) 0
PRESSURE:	Max Net Pressure (psi) 1096
TIME:	Max Exposure to Form. Temp. (min) .. 54.0
	Time to Close (min) 1316.1
RATE:	Fluid Loss Rate during pad (bpm) ... 0.0
EFFICIENCY:	at end of pumping schedule 0.80
PROPPANT:	Average In Situ Conc. (#/sq ft) 0.0
	Average Conductivity (md-ft) 0
HEIGHT:	Max Fracture Height (ft) 140
WIDTH:	Avg width at end of pumping (in) ... 0.06

Time History * NSI STIMPLAN 3-D Fracture Simulation
MWX-1, MINIFRAC #2

Time (min)	Pen (ft)	Pres (psi)	Rate (bpm)	Prop (PPG)	Sl Vol (MGal)	Eff- ciency	Loss (bpm)	Hght (ft)	W-Avg (in)
0.7	168	609	9.9	0.0	0.3	0.76	1.3	72	0.01
1.3	288	594	9.9	0.0	0.5	0.63	1.8	72	0.01
2.0	408	674	9.9	0.0	0.8	0.60	2.0	72	0.01
3.1	528	766	9.9	0.0	1.3	0.62	2.0	73	0.02
4.3	648	828	9.9	0.0	1.8	0.64	2.1	92	0.02
6.5	768	788	9.9	0.0	2.7	0.67	1.9	92	0.02
8.6	888	829	9.9	0.0	3.6	0.69	1.9	97	0.03
11.1	1008	822	9.9	0.0	4.6	0.70	1.9	98	0.03
13.6	1128	895	9.9	0.0	5.7	0.71	1.9	106	0.03
17.0	1248	906	9.9	0.0	7.1	0.72	1.9	109	0.04
20.1	1368	983	9.9	0.0	8.4	0.73	1.9	119	0.04
24.6	1488	957	9.9	0.0	10.3	0.74	1.9	119	0.04
28.4	1608	1041	9.9	0.0	11.8	0.74	1.9	129	0.04
33.7	1668	964	9.9	0.0	14.0	0.76	1.7	129	0.05
38.3	1788	1045	9.9	0.0	16.0	0.76	1.7	130	0.05
44.6	1908	1053	9.9	0.0	18.6	0.77	1.7	133	0.05
50.0	1938	1045	9.9	0.0	20.8	0.78	1.5	133	0.06
55.5	1998	1093	9.9	0.0	23.1	0.78	1.5	139	0.06
61.2	2028	1025	9.9	0.0	25.5	0.79	1.4	139	0.06
66.3	2088	1075	9.9	0.0	27.6	0.80	1.4	139	0.06
72.2	2153	1096	9.9	0.0	30.1	0.80	1.4	140	0.07
78.0	2183	958	0.0	0.0	30.1	0.79	1.3	140	0.06
134.3	2183	862	0.0	0.0	30.1	0.71	0.8	140	0.06
214.5	2183	767	0.0	0.0	30.1	0.63	0.7	140	0.05
316.8	2183	671	0.0	0.0	30.1	0.55	0.5	140	0.04
441.0	2183	575	0.0	0.0	30.1	0.47	0.4	140	0.04
586.9	2183	479	0.0	0.0	30.1	0.40	0.4	140	0.03
754.6	2183	383	0.0	0.0	30.1	0.32	0.3	140	0.02
944.1	2183	287	0.0	0.0	30.1	0.24	0.3	140	0.02
1155.3	2183	192	0.0	0.0	30.1	0.16	0.3	140	0.01
1388.3	2183	96	0.0	0.0	30.1	0.08	0.2	140	0.01

GEOMETRY SUMMARY * At End of Pumping Schedule
MWX-1, MINIFRAC #2

Dstnce (ft)	Press (psi)	W-Avg (in)	Q (bpm)	Sh-Rate (1/sec)	-----Hght (ft)-----			Bank Prop Fraction	Prop (PSF)	
					Total	Up	Dn			
54	1088	0.15	5.0	53	140	55	23	125	0.00	0.00
138	1070	0.14	4.8	60	138	53	22	123	0.00	0.00
228	1051	0.14	4.7	61	138	49	20	128	0.00	0.00
348	1024	0.13	4.6	73	134	48	20	124	0.00	0.00
468	996	0.12	4.4	87	131	46	18	123	0.00	0.00
588	968	0.11	4.3	106	128	43	17	119	0.00	0.00
708	947	0.10	4.2	131	122	41	16	111	0.00	0.00
828	927	0.09	3.9	133	121	39	15	114	0.00	0.00
948	906	0.09	3.6	148	117	37	14	110	0.00	0.00
1068	884	0.08	3.3	156	114	34	12	107	0.00	0.00
1188	860	0.07	2.8	174	109	32	11	101	0.00	0.00
1308	844	0.06	2.1	196	105	29	10	97	0.00	0.00
1428	752	0.03	0.9	581	89	20	5	81	0.00	0.00
1548	664	0.03	0.8	607	73	8	0	69	0.00	0.00
1638	593	0.02	0.7	645	72	4	0	72	0.00	0.00
1728	519	0.02	0.6	765	72	4	0	72	0.00	0.00
1848	386	0.01	0.5	1072	72	4	0	72	0.00	0.00
1923	315	0.01	0.4	1288	72	4	0	72	0.00	0.00
1968	280	0.01	0.3	1594	72	4	0	72	0.00	0.00
2013	238	0.01	0.3	1880	72	4	0	72	0.00	0.00
2058	183	0.01	0.3	2803	72	4	0	72	0.00	0.00
2121	120	0.00	0.2	4414	72	4	0	72	0.00	0.00

FLUID SUMMARY * At End of Pumping Schedule
MWX-1, MINIFRAC #2

Stage	Fluid	Prop	Pos	Concentration			Fl Vol	Ex Tim	Temp	Visc	Fall	
No	Gone	ID	ID	(ft)	In	Now	Desgn	(MGal)	(min)	(deg F)	(cp)	Frac
1	1	2	1	2153	0.0	0.0	0.0	0.3	11.8	180	4	0.00
1	1	2	1	2153	0.0	0.0	0.0	0.5	17.0	180	4	0.00
1	1	2	1	2153	0.0	0.0	0.0	0.8	24.0	180	5	0.00
1	1	2	1	2153	0.0	0.0	0.0	1.3	32.3	180	4	0.00
1	1	2	1	2153	0.0	0.0	0.0	1.8	45.2	180	6	0.00
1	1	2	1	2153	0.0	0.0	0.0	2.7	51.5	180	5	0.00
1	0	2	1	2080	0.0	0.0	0.1	3.6	54.0	180	5	0.00
1	0	2	1	1979	0.0	0.0	0.3	3.8	54.0	180	5	0.00
2	0	1	1	1830	0.0	0.0	0.4	4.6	50.7	180	12	0.00
2	0	1	1	1576	0.0	0.0	0.6	5.6	42.7	180	16	0.00
2	0	1	1	1344	0.0	0.0	0.8	7.0	38.2	180	25	0.00
2	0	1	1	1198	0.0	0.0	0.8	8.2	33.3	180	29	0.00
2	0	1	1	1072	0.0	0.0	0.9	10.1	22.0	180	32	0.00
2	0	1	1	944	0.0	0.0	0.9	11.6	16.5	180	34	0.00
2	0	1	1	818	0.0	0.0	0.9	13.7	10.9	180	37	0.00
2	0	1	1	686	0.0	0.0	0.9	15.5	0.0	180	41	0.00
2	0	1	1	555	0.0	0.0	0.9	18.0	0.0	151	53	0.00
2	0	1	1	430	0.0	0.0	1.0	20.2	0.0	92	80	0.00
2	0	1	1	324	0.0	0.0	1.0	22.4	0.0	87	89	0.00
2	0	1	1	224	0.0	0.0	1.0	24.7	0.0	82	99	0.00
2	0	1	1	133	0.0	0.0	1.0	26.7	0.0	76	105	0.00
2	0	1	1	45	0.0	0.0	1.0	29.0	0.0	73	112	0.00

A.7

MINIFRAC NO. 2, C = 0.0002 ft/min**0.5

Frac Summary * MWX-1, MINIFRAC #2

Design Data					
FLUID LOSS:	Coefficient (ft/sqrt(min))	0.0002		
	Spurt Loss (gal/100 sq ft)	0.00		
FORMATION:	Modulus (MM psi)	4.50		
	Fracture Height (ft)	72.0		
	Fluid Loss Height (ft)	55.0		
	Perforated Height (ft)	68.0		
TEMPERATURE:	Bottom Hole (deg F)	180		
PRESSURE:	Reservoir Pressure (psi)	5200.0		
	Closure Pressure (psi)	5890.0		
DEPTH:	Well Depth (ft)	7076		
FROMATION LAYER DATA:					
Depth	Stress at Top	Stres Grad	Modulus	Toughnesss	
6952	6520.0	0.000	4.50	1.00	
6969	8120.0	0.000	4.50	1.00	
6992	6240.0	0.000	4.50	1.00	
7015	7275.0	0.000	4.50	1.00	
7049	7300.0	0.000	4.50	1.00	
7057	6800.0	0.000	4.50	1.00	
7072	5890.0	0.000	4.00	1.00	
7104	7660.0	0.000	4.00	1.00	
7116	6410.0	0.000	4.00	1.00	
7147	7000.0	0.000	4.50	1.00	
7165	8000.0	0.000	4.50	1.00	
7175	6800.0	0.000	4.50	1.00	
7190	8420.0	0.000	4.50	1.00	
7201	7300.0	0.000	4.50	1.00	
7242	6360.0	0.433	4.50	1.00	
	Fluid Pressure Gradient (psi/ft)	0.433		
	Fracture Top (ft)	7076		
	Fracture Bottom (ft)	7144		

Calculated Results from 3-D Simulator	
STIMPLAN (TM) , NSI , Tulsa,OK	
Licensed To: Internal Use - NSI Technologies	
1/2 LENGTH:	'Hydraulic' length (ft) 1828
	Propped length (ft) 0
PRESSURE:	Max Net Pressure (psi) 1082
TIME:	Max Exposure to Form. Temp. (min) .. 47.5
	Time to Close (min) 457.1
RATE:	Fluid Loss Rate during pad (bpm) ... 0.0
EFFICIENCY:	at end of pumping schedule 0.70
PROPPANT:	Average In Situ Conc. (#/sq ft) 0.0
	Average Conductivity (md-ft) 0
HEIGHT:	Max Fracture Height (ft) 140
WIDTH:	Avg width at end of pumping (in) ... 0.07

Time History * NSI STIMPLAN 3-D Fracture Simulation
MWX-1, MINIFRAC #2

Time (min)	Pen (ft)	Pres (psi)	Rate (bpm)	Prop (PPG)	Sl Vol (MGal)	Eff- ciency	Loss (bpm)	Hght (ft)	W-Avg (in)
0.7	150	577	9.9	0.0	0.3	0.68	2.3	72	0.01
1.2	250	579	9.9	0.0	0.5	0.56	3.2	72	0.01
1.9	350	648	9.9	0.0	0.8	0.52	3.5	72	0.01
3.0	450	728	9.9	0.0	1.3	0.53	3.5	73	0.02
4.2	550	787	9.9	0.0	1.8	0.53	3.5	89	0.02
6.3	650	774	9.9	0.0	2.7	0.56	3.2	91	0.02
8.1	750	841	9.9	0.0	3.4	0.57	3.3	100	0.02
10.7	850	789	9.9	0.0	4.5	0.58	3.3	100	0.03
13.1	950	856	9.9	0.0	5.5	0.59	3.3	103	0.03
16.0	1050	902	9.9	0.0	6.7	0.60	3.3	110	0.04
19.2	1150	944	9.9	0.0	8.0	0.61	3.3	117	0.04
23.8	1250	966	9.9	0.0	9.9	0.62	3.1	121	0.04
29.6	1350	1029	9.9	0.0	12.3	0.63	3.0	130	0.04
36.1	1356	995	9.9	0.0	15.1	0.66	2.4	130	0.05
40.3	1369	1044	9.9	0.0	16.8	0.67	2.1	134	0.05
45.8	1394	1012	9.9	0.0	19.1	0.68	2.1	134	0.06
50.5	1444	1054	9.9	0.0	21.0	0.69	2.1	136	0.06
55.4	1494	1025	9.9	0.0	23.1	0.70	2.2	136	0.06
60.0	1594	1062	9.9	0.0	25.0	0.70	2.5	137	0.06
65.8	1694	1047	9.9	0.0	27.4	0.70	2.6	137	0.07
72.2	1816	1082	9.9	0.0	30.1	0.70	2.8	140	0.07
77.0	1828	927	0.0	0.0	30.1	0.69	2.4	140	0.07
102.3	1828	835	0.0	0.0	30.1	0.62	1.7	140	0.06
134.6	1828	742	0.0	0.0	30.1	0.55	1.5	140	0.05
173.2	1828	649	0.0	0.0	30.1	0.48	1.3	140	0.05
217.8	1828	556	0.0	0.0	30.1	0.41	1.1	140	0.04
268.3	1828	464	0.0	0.0	30.1	0.34	1.0	140	0.03
324.7	1828	371	0.0	0.0	30.1	0.27	0.9	140	0.03
387.0	1828	278	0.0	0.0	30.1	0.21	0.8	140	0.02
455.2	1828	185	0.0	0.0	30.1	0.14	0.7	140	0.01
529.3	1828	93	0.0	0.0	30.1	0.07	0.7	140	0.01

GEOMETRY SUMMARY * At End of Pumping Schedule
MWX-1, MINIFRAC #2

Dstnce (ft)	Press (psi)	W-Avg (in)	Q (bpm)	Sh-Rate (1/sec)	-----Hght (ft)-----			Bank Prop Fraction	Prop (PSF)	
					Total	Up	Dn			
50	1074	0.14	4.9	58	140	53	22	127	0.00	0.00
125	1058	0.14	4.7	63	138	52	21	125	0.00	0.00
200	1042	0.13	4.6	64	138	50	21	128	0.00	0.00
300	1020	0.12	4.4	73	135	48	19	125	0.00	0.00
400	996	0.11	4.2	90	129	45	18	117	0.00	0.00
500	975	0.11	4.0	97	126	43	17	116	0.00	0.00
600	957	0.10	3.8	104	125	42	16	115	0.00	0.00
700	942	0.10	3.6	110	123	40	15	116	0.00	0.00
800	925	0.09	3.5	133	118	38	15	108	0.00	0.00
900	908	0.08	3.3	153	114	36	14	104	0.00	0.00
1000	890	0.08	3.1	159	114	34	13	106	0.00	0.00
1100	875	0.07	2.8	184	111	33	12	103	0.00	0.00
1200	912	0.06	2.5	246	105	31	11	95	0.00	0.00
1300	762	0.03	1.5	931	92	20	5	86	0.00	0.00
1353	704	0.03	1.3	900	73	11	0	67	0.00	0.00
1363	694	0.03	1.3	917	73	10	0	68	0.00	0.00
1381	676	0.03	1.3	954	73	9	0	69	0.00	0.00
1419	636	0.02	1.2	1040	73	6	0	72	0.00	0.00
1469	579	0.02	1.1	1142	72	4	0	72	0.00	0.00
1544	482	0.02	1.0	1496	72	4	0	72	0.00	0.00
1644	321	0.01	0.8	2559	72	4	0	72	0.00	0.00
1755	184	0.01	0.5	4952	72	4	0	72	0.00	0.00

FLUID SUMMARY * At End of Pumping Schedule
MWX-1, MINIFRAC #2

Stage No	Fluid Gone	Prop ID	Pos ID	Pos (ft)	Concentration In	Concentration Now	Concentration Desgn	Fl Vol (MGal)	Ex Tim (min)	Temp (deg F)	Visc (cp)	Fall Frac
1	1	2	1	1816	0.0	0.0	0.0	0.3	4.8	180	3	0.00
1	1	2	1	1816	0.0	0.0	0.0	0.5	7.9	180	3	0.00
1	1	2	1	1816	0.0	0.0	0.0	0.8	9.5	180	3	0.00
1	1	2	1	1816	0.0	0.0	0.0	1.3	14.0	180	4	0.00
1	1	2	1	1816	0.0	0.0	0.0	1.8	16.2	180	4	0.00
1	1	2	1	1816	0.0	0.0	0.0	2.7	28.8	180	5	0.00
1	1	2	1	1816	0.0	0.0	0.0	3.4	31.2	180	4	0.00
1	1	2	1	1816	0.0	0.0	0.0	3.8	38.4	180	4	0.00
2	1	1	1	1816	0.0	0.0	0.0	4.4	45.2	180	8	0.00
2	1	1	1	1816	0.0	0.0	0.0	5.5	47.5	180	8	0.00
2	0	1	1	1673	0.0	0.0	0.2	6.7	42.3	180	8	0.00
2	0	1	1	1400	0.0	0.0	0.6	8.0	36.1	180	14	0.00
2	0	1	1	1159	0.0	0.0	0.8	9.8	30.7	180	28	0.00
2	0	1	1	987	0.0	0.0	0.8	12.1	20.8	180	32	0.00
2	0	1	1	808	0.0	0.0	0.9	14.8	16.0	180	36	0.00
2	0	1	1	667	0.0	0.0	0.9	16.4	11.3	180	41	0.00
2	0	1	1	552	0.0	0.0	0.9	18.6	0.0	180	46	0.00
2	0	1	1	437	0.0	0.0	0.9	20.5	0.0	125	63	0.00
2	0	1	1	336	0.0	0.0	0.9	22.5	0.0	90	83	0.00
2	0	1	1	246	0.0	0.0	1.0	24.3	0.0	85	93	0.00
2	0	1	1	155	0.0	0.0	1.0	26.6	0.0	80	99	0.00
2	0	1	1	52	0.0	0.0	1.0	29.1	0.0	73	108	0.00

A.8

MAIN FRACTURE TREATMENT, $C = 0.0001 \text{ ft/min}^{**0.5}$

Frac Summary * MWX-1, MAIN FRAC TREATMENT, PALUDAL

Design Data					
FLUID LOSS:	Coefficient (ft/sqrt(min))	0.0001		
	Spurt Loss (gal/100 sq ft)	0.00		
FORMATION:	Modulus (MM psi)	4.50		
	Fracture Height (ft)	72.0		
	Fluid Loss Height (ft)	55.0		
	Perforated Height (ft)	68.0		
TEMPERATURE:	Bottom Hole (deg F)	200		
PRESSURE:	Reservoir Pressure (psi)	5200.0		
	Closure Pressure (psi)	5890.0		
DEPTH:	Well Depth (ft)	7076		
FORMATION LAYER DATA:					
Depth	Stress at Top	Stres Grad	Modulus	Toughness	
6952	6520.0	0.000	4.50	1.00	
6969	8120.0	0.000	4.50	1.00	
6992	6240.0	0.000	4.50	1.00	
7015	7275.0	0.000	4.50	1.00	
7049	7300.0	0.000	4.50	1.00	
7057	6800.0	0.000	4.50	1.00	
7072	5890.0	0.000	4.00	1.00	
7104	7660.0	0.000	4.00	1.00	
7116	6410.0	0.000	4.00	1.00	
7147	7000.0	0.000	4.50	1.00	
7165	8000.0	0.000	4.50	1.00	
7175	6800.0	0.000	4.50	1.00	
7190	8420.0	0.000	4.50	1.00	
7201	7300.0	0.000	4.50	1.00	
7242	6360.0	0.433	4.50	1.00	
	Fluid Pressure Gradient (psi/ft)		0.433	
	Fracture Top (ft)			7076
	Fracture Bottom (ft)			7144

Calculated Results from 3-D Simulator	
STIMPLAN (TM) , NSI , Tulsa,OK	
Licensed To: Internal Use - NSI Technologies	
1/2 LENGTH:	'Hydraulic' length (ft) 2670
	Propped length (ft) 1687
PRESSURE:	Max Net Pressure (psi) 1234
TIME:	Max Exposure to Form. Temp. (min) .. 82.4
	Time to Close (min) 2929.1
RATE:	Fluid Loss Rate during pad (bpm) ... 1.2
EFFICIENCY:	at end of pumping schedule 0.90
PROPPANT:	Average In Situ Conc. (#/sq ft) 0.4
	Average Conductivity (md-ft) 160
HEIGHT:	Max Fracture Height (ft) 207
WIDTH:	Avg width at end of pumping (in) ... 0.13

Fluid ID No. 1		APOLLO				
Specific Gravity						1.04
	@Welbor	@FormTmp	@1Hr	@2Hr	@4Hr	@8Hr
vis (cp @ 170 1/sec)	92	89	85	82	77	66
non-Newtonian n'	0.52	0.56	0.60	0.64	0.71	0.85

Fluid ID No. 2		APOLLO				
Specific Gravity						1.04
	@Welbor	@FormTmp	@1Hr	@2Hr	@4Hr	@8Hr
vis (cp @ 170 1/sec)	74	72	70	68	64	57
non-Newtonian n'	0.63	0.66	0.69	0.72	0.77	0.88

Fluid ID No. 3		APOLLO				
Specific Gravity						1.04
	@Welbor	@FormTmp	@1Hr	@2Hr	@4Hr	@8Hr
vis (cp @ 170 1/sec)	55	50	45	38	5	5
non-Newtonian n'	0.72	0.77	0.87	0.89	0.97	0.97

Proppant ID No. 2		12- 20 Ottawa_Snd				
Specific Gravity						2.65
'Damage Factor'						0.70
Closure Pres (Mpsi)	0	2	4	8		16
KfW @ 2 #/sq ft (md-ft)	16000	13000	6500	1300		50

Time History * NSI STIMPLAN 3-D Fracture Simulation
MWX-1, MAIN FRAC TREATMENT, PALUDAL

Time (min)	Pen (ft)	Pres (psi)	Rate (bpm)	Prop (PPG)	Sl Vol (MGal)	Eff- ciency	Loss (bpm)	Hght (ft)	W-Avg (in)
0.3	120	588	15.0	0.0	0.2	0.70	1.3	72	0.01
0.5	180	581	15.0	0.0	0.3	0.64	1.8	72	0.01
0.7	240	620	15.0	0.0	0.4	0.63	2.0	72	0.01
1.0	300	672	15.0	0.0	0.6	0.65	2.0	73	0.02
1.4	360	714	15.0	0.0	0.9	0.67	2.1	77	0.02
1.8	420	725	15.0	0.0	1.1	0.69	2.1	79	0.02
2.2	480	748	15.0	0.0	1.4	0.70	2.1	90	0.02
2.7	540	736	15.0	0.0	1.7	0.72	2.1	90	0.02
3.2	600	815	15.0	0.0	2.0	0.73	2.2	98	0.02
3.9	660	809	15.0	0.0	2.5	0.74	2.1	99	0.03
4.6	720	909	15.0	0.0	2.9	0.75	2.2	112	0.03
5.6	780	857	15.0	0.0	3.5	0.76	2.1	112	0.03
6.5	840	957	15.0	0.0	4.1	0.77	2.0	121	0.03
8.1	900	920	15.0	0.0	5.1	0.79	1.9	121	0.04
9.3	943	986	15.0	0.0	5.9	0.79	1.7	127	0.04
10.5	948	856	0.2	0.0	5.9	0.78	1.3	127	0.04
12.7	1008	983	15.0	0.0	7.3	0.80	1.6	127	0.04
14.9	1068	1062	15.0	0.0	8.7	0.82	1.6	138	0.04
16.8	1095	915	15.0	0.0	9.9	0.83	1.3	138	0.05
18.0	1097	907	0.2	0.0	9.9	0.82	0.9	138	0.05
21.6	1157	1037	15.0	0.0	12.2	0.84	1.3	138	0.06
24.4	1209	1097	15.0	0.0	13.9	0.84	1.3	144	0.06
25.5	1210	952	0.2	0.0	13.9	0.84	0.9	144	0.06
31.5	1270	1073	15.0	0.0	17.7	0.86	1.2	144	0.08
35.0	1327	1133	15.0	0.0	19.9	0.86	1.2	150	0.08
39.7	1387	1103	21.0	1.5	24.0	0.88	1.2	150	0.09
43.1	1447	1173	21.0	2.0	27.0	0.88	1.3	188	0.09
47.7	1507	1049	21.0	2.0	31.1	0.89	1.3	188	0.10
50.8	1567	1115	21.0	3.0	33.8	0.89	1.3	188	0.11
53.5	1627	1155	21.0	3.0	36.3	0.89	1.4	188	0.11
56.0	1687	1175	21.0	4.0	38.4	0.89	1.5	188	0.11
58.8	1747	1128	21.0	4.0	40.9	0.90	1.5	188	0.12
61.2	1807	1163	21.0	4.0	43.0	0.90	1.5	188	0.12
63.7	1867	1186	21.0	4.0	45.2	0.90	1.6	189	0.12
66.4	1927	1160	21.0	4.0	47.6	0.90	1.6	189	0.12
68.8	1987	1186	21.0	4.0	49.7	0.90	1.6	189	0.12
71.3	2047	1203	21.0	4.0	52.0	0.90	1.7	189	0.12
74.2	2107	1160	21.0	5.5	54.5	0.90	1.7	189	0.12
76.8	2167	1184	21.0	5.5	56.8	0.90	1.7	189	0.13
79.4	2227	1207	21.0	5.5	59.1	0.90	1.7	190	0.12
82.6	2287	1162	21.0	5.5	61.9	0.90	1.7	190	0.13
85.5	2347	1183	21.0	5.5	64.5	0.90	1.8	190	0.13
88.4	2407	1206	21.0	5.5	67.0	0.90	1.8	190	0.13
91.3	2467	1215	21.0	5.5	69.6	0.90	1.8	190	0.13
94.2	2527	1209	21.0	5.5	72.2	0.90	1.8	190	0.13
98.2	2610	1234	21.0	5.5	75.7	0.90	1.9	207	0.13
102.2	2670	1053	0.0	0.0	75.7	0.90	1.8	207	0.13
252.8	2670	948	0.0	0.0	75.7	0.81	0.8	207	0.12

517.9	2670	843	0.0	0.0	75.7	0.72	0.5	207	0.10
866.2	2670	737	0.0	0.0	75.7	0.64	0.4	207	0.09
1255.6	2670	632	0.0	0.0	75.7	0.57	0.3	207	0.08
1663.5	2670	527	0.0	0.0	75.7	0.51	0.3	207	0.07
2100.6	2670	421	0.0	0.0	75.7	0.45	0.2	207	0.06
2559.9	2670	316	0.0	0.0	75.7	0.39	0.2	207	0.06
3027.3	2670	211	0.0	0.0	75.7	0.34	0.2	207	0.05

GEOMETRY SUMMARY * At End of Pumping Schedule
MWX-1, MAIN FRAC TREATMENT, PALUDAL

Dstnce (ft)	Press (psi)	W-Avg (in)	Q (bpm)	Sh-Rate (1/sec)	-----Hght (ft)-----			Bank Prop Fraction	Prop (PSF)	
					Total	Up	Dn			
30	1231	0.25	10.6	32	207	92	47	206	0.02	0.72
90	1226	0.22	10.4	38	205	92	47	203	0.02	0.64
150	1221	0.22	10.1	38	205	92	46	204	0.02	0.78
210	1216	0.23	9.9	38	188	92	31	186	0.02	0.66
270	1210	0.23	9.7	38	188	90	31	188	0.02	0.79
330	1205	0.23	9.5	37	188	90	31	188	0.01	0.78
390	1201	0.23	9.3	36	188	90	31	188	0.01	0.77
450	1195	0.23	9.0	34	184	91	31	176	0.01	0.53
510	1187	0.21	8.8	42	172	90	31	151	0.01	0.52
570	1181	0.21	8.6	41	172	77	29	167	0.01	0.47
630	1174	0.21	8.3	41	172	77	27	168	0.01	0.46
690	1166	0.17	8.1	60	172	79	29	164	0.01	0.39
750	1158	0.13	7.9	102	172	88	31	154	0.01	0.31
810	1149	0.14	7.8	92	155	61	26	144	0.01	0.30
870	1141	0.15	7.6	88	149	60	26	134	0.01	0.27
924	1133	0.15	7.5	88	149	57	24	138	0.01	0.26
978	1126	0.15	7.4	85	145	59	25	129	0.01	0.27
1052	1116	0.15	7.2	85	145	58	24	130	0.01	0.23
1127	1106	0.13	7.0	118	132	57	24	106	0.00	0.18
1183	1097	0.13	6.9	118	132	47	19	121	0.00	0.15
1240	1088	0.13	6.8	117	132	46	18	123	0.00	0.15
1299	1079	0.13	6.7	117	132	47	19	120	0.00	0.12
1357	1071	0.13	6.5	117	132	48	20	119	0.00	0.11
1417	1060	0.13	6.4	116	132	48	20	119	0.00	0.07
1477	1048	0.12	6.2	114	132	48	20	119	0.00	0.00
1537	1037	0.12	6.1	114	132	48	20	119	0.00	0.00
1597	1037	0.12	6.0	112	132	49	20	119	0.00	0.00
1657	1026	0.12	5.7	115	132	48	20	119	0.00	0.00
1717	1014	0.11	5.4	122	130	47	19	117	0.00	0.00
1777	1002	0.11	5.1	127	128	46	18	116	0.00	0.00
1837	990	0.10	4.8	129	127	45	18	115	0.00	0.00
1897	977	0.10	4.5	137	125	43	17	113	0.00	0.00
1957	965	0.09	4.2	145	122	42	16	111	0.00	0.00
2017	953	0.09	3.8	149	122	40	16	111	0.00	0.00
2077	943	0.08	3.4	163	119	39	15	109	0.00	0.00
2137	936	0.07	3.0	183	117	38	14	107	0.00	0.00
2197	1014	0.07	2.4	181	112	34	12	102	0.00	0.00
2257	810	0.03	1.2	712	97	25	7	90	0.00	0.00
2317	708	0.03	1.0	711	73	10	0	67	0.00	0.00
2377	606	0.02	0.9	831	72	4	0	72	0.00	0.00
2437	471	0.02	0.7	1128	72	4	0	72	0.00	0.00
2497	316	0.01	0.6	1909	72	4	0	72	0.00	0.00
2569	222	0.01	0.4	2676	72	4	0	72	0.00	0.00

FLUID SUMMARY * At End of Pumping Schedule
MWX-1, MAIN FRAC TREATMENT, PALUDAL

Stage No	Fluid Gone	Prop ID	Pos ID	Pos (ft)	Concentration In	Concentration Now	Concentration Design	Fl Vol (MGal)	Ex Tim (min)	Temp (deg F)	Visc (cp)	Fall Frac
1	1	5	1	2610	0.0	0.0	0.0	0.2	6.7	200	3	0.00
1	1	5	1	2610	0.0	0.0	0.0	0.3	9.3	200	3	0.00
1	1	5	1	2610	0.0	0.0	0.0	0.4	16.5	200	3	0.00
1	1	5	1	2610	0.0	0.0	0.0	0.6	18.3	200	2	0.00
1	1	5	1	2610	0.0	0.0	0.0	0.9	26.6	200	2	0.00
1	1	5	1	2610	0.0	0.0	0.0	1.1	30.3	200	2	0.00
1	1	5	1	2610	0.0	0.0	0.0	1.4	41.2	200	1	0.00
2	1	1	1	2610	0.0	0.0	0.0	1.7	49.7	200	21	0.00
2	1	1	1	2610	0.0	0.0	0.0	2.0	57.8	200	21	0.00
2	1	1	1	2610	0.0	0.0	0.0	2.5	66.8	200	22	0.00
2	1	1	1	2610	0.0	0.0	0.0	2.9	81.2	200	23	0.00
2	1	1	1	2610	0.0	0.0	0.0	3.5	82.4	200	23	0.00
2	0	1	1	2527	0.0	0.0	1.0	4.1	82.4	200	23	0.00
2	0	1	1	2340	0.0	0.0	3.0	4.9	76.4	200	36	0.00
2	0	1	1	2190	0.0	0.0	3.9	5.6	73.2	200	61	0.00
3	0	1	1	2159	0.0	0.0	4.0	5.6	73.2	200	59	0.00
4	0	1	1	2110	0.0	0.0	4.2	6.8	67.7	200	60	0.00
4	0	1	1	2017	0.0	0.0	4.4	7.9	67.7	200	62	0.00
4	0	1	1	1938	0.0	0.0	4.5	8.9	58.8	200	63	0.00
5	0	1	1	1903	0.0	0.0	4.6	8.9	58.8	200	64	0.00
6	0	1	1	1842	0.0	0.0	4.6	10.8	58.8	200	65	0.00
6	0	1	1	1738	0.0	0.0	4.8	12.3	54.8	200	66	0.00
7	0	1	1	1695	0.0	0.0	4.8	12.3	54.8	200	67	0.00
8	0	1	1	1609	0.0	0.0	4.9	15.3	44.0	200	68	0.00
8	0	1	1	1474	0.0	0.0	5.0	17.1	41.4	200	68	0.00
9	0	2	1	1353	1.5	1.6	5.1	19.7	33.7	200	60	0.14
10	0	2	1	1261	2.0	2.2	5.1	20.5	31.2	200	60	0.14
10	0	2	1	1174	2.0	2.1	5.1	23.0	26.1	200	60	0.12
10	0	2	1	1082	2.0	2.1	5.2	24.1	20.7	200	66	0.10
11	0	2	1	1011	3.0	3.2	5.2	26.2	18.1	200	67	0.10
11	0	2	1	919	3.0	3.1	5.2	28.4	12.2	200	67	0.07
11	0	2	1	845	3.0	3.1	5.3	29.7	9.3	200	67	0.06
12	0	2	1	802	4.0	4.2	5.3	30.4	6.4	200	67	0.06
12	0	2	1	750	4.0	4.1	5.3	32.2	0.0	200	69	0.05
12	0	2	1	682	4.0	4.1	5.3	34.1	0.0	183	80	0.05
12	0	2	1	628	4.0	4.1	5.3	35.9	0.0	101	88	0.04
12	0	2	1	581	4.0	4.1	5.3	37.6	0.0	99	87	0.04
12	0	2	1	532	4.0	4.1	5.4	39.5	0.0	96	87	0.03
12	0	2	1	485	4.0	4.1	5.4	41.3	0.0	94	90	0.03
12	0	2	1	443	4.0	4.1	5.4	43.0	0.0	92	94	0.03
13	0	3	1	423	5.5	5.6	5.4	43.1	0.0	92	66	0.04
13	0	3	1	399	5.5	5.6	5.4	45.1	0.0	90	65	0.03
13	0	3	1	355	5.5	5.6	5.4	46.9	0.0	88	65	0.03
13	0	3	1	312	5.5	5.6	5.4	48.8	0.0	86	65	0.03
13	0	3	1	264	5.5	5.6	5.4	51.0	0.0	83	65	0.02
13	0	3	1	215	5.5	5.6	5.4	53.1	0.0	80	65	0.02
13	0	3	1	168	5.5	5.5	5.5	55.1	0.0	78	66	0.01
13	0	3	1	123	5.5	5.5	5.5	57.2	0.0	76	67	0.01

13	0	3	1	77	5.5	5.5	5.5	59.3	0.0	74	67	0.01
13	0	3	1	37	5.5	5.5	5.5	61.1	0.0	71	71	0.00
14	0	3	2	10	5.5	5.5	5.5	62.1	0.0	71	71	0.02

PROPPANT SUMMARY * At End of Pumping Schedule
MWX-1, MAIN FRAC TREATMENT, PALUDAL

Distance (ft)	KfW (md-ft)	Proppant Concentration (lb/sq foot)	
		Prop ID--> 1	2
30	431	0.50	0.20
90	283	0.60	0.00
150	350	0.80	0.00
210	290	0.70	0.00
270	351	0.80	0.00
330	347	0.80	0.00
390	344	0.80	0.00
450	227	0.50	0.00
510	224	0.50	0.00
570	198	0.50	0.00
630	194	0.50	0.00
690	160	0.40	0.00
750	124	0.30	0.00
810	120	0.30	0.00
870	106	0.30	0.00
924	100	0.30	0.00
978	106	0.30	0.00
1052	85	0.20	0.00
1127	61	0.20	0.00
1183	50	0.20	0.00
1240	47	0.10	0.00
1299	34	0.10	0.00
1357	30	0.10	0.00
1417	9	0.10	0.00
1477	0	0.00	0.00
1537	0	0.00	0.00
1597	0	0.00	0.00
1657	0	0.00	0.00
1717	0	0.00	0.00
1777	0	0.00	0.00
1837	0	0.00	0.00
1897	0	0.00	0.00
1957	0	0.00	0.00
2017	0	0.00	0.00
2077	0	0.00	0.00
2137	0	0.00	0.00
2197	0	0.00	0.00
2257	0	0.00	0.00
2317	0	0.00	0.00
2377	0	0.00	0.00
2437	0	0.00	0.00
2497	0	0.00	0.00
2569	0	0.00	0.00
Average Conductivity (md-ft)		178	

PROPPANT SUMMARY * At Fracture Closure
 MWX-1, MAIN FRAC TREATMENT, PALUDAL

Distance (ft)	KfW (md-ft)	Proppant Concentration (lb/sq foot)	
		Prop ID--> 1	2
30	376	0.40	0.20
90	254	0.60	0.00
150	318	0.70	0.00
210	235	0.50	0.00
270	287	0.60	0.00
330	284	0.60	0.00
390	282	0.60	0.00
450	228	0.50	0.00
510	203	0.50	0.00
570	127	0.30	0.00
630	130	0.30	0.00
690	154	0.40	0.00
750	174	0.40	0.00
810	228	0.50	0.00
870	180	0.40	0.00
924	151	0.40	0.00
978	144	0.30	0.00
1052	138	0.30	0.00
1127	125	0.30	0.00
1183	82	0.20	0.00
1240	78	0.20	0.00
1299	73	0.20	0.00
1357	62	0.20	0.00
1417	49	0.20	0.00
1477	46	0.10	0.00
1537	39	0.10	0.00
1597	25	0.10	0.00
1657	6	0.10	0.00
1717	0	0.00	0.00
1777	0	0.00	0.00
1837	0	0.00	0.00
1897	0	0.00	0.00
1957	0	0.00	0.00
2017	0	0.00	0.00
2077	0	0.00	0.00
2137	0	0.00	0.00
2197	0	0.00	0.00
2257	0	0.00	0.00
2317	0	0.00	0.00
2377	0	0.00	0.00
2437	0	0.00	0.00
2497	0	0.00	0.00
2569	0	0.00	0.00
2640	0	0.00	0.00
Average Conductivity (md-ft)			160

A.9

MAIN FRACTURE TREATMENT, FORCING SCREEN-OUT AT 50 MIN.

MWX-1, MAIN FRAC TREATMENT, PALUDAL
Input Data

Well Data
 Depth (ft)..... 7076.
 Perforated Height (ft)..... 68.
 Reservoir Pressure (psi)..... 5200.
 Closure Pressure (psi)..... 5890.

Formation Data
 Fracture Height (ft)..... 72.
 Fluid Loss Height (ft)..... 55.
 Modulus (e6 psi)..... 4.5

Fluid Data
 Loss Coefficient (ft/sq root min)... .0001
 Spurt Loss (gal/100 sq ft)..... .00
 Viscosity (cp)
 at wellbore 148.
 at formation temperature 50.
 at fracture tip 30.
 n-prime50
 Proppant Fall Correction50

Proppant Data (Prop Type No 1)
 Mesh 20/40
 Specific Gravity 2.65
 KfW (md-ft at 2 lb/sq ft)..... 2000.

Max Exposure Time to Reservoir Temperature ... 47.5 min
 Pad Fluid Loss Rate 1.2 bpm

Stage	Sl Vol (M Gal)	Fl Vol (M Gal)	Prop Conc (PPG)	Rate (bpm)	Fluid Code	Prop Code	Pump Time (min)
1	1.5	1.5	.0	15.0	5	1	2.4
2	4.3	4.3	.0	15.0	1	1	6.9
3	.0	.0	.0	.2	1	1	1.2
4	4.0	4.0	.0	15.0	1	1	6.3
5	.0	.0	.0	.2	1	1	1.2
6	4.0	4.0	.0	15.0	1	1	6.3
7	.0	.0	.0	.2	1	1	1.2
8	5.9	5.9	.0	15.0	1	1	9.4
9	3.2	3.0	1.5	21.0	2	1	3.6
10	5.5	5.0	2.0	21.0	2	1	6.2
11	6.8	6.0	3.0	21.0	2	1	7.7
12	16.5	14.0	4.0	21.0	2	1	18.7
13	22.5	18.0	5.5	21.0	3	1	25.5
14	1.2	1.0	5.5	21.0	3	2	1.4

Total Fluid Volume is 66.8 M-gal
 Total Prop Volume is 193.0 M-lbs
 Gross Average Concentration is 2.9 lb/gal

***** Height Growth *****

Net Pressure (psi)	Height (ft)	Height Up	Height Down	Cs	Cf		
100.	68.	0.	0.	9.100	.123	0.	0.
581.	72.	4.	0.	7.347	.156	4.	0.
692.	80.	12.	0.	3.652	.273	9.	0.
693.	87.	16.	3.	3.629	.277	13.	3.
1144.	155.	61.	26.	1.510	.859	50.	26.
1145.	179.	85.	26.	1.611	.723	85.	26.
1146.	182.	88.	26.	1.463	.619	85.	26.
1147.	188.	89.	31.	1.499	.753	89.	31.
1213.	191.	92.	31.	1.238	.808	89.	31.
1214.	206.	92.	46.	1.291	1.016	92.	46.
1690.	267.	99.	99.	.658	4.169	99.	66.
1691.	572.	99.	404.	.422	7.466	99.	404.
1692.	629.	99.	461.	.329	10.439	99.	461.
9999.	639.	104.	466.	.329	10.439	102.	464.

Proppant No. 1, 20- 40 Ottawa_Snd , Sp.Gr. 2.65, Dmg .70

Stress (M psi)	0	2	4	8	16
Conductivity (d-ft)	4.60	4.00	2.70	.68	.05

Proppant No. 2, 12- 20 Ottawa_Snd , Sp.Gr. 2.65, Dmg .70

Stress (M psi)	0	2	4	8	16
Conductivity (d-ft)	16.00	13.00	6.50	1.30	.05

Fluid No. 5 , APOLLO Sp. Gr. 1.04 Quality 0

	At		Reservoir			
	Wellbore	Temperature	After Exposure of (hrs)			
Viscosity (cp) ...	20.	10.	1.	1.	1.	1.
n'70	.76	.95	.95	.95	.95

Fluid No. 1 , APOLLO Sp. Gr. 1.04 Quality 0

	At		Reservoir			
	Wellbore	Temperature	After Exposure of (hrs)			
Viscosity (cp) ...	92.	89.	85.	82.	77.	66.
n'52	.56	.60	.64	.71	.85

Fluid No. 2 , APOLLO Sp. Gr. 1.04 Quality 0

	At		Reservoir			
	Wellbore	Temperature	After Exposure of (hrs)			
Viscosity (cp) ...	74.	72.	70.	68.	64.	57.
n'63	.66	.69	.72	.77	.88

Fluid No. 3 , AFCLLO Sp. Gr. 1.04 Quality 0

	At	Reservoir	After Exposure of (hrs)			
	Wellbore	Temperature	1	2	4	8
Viscosity (cp) ...	55.	50.	45.	38.	5.	5.
n'72	.77	.87	.89	.97	.97

Time History * NSI STIMPLAN 3-D Fracture Simulation
MWX-1, MAIN FRAC TREATMENT, PALUDAL

Time (min)	Pen (ft)	Pres (psi)	Rate (bpm)	Prop (PPG)	Sl Vol (MGal)	Eff- ciency	Loss (bpm)	Hght (ft)	W-Avg (in)
.3	120.	588.	15.0	.0	.2	.70	1.3	72.	.01
.5	180.	581.	15.0	.0	.3	.64	1.8	72.	.01
.7	240.	620.	15.0	.0	.5	.63	2.0	72.	.01
1.0	300.	672.	15.0	.0	.6	.65	2.0	73.	.02
1.3	360.	713.	15.0	.0	.9	.67	2.1	77.	.02
1.8	420.	725.	15.0	.0	1.1	.69	2.1	79.	.02
2.2	480.	748.	15.0	.0	1.4	.70	2.1	90.	.02
2.7	540.	736.	15.0	.0	1.7	.72	2.1	90.	.02
3.2	600.	815.	15.0	.0	2.0	.73	2.2	98.	.02
3.9	660.	809.	15.0	.0	2.5	.74	2.1	99.	.03
4.6	720.	909.	15.0	.0	2.9	.75	2.2	112.	.03
5.6	780.	857.	15.0	.0	3.5	.76	2.1	112.	.03
6.5	840.	957.	15.0	.0	4.1	.77	2.0	121.	.03
8.1	900.	920.	15.0	.0	5.1	.79	1.9	121.	.04
9.3	943.	986.	15.0	.0	5.9	.79	1.7	127.	.04
10.5	948.	856.	.2	.0	5.9	.78	1.2	127.	.04
12.7	1008.	983.	15.0	.0	7.2	.80	1.6	127.	.04
14.9	1068.	1062.	15.0	.0	8.7	.82	1.6	138.	.04
16.8	1095.	915.	15.0	.0	9.9	.83	1.3	138.	.05
18.0	1097.	907.	.2	.0	9.9	.82	.9	138.	.05
21.6	1157.	1037.	15.0	.0	12.2	.84	1.3	138.	.06
24.4	1209.	1097.	15.0	.0	13.9	.84	1.3	144.	.06
25.6	1210.	952.	.2	.0	13.9	.84	.9	144.	.06
31.5	1270.	1073.	15.0	.0	17.7	.86	1.2	144.	.08
35.0	1327.	1133.	15.0	.0	19.9	.86	1.2	150.	.08
39.7	1387.	1103.	21.0	1.5	24.0	.88	1.2	150.	.09
43.1	1447.	1173.	21.0	2.0	27.0	.88	1.3	188.	.09
47.7	1507.	1049.	21.0	2.0	31.1	.89	1.3	188.	.10
50.8	1567.	1115.	21.0	3.0	33.8	.89	1.3	188.	.11
53.5	1627.	1155.	21.0	3.0	36.2	.89	1.4	188.	.11
56.0	1687.	1175.	21.0	4.0	38.4	.89	1.5	188.	.12
71.0	1687.	2012.	21.0	4.0	51.7	.92	1.1	188.	.16
86.0	1687.	2858.	21.0	5.5	64.9	.93	.9	188.	.19
98.2	1687.	3551.	21.0	5.5	75.7	.94	.8	188.	.23
*****	1687.	3196.	.0	.0	75.7	.67	.2	188.	.15
*****	1687.	2841.	.0	.0	75.7	.62	.2	188.	.14
*****	1687.	2486.	.0	.0	75.7	.57	.1	188.	.13
*****	1687.	2131.	.0	.0	75.7	.52	.1	188.	.12
*****	1687.	1776.	.0	.0	75.7	.47	.1	188.	.11
*****	1687.	1420.	.0	.0	75.7	.43	.1	188.	.10
*****	1687.	1065.	.0	.0	75.7	.38	.1	188.	.09
*****	1687.	710.	.0	.0	75.7	.35	.1	188.	.08
*****	1687.	710.	.0	.0	75.7	.35	.1	188.	.08

GEOMETRY SUMMARY * At End of Pumping Schedule
MWX-1, MAIN FRAC TREATMENT, PALUDAL

Dstnce (ft)	Press (psi)	W-Avg (in)	Q (bpm)	Sh-Rate (1/sec)	Hght (ft)	Bank Fraction	Prop (PSF)
30.	3551.	.67	10.5	4.	188.	.01	2.31
90.	3551.	.68	8.6	4.	186.	.01	1.91
150.	3550.	.66	6.8	4.	155.	.01	1.78
210.	3550.	.62	5.4	3.	152.	.01	1.33
270.	3550.	.62	4.0	3.	152.	.01	1.31
330.	3550.	.62	2.6	2.	151.	.00	1.04
390.	3550.	.60	1.3	1.	150.	.01	.66
450.	1126.	.17	.0	83.	142.	.00	.00
510.	1114.	.14	8.8	134.	129.	.00	.00
570.	1102.	.14	8.6	134.	129.	.00	.00
630.	1089.	.13	8.5	135.	129.	.00	.00
690.	1076.	.13	8.3	136.	129.	.00	.00
750.	1061.	.12	8.2	162.	124.	.00	.00
810.	1046.	.12	7.7	158.	124.	.00	.00
870.	1031.	.12	7.3	153.	124.	.00	.00
924.	1017.	.12	6.8	148.	124.	.00	.00
978.	1003.	.11	6.5	149.	123.	.00	.00
1052.	980.	.11	5.8	153.	120.	.00	.00
1127.	948.	.08	4.7	236.	101.	.00	.00
1183.	918.	.08	4.1	219.	101.	.00	.00
1240.	888.	.08	3.5	204.	101.	.00	.00
1299.	848.	.07	2.8	236.	92.	.00	.00
1357.	781.	.03	1.4	671.	73.	.00	.00
1417.	687.	.03	1.2	861.	72.	.00	.00
1477.	571.	.02	1.0	1078.	72.	.00	.00
1537.	429.	.02	.8	1560.	72.	.00	.00
1597.	282.	.01	.6	2746.	72.	.00	.00
1657.	164.	.01	.4	4044.	72.	.00	.00

FLUID SUMMARY * At End of Pumping Schedule
 MWX-1, MAIN FRAC TREATMENT, PALUDAL

Stage No	Fluid Gone	Prop ID	Pos ID	Pos (ft)	Concentration			Fl Vol (MGal)	Ex Tim (min)	Temp (deg F)	Visc (cp)	Fall Frac
					In	Now	Desgn					
1	1	5	1	1687.	.0	.0	.0	.2	6.7	200.	3.	.00
1	1	5	1	1687.	.0	.0	.0	.3	9.3	200.	3.	.00
1	1	5	1	1687.	.0	.0	.0	.5	16.5	200.	3.	.00
1	1	5	1	1687.	.0	.0	.0	.6	18.3	200.	2.	.00
1	1	5	1	1687.	.0	.0	.0	.9	26.6	200.	2.	.00
1	1	5	1	1687.	.0	.0	.0	1.1	30.3	200.	2.	.00
1	1	5	1	1687.	.0	.0	.0	1.4	41.2	200.	1.	.00
2	1	1	1	1687.	.0	.0	.0	1.7	47.1	200.	20.	.00
2	0	1	1	1670.	.0	.0	.0	2.0	47.5	200.	20.	.00
2	0	1	1	1598.	.0	.0	.0	2.4	46.1	200.	20.	.00
2	0	1	1	1483.	.0	.0	.0	2.8	43.2	200.	27.	.00
2	0	1	1	1365.	.0	.0	.0	3.4	41.0	200.	39.	.00
2	0	1	1	1277.	.0	.0	.0	3.9	41.0	200.	51.	.00
2	0	1	1	1208.	.0	.0	.0	4.7	34.9	200.	52.	.00
2	0	1	1	1136.	.0	.0	.0	5.3	31.8	200.	50.	.00
3	0	1	1	1105.	.0	.0	.0	5.3	31.8	200.	50.	.00
4	0	1	1	1065.	.0	.0	.0	6.5	26.2	200.	59.	.00
4	0	1	1	987.	.0	.0	.0	7.7	26.2	200.	60.	.00
4	0	1	1	919.	.0	.0	.0	8.7	17.4	200.	60.	.00
5	0	1	1	888.	.0	.0	.0	8.7	17.4	200.	60.	.00
6	0	1	1	830.	.0	.0	.0	10.6	17.4	200.	59.	.00
6	0	1	1	731.	.0	.0	.0	12.0	13.3	200.	60.	.00
7	0	1	1	690.	.0	.0	.0	12.0	13.3	200.	63.	.00
8	0	1	1	606.	.0	.0	.0	15.1	2.6	200.	63.	.00
8	0	1	1	482.	.0	.0	.0	16.9	.0	200.	71.	.00
9	1	2	1	396.	1.5	44.1	.0	20.1	.0	119.	74.	.00
10	0	2	1	381.	2.0	.0	5.5	21.0	.0	200.	266.	1.00
10	0	2	1	398.	2.0	1.9	5.9	23.4	.0	200.	267.	.06
10	0	2	1	376.	2.0	1.9	5.9	24.5	.0	200.	268.	.05
11	0	2	1	358.	3.0	2.8	6.0	26.5	.0	200.	269.	.05
11	0	2	1	333.	3.0	2.8	6.0	28.7	.0	200.	270.	.04
11	0	2	1	314.	3.0	2.8	6.0	29.9	.0	200.	271.	.04
12	0	2	1	303.	4.0	3.7	6.0	30.6	.0	200.	272.	.04
12	0	2	1	289.	4.0	3.7	6.0	32.3	.0	200.	246.	.03
12	0	2	1	219.	4.0	3.7	6.1	42.7	.0	200.	226.	.03
13	0	3	1	114.	5.5	5.5	5.5	53.3	.0	137.	119.	.02
13	0	3	1	38.	5.5	5.5	5.5	60.9	.0	82.	109.	.01
14	0	3	2	4.	5.5	5.5	5.5	61.9	.0	79.	108.	.03

***** Proppant Summary *****
 At End of Pumping Schedule
 MWX-1, MAIN FRAC TREATMENT, PALUDAL

Distance (ft)	KfW (md-ft)	Proppant Concentration (lb/sq ft)	
		Prop ID Code --> 1	2
30.	951.	2.0	.3
90.	688.	1.9	.0
150.	638.	1.8	.0
210.	474.	1.3	.0
270.	465.	1.3	.0
330.	364.	1.0	.0
390.	224.	.7	.0
450.	0.	.0	.0
510.	0.	.0	.0
570.	0.	.0	.0
630.	0.	.0	.0
690.	0.	.0	.0
750.	0.	.0	.0
810.	0.	.0	.0
870.	0.	.0	.0
924.	0.	.0	.0
978.	0.	.0	.0
1052.	0.	.0	.0
1127.	0.	.0	.0
1183.	0.	.0	.0
1240.	0.	.0	.0
1299.	0.	.0	.0
1357.	0.	.0	.0
1417.	0.	.0	.0
1477.	0.	.0	.0
1537.	0.	.0	.0
1597.	0.	.0	.0
1657.	0.	.0	.0

***** Average Conductivity is 543. md-ft *****

***** Proppant Summary *****
 At Fracture Closure
 MWX-1, MAIN FRAC TREATMENT, PALUDAL

Distance (ft)	KfW (md-ft)	Proppant Concentration (lb/sq ft)	
		Prop ID Code --> 1	2
30.	946.	2.0	.3
90.	684.	1.9	.0
150.	645.	1.8	.0
210.	478.	1.3	.0
270.	469.	1.3	.0
330.	369.	1.0	.0
390.	228.	.7	.0
450.	0.	.0	.0
510.	0.	.0	.0
570.	0.	.0	.0
630.	0.	.0	.0
690.	0.	.0	.0
750.	0.	.0	.0
810.	0.	.0	.0
870.	0.	.0	.0
924.	0.	.0	.0
978.	0.	.0	.0
1052.	0.	.0	.0
1127.	0.	.0	.0
1183.	0.	.0	.0
1240.	0.	.0	.0
1299.	0.	.0	.0
1357.	0.	.0	.0
1417.	0.	.0	.0
1477.	0.	.0	.0
1537.	0.	.0	.0
1597.	0.	.0	.0
1657.	0.	.0	.0

***** Average Conductivity is 545. md-ft *****

A.10

MAIN FRACTURE TREATMENT, SIMULATING PROPPED LENGTH AT 50 MIN.

Frac Summary * MWX-1, MAIN FRAC TREATMENT, PALUDAL

Design Data				
FLUID LOSS:	Coefficient (ft/sqrt(min)) 0.0001			
	Spurt Loss (gal/100 sq ft) 0.00			
FORMATION:	Modulus (MM psi) 4.50			
	Fracture Height (ft) 72.0			
	Fluid Loss Height (ft) 55.0			
	Perforated Height (ft) 68.0			
TEMPERATURE:	Bottom Hole (deg F) 200			
PRESSURE:	Reservoir Pressure (psi) 5200.0			
	Closure Pressure (psi) 5890.0			
DEPTH:	Well Depth (ft) 7076			
FROMATION LAYER DATA:				
Depth	Stress at Top	Stres Grad	Modulus	Toughnesss
6952	6520.0	0.000	4.50	1.00
6969	8120.0	0.000	4.50	1.00
6992	6240.0	0.000	4.50	1.00
7015	7275.0	0.000	4.50	1.00
7049	7300.0	0.000	4.50	1.00
7057	6800.0	0.000	4.50	1.00
7072	5890.0	0.000	4.00	1.00
7104	7660.0	0.000	4.00	1.00
7116	6410.0	0.000	4.00	1.00
7147	7000.0	0.000	4.50	1.00
7165	8000.0	0.000	4.50	1.00
7175	6800.0	0.000	4.50	1.00
7190	8420.0	0.000	4.50	1.00
7201	7300.0	0.000	4.50	1.00
7242	6360.0	0.433	4.50	1.00
Fluid Pressure Gradient (psi/ft)				0.433
Fracture Top (ft)				7076
Fracture Bottom (ft)				7144

Calculated Results from 3-D Simulator STIMPLAN (TM) , NSI , Tulsa,OK Licensed To: Internal Use - NSI Technologies	
1/2 LENGTH:	'Hydraulic' length (ft) 1616
	Propped length (ft) 480
PRESSURE:	Max Net Pressure (psi) 1173
TIME:	Max Exposure to Form. Temp. (min) .. 43.9
	Time to Close (min) 2169.6
RATE:	Fluid Loss Rate during pad (bpm) ... 1.2
EFFICIENCY:	at end of pumping schedule 0.89
PROPPANT:	Average In Situ Conc. (#/sq ft) 0.2
	Average Conductivity (md-ft) 70
HEIGHT:	Max Fracture Height (ft) 188
WIDTH:	Avq width at end of pumping (in) ... 0.11

Fluid ID No. 1		APOLLO					
Specific Gravity							1.04
	@Welbor	@FormTmp	@1Hr	@2Hr	@4Hr	@8Hr	
vis (cp @ 170 1/sec)	92	89	85	82	77	66	
non-Newtonian n'	0.52	0.56	0.60	0.64	0.71	0.85	

Fluid ID No. 2		APOLLO					
Specific Gravity							1.04
	@Welbor	@FormTmp	@1Hr	@2Hr	@4Hr	@8Hr	
vis (cp @ 170 1/sec)	74	72	70	68	64	57	
non-Newtonian n'	0.63	0.66	0.69	0.72	0.77	0.88	

Time History * NSI STIMPLAN 3-D Fracture Simulation
MWX-1, MAIN FRAC TREATMENT, PALUDAL

Time (min)	Pen (ft)	Pres (psi)	Rate (bpm)	Prop (PPG)	Sl Vol (MGal)	Eff- ciency	Loss (bpm)	Hght (ft)	W-Avg (in)
0.3	120	588	15.0	0.0	0.2	0.70	1.3	72	0.01
0.5	180	581	15.0	0.0	0.3	0.64	1.8	72	0.01
0.7	240	620	15.0	0.0	0.4	0.63	2.0	72	0.01
1.0	300	672	15.0	0.0	0.6	0.65	2.0	73	0.02
1.4	360	714	15.0	0.0	0.9	0.67	2.1	77	0.02
1.8	420	725	15.0	0.0	1.1	0.69	2.1	79	0.02
2.2	480	748	15.0	0.0	1.4	0.70	2.1	90	0.02
2.7	540	736	15.0	0.0	1.7	0.72	2.1	90	0.02
3.2	600	815	15.0	0.0	2.0	0.73	2.2	98	0.02
3.9	660	809	15.0	0.0	2.5	0.74	2.1	99	0.03
4.6	720	909	15.0	0.0	2.9	0.75	2.2	112	0.03
5.6	780	857	15.0	0.0	3.5	0.76	2.1	112	0.03
6.5	840	957	15.0	0.0	4.1	0.77	2.0	121	0.03
8.1	900	920	15.0	0.0	5.1	0.79	1.9	121	0.04
9.3	943	986	15.0	0.0	5.9	0.79	1.7	127	0.04
10.5	948	856	0.2	0.0	5.9	0.78	1.3	127	0.04
12.7	1008	983	15.0	0.0	7.3	0.80	1.6	127	0.04
14.9	1068	1062	15.0	0.0	8.7	0.82	1.6	138	0.04
16.8	1095	915	15.0	0.0	9.9	0.83	1.3	138	0.05
18.0	1097	907	0.2	0.0	9.9	0.82	0.9	138	0.05
21.6	1157	1037	15.0	0.0	12.2	0.84	1.3	138	0.06
24.4	1209	1097	15.0	0.0	13.9	0.84	1.3	144	0.06
25.5	1210	952	0.2	0.0	13.9	0.84	0.9	144	0.06
31.5	1270	1073	15.0	0.0	17.7	0.86	1.2	144	0.08
35.0	1327	1133	15.0	0.0	19.9	0.86	1.2	150	0.08
39.7	1387	1103	21.0	1.5	24.0	0.88	1.2	150	0.09
43.1	1447	1173	21.0	2.0	27.0	0.88	1.3	188	0.09
47.7	1507	1049	21.0	2.0	31.1	0.89	1.3	188	0.10
50.2	1556	1102	21.0	3.0	33.3	0.89	1.3	188	0.11
54.1	1616	1036	0.0	0.0	33.3	0.88	1.3	188	0.11
141.6	1616	932	0.0	0.0	33.3	0.79	0.6	188	0.09
292.6	1616	829	0.0	0.0	33.3	0.71	0.4	188	0.08
502.1	1616	725	0.0	0.0	33.3	0.62	0.3	188	0.07
766.5	1616	621	0.0	0.0	33.3	0.53	0.3	188	0.06
1080.1	1616	518	0.0	0.0	33.3	0.45	0.2	188	0.05
1433.4	1616	414	0.0	0.0	33.3	0.37	0.2	188	0.04
1814.7	1616	311	0.0	0.0	33.3	0.29	0.2	188	0.03
2219.8	1616	207	0.0	0.0	33.3	0.22	0.1	188	0.03

GEOMETRY SUMMARY * At End of Pumping Schedule
MWX-1, MAIN FRAC TREATMENT, PALUDAL

Dstnce (ft)	Press (psi)	W-Avg (in)	Q (bpm)	Sh-Rate (1/sec)	-----Hght (ft)-----			Bank Prop Fraction	Prop (PSF)	
					Total	Up	Dn			
30	1099	0.21	10.4	47	188	89	31	187	0.00	0.43
90	1092	0.21	9.6	44	186	89	31	183	0.00	0.31
150	1086	0.20	9.0	53	155	61	26	143	0.00	0.25
210	1080	0.19	8.4	58	152	60	26	138	0.00	0.23
270	1074	0.19	7.9	55	152	59	25	141	0.00	0.18
330	1068	0.19	7.3	52	151	58	25	140	0.00	0.07
390	1060	0.18	6.8	52	150	57	24	139	0.00	0.00
450	1052	0.16	6.3	65	142	56	24	127	0.00	0.00
510	1041	0.13	5.8	103	129	55	23	103	0.00	0.00
570	1029	0.13	5.5	99	129	44	18	119	0.00	0.00
630	1017	0.12	5.2	95	129	43	17	120	0.00	0.00
690	1006	0.12	4.8	91	129	46	19	116	0.00	0.00
750	992	0.11	4.4	111	121	48	20	99	0.00	0.00
810	977	0.11	4.1	106	121	38	15	114	0.00	0.00
870	962	0.11	3.8	101	121	41	16	109	0.00	0.00
924	949	0.11	3.4	94	121	38	15	114	0.00	0.00
978	933	0.09	3.1	115	115	38	15	102	0.00	0.00
1052	901	0.07	2.8	166	111	35	13	100	0.00	0.00
1127	787	0.05	2.3	407	83	24	7	63	0.00	0.00
1183	755	0.04	1.6	436	83	15	2	78	0.00	0.00
1240	719	0.03	1.2	766	83	13	2	79	0.00	0.00
1299	637	0.02	1.0	850	73	6	0	71	0.00	0.00
1357	525	0.02	0.9	1058	72	4	0	72	0.00	0.00
1417	388	0.02	0.7	1571	72	4	0	72	0.00	0.00
1477	253	0.01	0.5	2776	72	4	0	72	0.00	0.00
1532	132	0.01	0.4	7132	72	4	0	72	0.00	0.00

FLUID SUMMARY * At End of Pumping Schedule
MWX-1, MAIN FRAC TREATMENT, PALUDAL

Stage	Fluid No	Prop ID	Prop ID	Pos (ft)	Concentration			Fl Vol (MGal)	Ex Tim (min)	Temp (deg F)	Visc (cp)	Fall Frac
	Gone				In	Now	Desgn					
1	1	5	1	1556	0.0	0.0	0.0	0.2	6.7	200	3 0.00	
1	1	5	1	1556	0.0	0.0	0.0	0.3	9.3	200	3 0.00	
1	1	5	1	1556	0.0	0.0	0.0	0.4	16.5	200	3 0.00	
1	1	5	1	1556	0.0	0.0	0.0	0.6	18.3	200	2 0.00	
1	1	5	1	1556	0.0	0.0	0.0	0.9	26.6	200	2 0.00	
1	1	5	1	1556	0.0	0.0	0.0	1.1	30.3	200	2 0.00	
1	1	5	1	1556	0.0	0.0	0.0	1.4	41.2	200	1 0.00	
2	1	1	1	1556	0.0	0.0	0.0	1.7	43.9	200	18 0.00	
2	0	1	1	1503	0.0	0.0	0.4	2.0	41.7	200	19 0.00	
2	0	1	1	1404	0.0	0.0	1.2	2.4	40.3	200	24 0.00	
2	0	1	1	1286	0.0	0.0	1.7	2.8	37.4	200	30 0.00	
2	0	1	1	1175	0.0	0.0	2.3	3.4	35.2	200	39 0.00	
2	0	1	1	1089	0.0	0.0	2.4	3.9	35.2	200	55 0.00	
2	0	1	1	1022	0.0	0.0	2.5	4.8	29.1	200	63 0.00	
2	0	1	1	959	0.0	0.0	2.6	5.5	25.9	200	69 0.00	
3	0	1	1	935	0.0	0.0	2.7	5.5	25.9	200	73 0.00	
4	0	1	1	896	0.0	0.0	2.7	6.7	20.4	200	72 0.00	
4	0	1	1	816	0.0	0.0	2.8	8.0	20.4	200	70 0.00	
4	0	1	1	743	0.0	0.0	2.8	9.1	11.6	200	69 0.00	
5	0	1	1	710	0.0	0.0	2.8	9.1	11.6	200	75 0.00	
6	0	1	1	655	0.0	0.0	2.8	11.1	11.6	200	74 0.00	
6	0	1	1	560	0.0	0.0	2.9	12.6	7.5	200	72 0.00	
7	0	1	1	519	0.0	0.0	2.9	12.6	7.5	200	71 0.00	
8	0	1	1	452	0.0	0.0	2.9	15.9	0.0	200	85 0.00	
8	0	1	1	354	0.0	0.0	2.9	17.9	0.0	138	97 0.00	
9	0	2	1	279	1.5	1.5	3.0	20.7	0.0	94	79 0.03	
10	0	2	1	221	2.0	2.0	3.0	21.6	0.0	88	77 0.04	
10	0	2	1	169	2.0	2.0	3.0	24.2	0.0	84	79 0.02	
10	0	2	1	114	2.0	2.0	3.0	25.5	0.0	79	84 0.01	
11	0	2	1	71	3.0	3.0	3.0	27.8	0.0	76	85 0.02	
11	0	2	1	23	3.0	3.0	3.0	29.7	0.0	73	84 0.00	

PROPPANT SUMMARY * At End of Pumping Schedule
 MWX-1, MAIN FRAC TREATMENT, PALUDAL

Distance (ft)	KfW (md-ft)	Proppant Concentration (lb/sq foot) Prop ID--> 1
30	190	0.40
90	131	0.30
150	101	0.30
210	91	0.20
270	64	0.20
330	9	0.10
390	0	0.00
450	0	0.00
510	0	0.00
570	0	0.00
630	0	0.00
690	0	0.00
750	0	0.00
810	0	0.00
870	0	0.00
924	0	0.00
978	0	0.00
1052	0	0.00
1127	0	0.00
1183	0	0.00
1240	0	0.00
1299	0	0.00
1357	0	0.00
1417	0	0.00
1477	0	0.00
1532	0	0.00
Average Conductivity (md-ft)		98

PROPPANT SUMMARY * At Fracture Closure
 MWX-1, MAIN FRAC TREATMENT, PALUDAL

Distance (ft)	KfW (md-ft)	Proppant Concentration (lb/sq foot) Prop ID--> 1
30	123	0.30
90	98	0.20
150	95	0.20
210	74	0.20
270	65	0.20
330	56	0.20
390	36	0.10
450	9	0.10
510	0	0.00
570	0	0.00
630	0	0.00
690	0	0.00
750	0	0.00
810	0	0.00
870	0	0.00
924	0	0.00
978	0	0.00
1052	0	0.00
1127	0	0.00
1183	0	0.00
1240	0	0.00
1299	0	0.00
1357	0	0.00
1417	0	0.00
1477	0	0.00
1532	0	0.00
1586	0	0.00
Average Conductivity (md-ft)		70